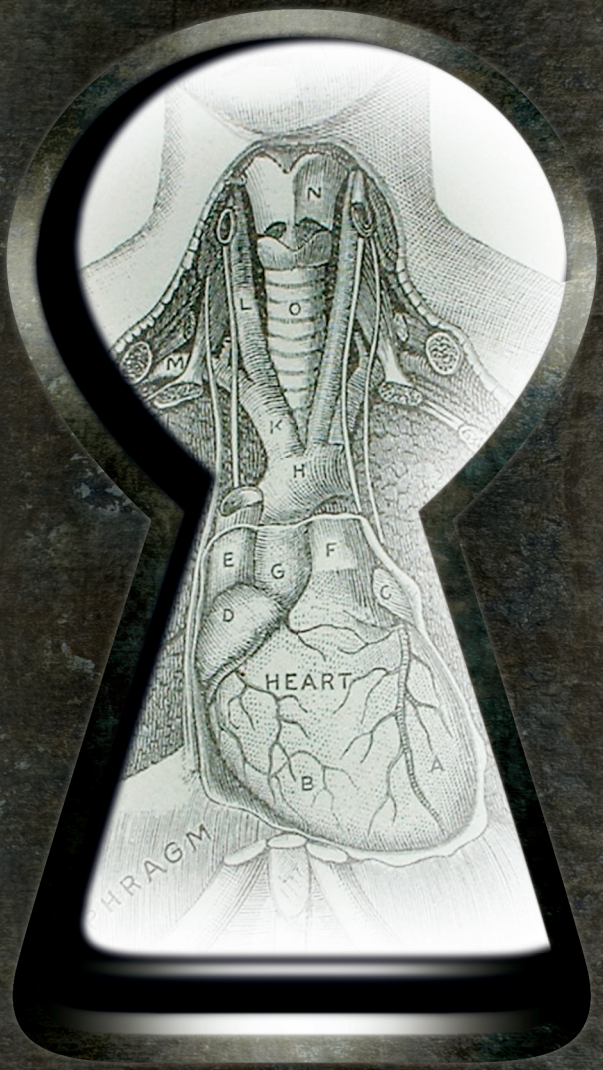

Inflammatory mediators in diet-induced cardiac dysfunction

Mieke Louwe

Inflammatory mediators in diet-induced cardiac dysfunction

Mieke Louwe

Inflammatory mediators in diet-induced cardiac dysfunction

Cover design: Harald Pieper
Layout design: Koen Rotteveel & Tina van Houten
Printing: Wöhrmann Print Service

ISBN: 978-94-6203-380-1

Inflammatory mediators in diet-induced cardiac dysfunction

Proefschrift

ter verkrijging van
de graad van Doctor aan de Universiteit Leiden,
op gezag van Rector Magnificus prof.mr. C.J.J.M. Stolker,
volgens besluit van het College voor Promoties
te verdedigen op dinsdag 25 juni 2013
klokke 15.00 uur

door

Maria Cornelia Louwe

geboren te Egmond aan den Hoef
in 1984

Promotiecommissie

Promotores: Prof. dr. J.W.A. Smit
Prof. dr. K. Willems van Dijk

Co-promotor: Dr. P. Steendijk

Overige leden: Prof. dr. P.C.N. Rensen
Prof. dr. J.W. Jukema
Dr. M. van Eck (LACDR, Universiteit Leiden)
Prof. dr. M.H. Hofker (Rijksuniversiteit Groningen)

The work described in this thesis was performed at the department of Endocrinology and Metabolic Diseases at the Leiden University Medical Center, Leiden, the Netherlands.

The research described in this thesis was performed within the framework of CTMM, the Center for Translational Molecular Medicine (www.ctmm.nl), project PREDICCt (grant 01C-104), and supported by the Dutch Heart Foundation (DFH-2008T085), Dutch Diabetes Research Foundation and Dutch Kidney Foundation.

Financial support by the Dutch Heart Foundation for the publication of this thesis is gratefully acknowledged.

The printing of this thesis was kindly supported by:
Boehringer Ingelheim, Greiner Bio-One, Novo Nordisk B.V.

What is a scientist after all? It is a curious man looking through a keyhole, the keyhole of nature, trying to know what's going on.

Jacques Cousteau (1910-1997)

Table of contents

CHAPTER 1

General introduction

General introduction

Cardiovascular diseases

Cardiovascular diseases (CVD) are the leading cause of death in the Westernized world. In the Netherlands, 30% of the reported deaths were a result of CVD.[1] Similar percentages are listed globally, according to the World Health Organization.[2] Despite substantially improved treatment options during the last decades, the number of patients suffering from CVD is still increasing.[2]

Risk factors for CVD can be subdivided into non-modifiable and modifiable risk factors. Non-modifiable factors include genetic variation, gender and age, whereas modifiable factors include lifestyle (smoking, physical inactivity, diet, overweight), hypertension, hyperlipidemia and hyperglycemia.[3] Adequate changes in lifestyle such as a more healthy diet, smoking prevention, increased physical activity and weight control can avoid over 75% of deaths attributed to CVD.[4] However, harsh reality shows that this is rarely feasible for individuals. As a result, in the last decade research on the treatment options for CVD is increasingly focused on the role of non-modifiable factors. Primary prevention strategies focus on the identified risk factors, such as lowering of plasma lipid levels using statins. Despite all efforts CVD are projected to remain the leading cause of death in the future.[2] Therefore it is urgent to expand the knowledge of underlying mechanisms in order to develop new therapies based on targeting different pathways.

The main CVD events are myocardial infarction (MI) and stroke, both caused by atherosclerosis. An MI occurs when, due to a vicious cycle of lipid accumulation and inflammation, the assembled atherosclerotic lesion in the coronary artery ruptures thereby releasing thrombotic factors, causing formation of a thrombus that can occlude the blood flow. This results in ischemia in distal areas, which can cause damage and death of the myocardial cells, eventually leading to cardiac remodeling and dysfunction.

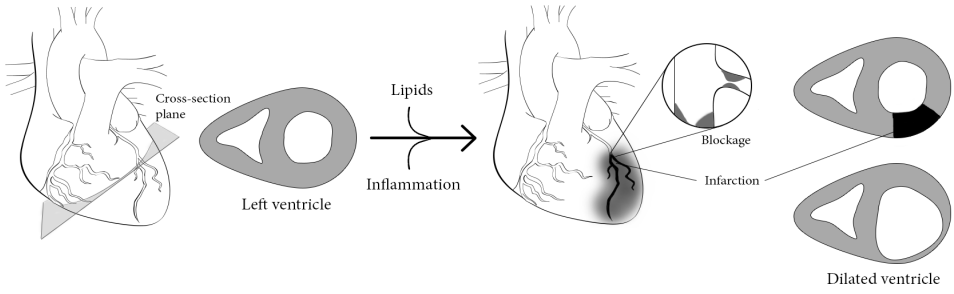

Figure 1 **Schematic representation of the role of inflammation and lipids on cardiac pathophysiology.** In a healthy heart with a normal functioning left ventricle a disturbed lipid metabolism as well as inflammation can contribute to cardiac dysfunction and atherosclerosis. The latter may lead to coronary occlusion and subsequent ischemia or even infarction, finally resulting in a dilated and less functional left ventricle.

The research reported in this thesis investigates the role of inflammation and lipid metabolism in the development of CVD (see figure 1). These two components are of particular interest as each, both individually and collectively, can lead to the onset or maintenance of pathological cardiac conditions. To study the influence of lipids and inflammation on cardiac function, specialized hemodynamic measurements were performed in mice. This chapter offers a general introduction to heart physiology and pathophysiology as well as to lipids and inflammation, two effectors of CVD that are both related to metabolic dysfunction.

Physiology

Heart function

Basal heart function

A well-functioning heart is essential for life as it pumps oxygen-rich blood with life-maintaining nutrients via the circulation to every part of the body. The blood flow originates by the coordinated contraction of the four chambers of the heart; two superior atria and two inferior ventricles. Via the right-sided cardiac chambers deoxygenated blood is pumped into the pulmonary circulation where it is enriched with oxygen. The left chambers of the heart pump blood into the systemic circuit. When left ventricular pressure is plotted as a function of its instantaneous volume, a pressure-volume loop (PV-loop) is generated, describing the function of the left ventricle (LV) during the different phases of one contractile cycle. These include a: filling phase, isovolumic contraction, ejection phase and isovolumic relaxation (see figure 2; upper panel).

The first phase in the cardiac cycle is passive filling of the LV (A), when blood flows from the atrium to the ventricle as a result of the atrial-ventricular pressure gradient. A second active ventricular filling is established by atrial contraction thereby increasing the atrial pressure and thus re-establishing a pressure gradient between the atrium and ventricle. The end-diastole (B), is the point where the ventricular volume is maximal, just prior to activation of the myocardium. Then isovolumic contraction takes place (C). After mitral valve closing, the ventricular chamber gradually develops sufficient pressure that exceeds the pressure in the aorta, thereby opening the aortic valve (D), followed by active ejection of the blood from the ventricular chamber into the aorta (E). Once the LV pressure drops below the aortic pressure the aortic valve closes as a result (F). This is described as the end-systolic point, with the lowest ventricular volume and a high ventricular pressure. During the subsequent isovolumic relaxation period (G) the ventricle muscle relaxes. When the LV pressure falls below atrial pressure the mitral valve opens (H), thereby starting the filling phase of the LV. From this loop a range of indices can be derived characterizing systolic and diastolic function of the LV and general hemodynamic indices (figure 2; middle and lower panel).

The following parameters can be obtained from PV-loops (figure 2):

Systolic function:

- end-systolic pressure (ESP): pressure in the ventricle at the end of systole, approximates mean arterial blood pressure
- end-systolic volume (ESV): blood volume remaining in the ventricle at end of systole (normally approximately the end of ejection)
- ejection fraction (EF; calculated as [EDV-ESV]/EDV): fraction of blood ejected from a ventricle per heartbeat, under normal circumstances ejection fraction is >60%
- dP/dt_{MAX}: maximum rate of pressure change in the LV, characterizing cardiac contractility
- end-systolic elastance (E_{ES}): the slope of the end-systolic pressure-volume relation (ESPVR). An increased slope as well as a leftward shift of the ESPVR indicates an increase in contractility

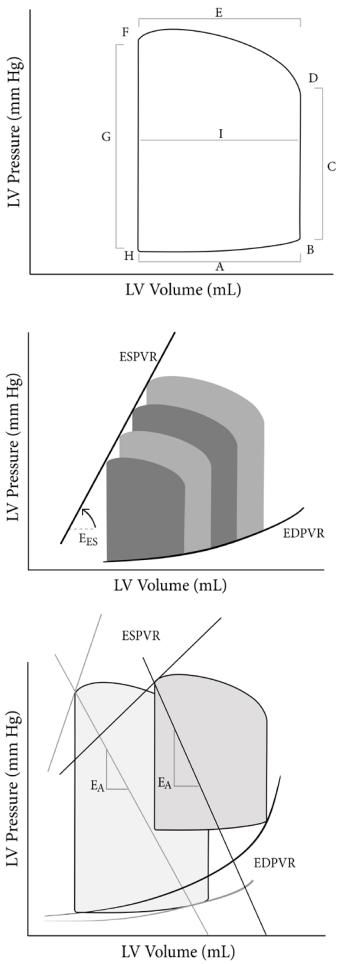

Figure 2 **Illustrations of left ventricular PV-loops.**

Upper panel: PV-loop of a regular cardiac cycle; see text for comprehensive explanation.

Middle panel: Calculations of end-systolic pressure–volume relation (ESPVR) and end-diastolic pressure–volume relation (EDPVR). A cluster of PV-loops under different loading conditions reveals the ESPVR and the EDPVR. The slope of the ESPVR indicates the end-systolic elastance (E_{ES}).

Lower panel: Illustration of a PV-loop from a dilated and failing left ventricle. A decrease in contractility is indicated by a decreased slope and a rightward shift of the ESPVR. The end-diastolic stiffness has increased indicated by the slope of the EDPVR. The left ventricular distensibility has decreased indicated by the upward shift of the EDPVR. Furthermore, LV performance has decreased indicated by decrease in the ventricular-arterial coupling ratio (E_{ES}/E_A). ESPVR, end-systolic pressure-volume relation; EDPVR, end-diastolic pressure-volume relation; E_A, effective arterial elastance; LV, left ventricle.

Diastolic function:

- end-diastolic pressure (EDP): pressure in a ventricle at the end of diastole, a measure of cardiac preload
- end-diastolic volume (EDV): blood volume at end of diastole at maximal stretch of cardiomyocytes prior to contraction (measure of preload)
- Tau: time constant of isovolumic exponential pressure decay during relaxation, measurement of LV relaxation
- $-dP/dt_{MIN}$: minimal rate of pressure change in the LV
- end-diastolic elastance (E_{ED}): the slope of the end-diastolic pressure-volume relation (EDPVR), representing the diastolic stiffness of the ventricle

General function:

- heart rate (HR): number of heart beats per minute
- stroke volume (SV; calculated as EDV-ESV): volume of blood ejected from a ventricle at each heartbeat, during heart failure stroke volume usually decreased or maintained only at the expenses of substantially increased filling pressure
- cardiac output (CO; calculated as HRxSV): total blood volume expelled by a ventricle per minute
- stroke work (SW): external work performed by the ventricle by ejecting stroke volume, represented by the area within the PV-loop
- effective arterial elastance (E_A; calculated as ESP/SV): index for afterload, load that the heart must eject blood against
- E_{ES}/E_A: ventricular-arterial coupling ratio, describes the coupling between LV performance and the systemic arterial system. Normal coupling ratio is approximately 1, the values decreases with heart failure

Assessment of left ventricular function in mice

Humans and mice display a 99% gene similarity[5], making mice suitable models for studying the function of human genes in health and disease. In addition, mice and rats are the most commonly used species for basic animal studies, as the understanding of their biology and genetics is well developed, breeding and housing are relatively inexpensive and a large number of specifically designed tools and techniques exist for this very purpose.

To reach the objectives of the current research program, functional assessment of the heart is essential. Considering the small size of the mouse heart and the high heart rate (approximately 500 beats per minute), highly specialized techniques are required to assess hemodynamic and ventricular function in the intact mouse. Magnetic resonance imaging (MRI), echocardiography and invasive PV-loop measurements have become available for cardiac phenotyping of small animals.

In this thesis, PV-loops by conductance catheter and transthoracic echocardiography were used to acquire cardiac function data. PV-loops are considered the gold standard in hemodynamic measurement, as they provide a direct volume signal and by combining these with LV pressure, pressure volume-relations can be obtained.[6] In addition, the pressure volume-relations yield very sensitive and load-independent indices. A disadvantage is that PV-loop measurements are highly invasive as the catheter is inserted in the right carotid artery and positioned into the LV. As a result, these measurements are routinely performed in mice as study ending. In contrast, echocardiography is a safe and non-invasive measurement and is one of the most widely used imaging tools in cardiology.[7, 8] It can be used relatively easy to obtain two dimensional movies and provides valuable information about cardiac chamber shape and size and allows tissue damage visualization.

Metabolism of the heart

Energy supply to the heart

Continuous contraction and relaxation of the heart results in a high energy demand by this organ. However, the heart has almost no internal energy reserves and thus has to produce energy (as adenosine triphosphate (ATP)) to maintain contractile function. Under normal conditions the heart preferably oxidizes fatty acids (FA), generating 70% of the cardiac energy demand. The remainder is covered by utilization of glucose (20-30%), lactate and ketones.[9] If necessary, the heart can shift its substrate utilization preferences during changed substrate availability and certain pathological conditions.[10] As *de novo* synthesis of FAs is low in heart tissue, the majority of FAs is derived from the circulation. FA uptake occurs via passive diffusion or via FA transporters (CD36/FATP)[11] by the cardiomyocytes which represent 75% of the cardiac cells and are the main site for fat oxidation.[12] After several modification steps FAs undergo β-oxidation yielding acetyl CoA, which subsequently enters the Krebs cycle and result in nicotinamide adenine dinucleotide hydrogen (NADH) and flavin adenine dinucleotide hydrogen ($FADH_2$) production, which are both used by the electron transport chain to generate ATP. Glucose is taken up via the glucose transporter (GLUT) and converted via the glycolysis pathway to acetyl CoA. Similar to FA derived Acetyl CoA, glucose derived Acetyl CoA is further processed in the Krebs cycle and electron transport chain. Since glucose utilization results in less production of ATP per carbon molecule, FAs are the preferred substrate in the aerobic heart.

Oxygen supply to the heart

To maintain adequate ATP concentrations in the heart, aerobic production of ATP is necessary since insufficient energy is produced in anaerobic conditions. Consequently, a constant supply of oxygen is essential to sustain cardiac function and viability.[13] The heart consumes large amounts of oxygen, especially compared to other organs. Under basal conditions the heart uses ~5–10 mL O_2/min/100g tissue, which can increase to more than ~70 mL O_2/min/100g myocardial tissue during heavy exercise. This is significantly

more than that consumed by the brain (~4 mL O_2/min/100g tissue) or skeletal muscle (~0.2 mL O_2/min/100 g) tissue under basal conditions.[14]

Adequate cardiac oxygen supply is achieved via the coronary circulation, as the myocardium itself is too thick to allow direct oxygen delivery from the chambers. Blockage of a coronary artery, for example by thrombus formation, therefore has major implications for the oxygen supply to the surrounding myocardium.

Pathophysiology

Atherosclerosis

Atherosclerosis is a complex, chronic and progressive inflammatory disorder which is characterized by thickening and hardening of medium-sized and larger arteries. Lipids, smooth muscle cells (SMC) and immune cells inside the vessel wall accumulate, resulting in narrowing of the blood vessel. Rupture of an advanced atherosclerotic lesion can lead to an MI, one of the most common causes of death in the Western world.[15]

The first step in the development of atherosclerosis is endothelial dysfunction, which has an impact on the cellular structure and function of the endothelium. Dysfunction can, among others, be caused by hypercholesterolemia, cigarette smoking, hypertension, diabetes mellitus or infections.[15, 16] As a consequence of the endothelial dysfunction, the vessel wall expresses adhesion molecules, such as vascular cell adhesion molecule (VCAM)-1, intercellular adhesion molecule (ICAM)-1 and E-selectin. Leukocytes, like monocytes and T-cells are attracted from the circulation by adhesion molecules and migrate through the endothelial layer into the intima via monocyte chemoattractant protein-1 (MCP-1).[17, 18] Monocytes differentiate into macrophages upon migration into the sub-endothelial space, where the macrophages start to ingest modified lipids, resulting in lipid-rich macrophages or foam cells. The foam cells excrete cytokines and chemokines that attract and activate additional immune cells, thereby amplifying the intralesional inflammatory response.[19] Lesions consisting of macrophage foam cells and T-cells are the earliest type of lesions, the so-called fatty streak. However, these lesions do not result in clinical symptoms.[20] At this stage the development of the lesion is still reversible, since cholesterol can be exported to cholesterol acceptors as high density lipoprotein (HDL) and lipid-poor apoA1 via cholesterol transporters like ATP-binding cassette transporter A1 (ABCA1).[15] Inflammatory stimuli activate SMC to migrate into the intima leading to the formation of an advanced lesion.[16, 20] In the lesion SMC are able to take up cholesterol and thereby contributing to the foam cell formation. Furthermore, they secrete extracellular matrix components like elastin and collagen which form an elastic fibrous cap covering the lesion. This cap forms a barrier between the circulating blood on one side and the content of the lesion on the other side, consisting of a core of extracellular lipid, necrotic material derived from death foam cells, macrophages, SMC, T-cells and other inflammatory cells.[16]

The lesion stability depends on the thickness of the fibrous cap and on the lesion composition. Matrix metalloproteinases, produced by foam cells, degrade the extracellular matrix, thereby reducing the stability of the atherosclerotic lesion.[20] In addition, a large number of macrophages and a relative high lipid content of the lesion also diminish the stability. Lesion instability can lead to rupture, thereby releasing pro-thrombotic material into the bloodstream which triggers thrombus formation. This can result in an occlusion of a blood vessel which may lead to an MI or stroke.

It is important to emphasize that atherosclerotic lesions in mice are not prone to rupture, although mouse lesions resemble human lesions in several aspects. As a consequence, atherosclerotic mouse models do not develop MIs and in order to study the effects of an MI an alternative intervention is required. The model of permanent ligation of the left anterior descending (LAD) artery is often used to induce MI in mice as well as the ischemia/reperfusion model.[21]

Myocardial infarctions

Occlusion of a coronary artery interrupts the blood flow towards the downstream myocardial tissue, causing ischemia and initiating tissue damage and starvation. Damage can be reduced by timely reperfusion of the tissue, which is the preferred clinical therapy after an MI. Prolonged occlusion of the coronary arteries initiates a slow cascade of events which transforms the endangered zone in order to maintain cardiac output.[22] This process is usually completed in 6 to 8 weeks in humans and is referred to as infarct healing or LV remodeling.

Infarct healing can be divided into three, somewhat overlapping, stages: inflammation, proliferation and maturation.[23] In the first stage apoptosis occurs, which is a major contributor to cardiomyocyte loss.[24] Subsequently, danger signals are released by the necrotic cardiomyocyte, thereby activating the innate immune mechanism, e.g. complement system and Toll-like receptors (TLR), causing an intense inflammatory response.[25, 26] Chemokines and cytokines are released, resulting in leukocyte infiltration and clearance of necrotic cells and debris in the infarcted zone. After approximately 3 days the acute inflammatory response diminishes, marking the onset of the next stage. Concomitantly, activated macrophages produce growth factors and cytokines leading to the formation of granulation tissue which replaces the dead cardiomyocytes.[25] Proliferation of fibroblasts deposits a network of extracellular matrix and collagen, thereby strengthening the wound.[27] Furthermore, neovascularization realizes renewed blood supply to the infarcted area, via new vessels derived from pre-existing blood vessels or from migrating endothelial cells.[28] As repair proceeds, in the maturation stage, fibroblasts undergo apoptosis and a collagen-rich scar is formed.

The ischemic inflammatory response is a critical factor in the balance between cardiac repair and adverse LV remodeling. Experimental models suggest that prolonged or expanded inflammation or a non-controlled infarct healing result in adverse remodeling of the infarcted heart.[29, 30] For instance, both TLR2 and TLR4 have shown to play an unfavorable role in LV remodeling, since disrupted TLR4 signaling prevents adverse remodeling and TLR2 inhibition reduces ischemia/reperfusion injury and improves

cardiac function.[31-33] Although morbidity after an MI is decreasing due to improved reperfusion strategies and medical therapy, 5-year morbidity remains high. Therefore, strategies to interfere with inflammatory pathways after MI are intensively studied.

Metabolic dysfunction

Lipid metabolism

FAs are preferentially used as energy source by the heart and derive from our diet or are produced *de novo* in the liver. Since FAs themselves are cytotoxic, they are transported through the circulation either bound to serum albumin or incorporated as triglycerides (TG) in lipoproteins. TG-derived FAs are also a main source of energy for activity of skeletal muscle, for heat production by brown adipose tissue or for storage in white adipose tissue (WAT) for usage at a later point in time. In addition to TGs, cholesterol is also an essential lipid for many of our body's functions. Cholesterol is of critical importance for maintenance of cellular membranes and serves as a precursor for steroid hormone and bile acid synthesis.[34, 35]

Lipids are insoluble in an aqueous environment like blood, therefore they are transported in the circulation in water-soluble spherical particles called lipoproteins. Lipoproteins consist of a lipid-rich core of neutral lipids containing TGs and cholesteryl esters (CE), surrounded by a single layer of phospholipids (PL), free cholesterol and proteins called apolipoproteins. The latter are necessary for lipoprotein formation, modulation of enzymes and proteins, and act as ligands for receptor-mediated binding.

Based on their composition and size, lipoproteins can be divided in several subclasses: chylomicrons, very low-density lipoproteins (VLDL), intermediate-density lipoproteins (IDL), low-density lipoproteins (LDL) and high-density lipoproteins (HDL).[36] The two particles with the lowest density, chylomicrons and VLDL, contain mainly TGs, whereas LDL and HDL particles mainly transport cholesterol in the form of CE. The metabolism of these lipoproteins and the subsequent distribution and cellular processing of TG-derived FA is described in the following sections and a schematic overview is depicted in figure 3.

After a meal, in the postprandial state, dietary TGs are lipolyzed by pancreatic lipases into 2-monoacylglycerol and FA. Together with dietary cholesterol these components are taken up by the intestinal cells and assembled into chylomicrons. These particles are transported from the lymph to the blood circulation, where TG in the core of the particle is hydrolyzed into glycerol and FA by endothelium-bound lipoprotein lipase (LPL).[37] FAs are taken up by the underlying peripheral tissue as an energy source for activity, thermogenesis or for storage.[38] The chylomicron-remnant particles, which are relatively enriched in CE and apolipoprotein E (apoE), are removed from the circulation by the liver e.g. via recognition of apoE by the LDL receptor (LDLr) and the LDLr-related (LRP).[39] Since remnant clearance results in the uptake of dietary cholesterol by the liver, it is clear that the liver plays a central role in cholesterol metabolism.

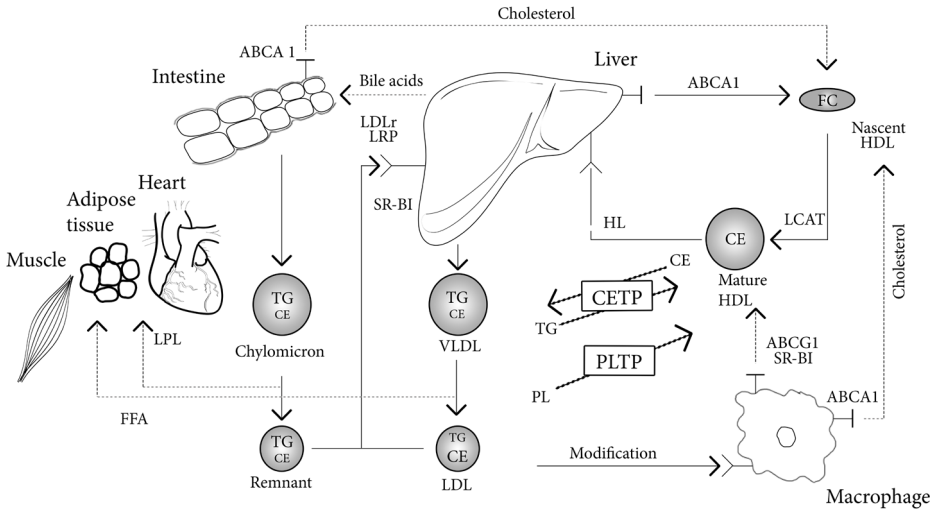

Figure 3 **Schematic representation of lipoprotein metabolism.** See text for explanation. ABCA1, ATP-binding casette transporter A1; ABCG1, ATP-binding casette transporter G1; CE, cholesteryl ester; CETP, cholesteryl ester transfer protein; FFA, free fatty acids; HDL, high density lipoprotein; HL, hepatic lipase; LCAT, lechitin-cholesterol acyltransferase; LDL, low density lipoprotein; LDLr, LDL receptor; LPL, lipoprotein lipase; LRP, LDLr related protein; PL, phospholipid; PLTP, phospholipid transfer protein; SR-B1, scavenger receptor B1; TG, triglycerides; VLDL, very low density lipoprotein

In the fasted state no food is taken up in the intestines and the body's energy supply rely on the production of TG-rich VLDL particles by the liver. These TG-rich VLDL particles serve as main donor of TG-derived FA for extrahepatic tissues. Cholesterol and FA, derived from WAT or *de novo* synthesis, are packed as TG into VLDL particles in the hepatocytes of the liver.[40] They are secreted into the circulation and, similarly to chylomicrons, the core TGs are hydrolyzed by LPL. The depletion of TG from the VLDL particle results in the formation of VLDL remnants. These remnant particles are partly cleared by the liver, while the remaining particles undergo further lipolysis that results in the formation of LDL particles. LDL particles are relatively enriched in CE as compared to TG and apolipoprotein B (apoB) is its primary apolipoprotein. The majority of LDL particles are taken up from the plasma by the LDLr, while the remainder is taken up by extrahepatic tissues where the CE are used for e.g. maintenance of cellular membranes. High levels of apoB-containing lipoproteins (VLDL, VLDL remnants and LDL) can lead to deposition of these lipoproteins in the vessel wall, where they are modified and taken up by macrophages. This is the initial step of atherosclerosis development.

In contrast to apoB-containing lipoproteins, HDL is generally believed to have anti-atherogenic properties. This is attributed to its involvement in reverse cholesterol transport (RCT). In RCT, excessive cholesterol from the periphery is transported via the plasma to the liver. In the liver, HDL-derived cholesterol can be recycled or converted to degradation products like bile acids which are excreted via the bile into the intestine and feces. ApoA1, the major HDL apolipoprotein, is synthesized in the

liver and the intestine and is secreted into the plasma in complex with PL.[41] The apoA1-rich nascent HDL particle is subsequently further lipidated with PL and cholesterol from peripheral cells, through the involvement of the cholesterol transporter protein ABCA1. The initial lipidation of HDL via ABCA1 is a crucial step in HDL formation since patients with ABCA1 gene mutations as well as mice lacking ABCA1 have very low HDL levels.[42,43] The acquired cholesterol is esterified by lecithin-cholesterol acyl transferase (LCAT) generating spherical mature HDL. This mature particle can take up PL from chylomicrons and VLDL particles, via interaction with the phospholipid transfer protein (PLTP). In addition, loading with cholesterol from the periphery can occur via Scavenger Receptor B1 (SR-B1) and/or another ABC-transporter, ABCG1. The accumulated CE are stored in the core of the HDL particle and these CE can be taken up directly by the liver via SR-B1.[41] Indirect uptake of CE can take place after exchange of CE from HDL with TGs from apoB-containing lipoproteins and this transport is facilitated by the cholesteryl ester transfer protein (CETP).[44] Importantly, CETP is not expressed in rodents, except for hamsters, and therefore in mice there is no bidirectional exchange of CE and TG between HDL and (V)LDL.

Cholesterol and triglycerides as risk factors for CVD

Numerous clinical studies have shown that both elevated LDL-cholesterol levels and low HDL-cholesterol levels correlate with an increased CVD risk.[45-48] Several anti-atherogenic drugs have been developed aimed at reduction of LDL-cholesterol levels in plasma. Statins (or HMG-CoA reductase inhibitors) are the most widely used drugs that efficiently lower plasma (V)LDL-cholesterol levels, leading to a decreased cardiovascular morbidity and mortality.[49] However, a substantial residual cardiovascular risk remains, thereby indicating that additional treatment is required.[47, 50] One of the experimental strategies aims at increasing the anti-atherogenic HDL-cholesterol concentration. It is thought that the removal of excess cholesterol from macrophages and foam cells by HDL is one of the important mechanisms underlying the atheroprotective property of HDL. Increase in HDL levels can be achieved through inhibition of CETP. As described above, CETP facilitates the transfer of CE from HDL to (V)LDL in exchange for TGs. Via this mechanism, cholesterol in the anti-atherogenic HDL particles is lowered whereas it is increased in the atherogenic (V)LDL particles. Lowering CETP activity can be achieved by using drugs such as anacetrapip and niacin.[51, 52]

In addition to cholesterol, elevated levels of plasma TGs, known as hypertriglyceridemia, are also associated with an increased risk for CVD. It has been debated to which extent TG independently promote CVD risk[53]. Previous population studies showed that high TG levels are inversely related with HDL-cholesterol levels. Thus, an adjustment of HDL-cholesterol attenuates the relationship between TG and CVD. Nevertheless many clinical studies provided evidence that increased TG levels act as an independent risk factor.[54-57]

Ectopic fat deposition

In a healthy person, FA that are not directly used as energy source, are stored in WAT for usage at a later point in time. Through a tightly regulated process only a small portion

of FAs are directed for storage to non-adipose tissue such as liver, pancreas, skeletal muscle, kidney and heart.[58] Despite the ability of WAT to increase adipocyte cell size (hypertrophy) as well as cellular number (hyperplasia), the expandability of WAT is limited, particularly when the FA flux is increased over a long period of time.[59] As a result, transportation of FAs towards the non-adipose tissue will be increased, leading to ectopic fat accumulation. While limited ectopic FA accumulation may be physiological, in pathological conditions, excess ectopic fat may disrupt cellular function probably via toxic intermediary metabolites like ceramides and diacylglycerol. This is believed to contribute to insulin resistance, non-alcoholic hepatosteatitis (NASH) or heart dysfunction.[60, 61]

Metabolic inflammation and the innate immune system

Although the exact molecular mechanisms responsible for the activation of inflammatory pathways in obesity are still poorly understood, both adipose tissue and the liver are thought to be involved in the onset and development of metabolic inflammation. In obese subjects, expanded adipocytes secrete chemokines and cytokines, including tumor necrosis factor alpha (TNFα) and monocyte chemotactic protein-1 (MCP-1), resulting in the recruitment and activation of macrophages.[62] These pro-inflammatory macrophages in turn produce large amounts of TNFα and interleukine-1ß thereby providing a negative feedback loop and further amplification of the inflammation.[63] Similar to adipose tissue, the liver also becomes inflamed during obesity, which is reflected by an increase in hepatic inflammation markers such as serum amyloid A and C-reactive protein and nuclear factor κB (NF-κB) activation in high-fat diet fed mice.[64, 65] In general, the consequent chronic low-grade systemic inflammation increases the risk for associated inflammatory diseases like atherosclerosis and type 2 diabetes mellitus.

TLRs, which are part of the innate immune system, are suggested to play an important role in the development of obesity, insulin resistance and atherosclerosis.[66-68] Several studies demonstrated that saturated FAs exert pro-inflammatory effects through these receptors, particularly via the subtypes TLR2 and TLR4. TLRs are pattern-recognition receptors (PRRs) and are predominantly expressed on immune cells, like macrophages and dendritic cells, but have also been identified on non-immune cells such as adipocytes and cardiomyocytes. TLRs, of which 12 different types have been identified thus far, are expressed on the cell surface or in intracellular compartments.[69] These PRRs detect microbial components and 'danger' signals released by injured host cells, thereby activating the immune system as a first line of defense.[70] In mammals, ligand recognition by TLRs leads to recruitment of cytoplasmic myeloid differentiation factor (MyD)88, a universal TLR adaptor protein. MyD88 recruits proteins of the IRAK family and TRAF6, resulting in the phosphorylation and activation of the IKK complex. Finally, this process causes translocation of NFκB to the nucleus and the transcription of pro-inflammatory cytokines (figure 4).[71]

It is interesting to note that medium-chain FAs might serve as exogenous ligands for TLR2 and TLR4, provoking a nutritionally or metabolically induced inflammatory response.[72, 73] The lipoid structures in bacterial membranes recognized by TLR2 (lipoteichoic acid,

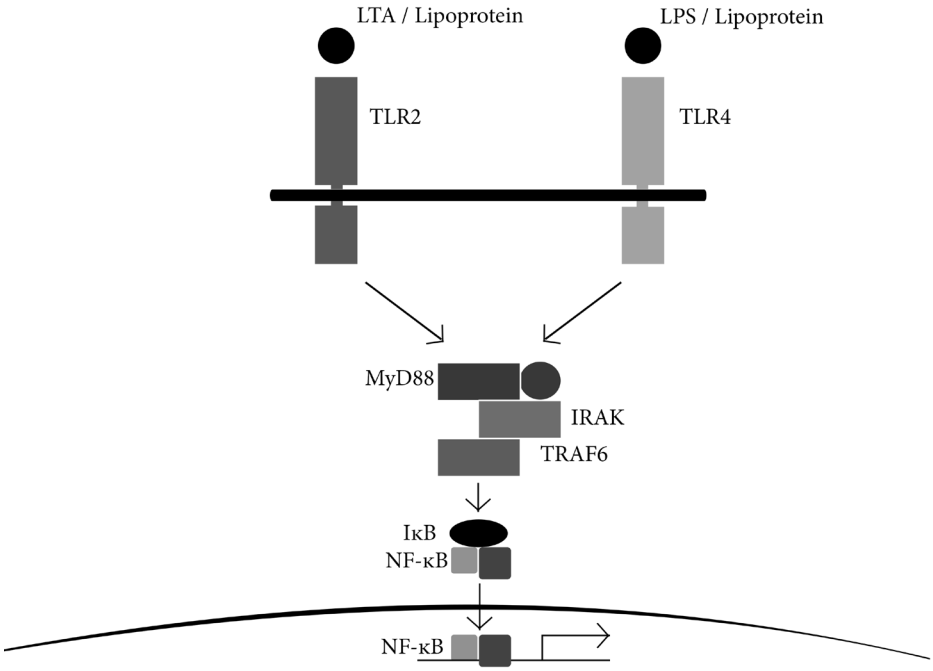

Figure 4 **TLR2 and TLR4 mediated signaling pathway.** Ligand recognition by TLR2 or TLR4 leads to the activation of MyD88 and the IRAK family, which in turn activates TRAF6. This results subsequently in the phosphorylation and activation of the IKK complex allowing NFκB to translocate into the nucleus. LTA, lipoteichoic acid; LPS, lipopolysaccharide,; IRAK, Interleukin-1 receptor-associated kinase; TRAF6, TNF receptor associated factor 6; IKK, IκB kinase.

(LTA)) and TLR4 (lipopolysacharide, (LPS)) share homology with endogenous lipids. Consequently, those TLRs can be activated by endogenous lipids and lipoproteins[74], including oxidized LDL[75], medium-chain FA component of LPS, as well as saturated FA.[76] In vivo animal experiments demonstrated that inhibition of TLR4 in mice resulted in protection from acute infused lipid induced insulin resistance[73], and also protection against diet-induced obesity has been reported.[68, 77] Similar findings, including improved insulin sensitivity[78] protection against died-induced adiposity and hepatic steatosis[79], are reported for TLR2 knock-out models. Furthermore, deletion of TLR2 or TLR4 reduces atherosclerotic lesion development in murine models.[80, 81]

Outline of thesis

The studies in this thesis are performed to provide additional and improved insight into the effects and interplay of dietary lipids and metabolic inflammation on cardiac performance in the presence or absence of atherosclerosis and myocardial infarctions. All studies are performed in mice and during the beginning of this PhD project little was known about the effect of gender on the relationship between diet-induced obesity, lipid metabolism and cardiac function in mice. Therefore, the effects of LV function after intermediate and long-term high-fat diet feeding in male and female mice are studied in **Chapter 2**. Subsequently, in **Chapter 3** the question is addressed if high-fat diet feeding results in more severe cardiac dysfunction after an MI, due to an increased inflammatory response induced by the dietary lipids, as compared to low-fat diet feeding. **Chapter 4** also examines effects after an MI, as the role of ABCA1 after an infarction is studied. **Chapter 5** focuses on the role of RP105, the physiological inhibitor of TLR4-signalling, in the process of LV remodeling after an MI. These effects are studied to investigate the role of TLR4 in cardiac function after an infarction. In addition, **Chapter 6** reports on the direct effects of TLR2 and TLR4 deficiency on cardiac function after high-fat diet feeding. In **Chapter 7**, it is investigated whether treatment with the LDL lowering drug simvastatin, in combination with the HDL raising drug niacin, leads to beneficial effects regarding plasma lipids and atherosclerotic development. **Chapter 8** provides a summary of the results obtained from the studies and discusses their implications.

References

1 http://www.hartstichting.nl/9800/13341/15305/HVZ_in_Nederland_2010. 2012. Internet Communication

2 http://www.who.int/mediacentre/factsheets/fs317/en/index.html. 2012. Internet Communication

3 Lusis AJ. Atherosclerosis. *Nature* 2000 September 14;407(6801):233-41.

4 Perk J, De BG, Gohlke H et al. European Guidelines on cardiovascular disease prevention in clinical practice (version 2012). The Fifth Joint Task Force of the European Society of Cardiology and Other Societies on Cardiovascular Disease Prevention in Clinical Practice (constituted by representatives of nine societies and by invited experts). Developed with the special contribution of the European Association for Cardiovascular Prevention & Rehabilitation (EACPR). *Eur Heart J* 2012 July;33(13):1635-701.

5 Lander ES, Linton LM, Birren B et al. Initial sequencing and analysis of the human genome. *Nature* 2001 February 15;409(6822):860-921.

6 Borlaug BA, Kass DA. Invasive hemodynamic assessment in heart failure. *Cardiol Clin* 2011 May;29(2):269-80.

7 Lu X, Xie M, Tomberlin D et al. How accurately, reproducibly, and efficiently can we measure left ventricular indices using M-mode, 2-dimensional, and 3-dimensional echocardiography in children? *Am Heart J* 2008 May;155(5):946-53.

8 Morgan EE, Faulx MD, McElfresh TA et al. Validation of echocardiographic methods for assessing left ventricular dysfunction in rats with myocardial infarction. *Am J Physiol Heart Circ Physiol* 2004 November;287(5):H2049-H2053.

9 Taegtmeyer H, Hems R, Krebs HA. Utilization of energy-providing substrates in the isolated working rat heart. *Biochem J* 1980 March 15;186(3):701-11.

10 Lopaschuk GD, Ussher JR, Folmes CD, Jaswal JS, Stanley WC. Myocardial fatty acid metabolism in health and disease. *Physiol Rev* 2010 January;90(1):207-58.

11 Glatz JF, Luiken JJ, Bonen A. Membrane fatty acid transporters as regulators of lipid metabolism: implications for metabolic disease. *Physiol Rev* 2010 January;90(1):367-417.

12 Stanley WC, Recchia FA, Lopaschuk GD. Myocardial substrate metabolism in the normal and failing heart. *Physiol Rev* 2005 July;85(3):1093-129.

13 Giordano FJ. Oxygen, oxidative stress, hypoxia, and heart failure. *J Clin Invest* 2005 March;115(3):500-8.

14 Henning R.J., Olsson R.A. Coronary Blood Flow and Myocardial Ischemia. *Essentials of cardiology, Principles and Practice.* Second ed. 2006. p. 439-49.

15 Glass CK, Witztum JL. Atherosclerosis. the road ahead. *Cell* 2001 February 23;104(4):503-16.

16 Ross R. Atherosclerosis--an inflammatory disease. *N Engl J Med* 1999 January 14;340(2):115-26.

17 Cybulsky MI, Gimbrone MA, Jr. Endothelial expression of a mononuclear leukocyte adhesion molecule during atherogenesis. *Science* 1991 February 15;251(4995):788-91.

18 Springer TA. Traffic signals for lymphocyte recirculation and leukocyte emigration: the multistep paradigm. *Cell* 1994 January 28;76(2):301-14.

19 Hansson GK. Immune mechanisms in atherosclerosis. *Arterioscler Thromb Vasc Biol* 2001 December;21(12):1876-90.

20 Hansson GK. Inflammation, atherosclerosis, and coronary artery disease. *N Engl J Med* 2005 April 21;352(16):1685-95.

21 Vandervelde S, van Amerongen MJ, Tio RA, Petersen AH, van Luyn MJ, Harmsen MC. Increased inflammatory response and neovascularization in reperfused vs. non-reperfused murine myocardial infarction. *Cardiovasc Pathol* 2006 March;15(2):83-90.

22 Lewis EF, Moye LA, Rouleau JL et al. Predictors of late development of heart failure in stable survivors of myocardial infarction: the CARE study. *J Am Coll Cardiol* 2003 October 15;42(8):1446-53.

23 Frangogiannis NG. The mechanistic basis of infarct healing. *Antioxid Redox Signal* 2006 November;8(11-12):1907-39.

24 Haunstetter A, Izumo S. Apoptosis: basic mechanisms and implications for cardiovascular disease. *Circ Res* 1998 June 15;82(11):1111-29.

25 Cleutjens JP, Blankesteijn WM, Daemen MJ, Smits JF. The infarcted myocardium: simply dead tissue, or a lively target for therapeutic interventions. *Cardiovasc Res* 1999 November;44(2):232-41.

26 Wang Y, Abarbanell AM, Herrmann JL et al. Toll-like receptor signaling pathways and the evidence linking toll-like receptor signaling to cardiac ischemia/reperfusion injury. *Shock* 2010 December;34(6):548-57.

27 Bishop JE, Laurent GJ. Collagen turnover and its regulation in the normal and hypertrophying heart. *Eur Heart J* 1995 May;16 Suppl C:38-44.

28 Nelissen-Vrancken HJ, Debets JJ, Snoeckx LH, Daemen MJ, Smits JF. Time-related normalization of maximal coronary flow in isolated perfused hearts of rats with myocardial infarction. *Circulation* 1996 January 15;93(2):349-55.

29 Dobaczewski M, Xia Y, Bujak M, Gonzalez-Quesada C, Frangogiannis NG. CCR5 signaling suppresses inflammation and reduces adverse remodeling of the infarcted heart, mediating recruitment of regulatory T cells. *Am J Pathol* 2010 May;176(5):2177-87.

30 Huebener P, Abou-Khamis T, Zymek P et al. CD44 is critically involved in infarct healing by regulating the inflammatory and fibrotic response. *J Immunol* 2008 February 15;180(4):2625-33.

31 Arslan F, Smeets MB, O'Neill LA et al. Myocardial ischemia/reperfusion injury is mediated by leukocytic toll-like receptor-2 and reduced by systemic administration of a novel anti-toll-like receptor-2 antibody. *Circulation* 2010 January 5;121(1):80-90.

32 Arslan F, Keogh B, McGuirk P, Parker AE. TLR2 and TLR4 in ischemia reperfusion injury. *Mediators Inflamm* 2010;2010:704202.

33 Timmers L, Sluijter JP, van Keulen JK et al. Toll-like receptor 4 mediates maladaptive left ventricular remodeling and impairs cardiac function after myocardial infarction. *Circ Res* 2008 February 1;102(2):257-64.

34 Mu H, Porsgaard T. The metabolism of structured triacylglycerols. *Prog Lipid Res* 2005 November;44(6):430-48.

35 Russell DW. Cholesterol biosynthesis and metabolism. *Cardiovasc Drugs Ther* 1992 April;6(2):103-10.

36 Brown MS, Goldstein JL. A receptor-mediated pathway for cholesterol homeostasis. *Science* 1986 April 4;232(4746):34-47.

37 Goldberg IJ. Lipoprotein lipase and lipolysis: central roles in lipoprotein metabolism and atherogenesis. *J Lipid Res* 1996 April;37(4):693-707.

38 Fielding CJ, Renston JP, Fielding PE. Metabolism of cholesterol-enriched chylomicrons. Catabolism of triglyceride by lipoprotein lipase of perfused heart and adipose tissues. *J Lipid Res* 1978 August;19(6):705-11.

39 Mahley RW, Hui DY, Innerarity TL, Beisiegel U. Chylomicron remnant metabolism. Role of hepatic lipoprotein receptors in mediating uptake. *Arteriosclerosis* 1989 January;9(1 Suppl):I14-I18.

40 Gibbons GF. Assembly and secretion of hepatic very-low-density lipoprotein. *Biochem J* 1990 May 15;268(1):1-13.

41 Rader DJ. Molecular regulation of HDL metabolism and function: implications for novel therapies. J Clin Invest 2006 December;116(12):3090-100.

42 Brooks-Wilson A, Marcil M, Clee SM et al. Mutations in ABC1 in Tangier disease and familial high-density lipoprotein deficiency. *Nat Genet* 1999 August;22(4):336-45.

43 McNeish J, Aiello RJ, Guyot D et al. High density lipoprotein deficiency and foam cell accumulation in mice with targeted disruption of ATP-binding cassette transporter-1. *Proc Natl Acad Sci U S A* 2000 April 11;97(8):4245-50.

44 Tall AR. Plasma high density lipoproteins. Metabolism and relationship to atherogenesis. *J Clin Invest* 1990 August;86(2):379-84.

45 Castelli WP. Cholesterol and lipids in the risk of coronary artery disease--the Framingham Heart Study. *Can J Cardiol* 1988 July;4 Suppl A:5A-10A.

46 Chapman MJ, Assmann G, Fruchart JC, Shepherd J, Sirtori C. Raising high-density lipoprotein cholesterol with reduction of cardiovascular risk: the role of nicotinic acid--a position paper developed by the European Consensus Panel on HDL-C. *Curr Med Res Opin* 2004 August;20(8):1253-68.

47 Cannon CP, Braunwald E, McCabe CH et al. Intensive versus moderate lipid lowering with statins after acute coronary syndromes. *N Engl J Med* 2004 April 8;350(15):1495-504.

48 Yaari S, Goldbourt, Even-Zohar S, Neufeld HN. Associations of serum high density lipoprotein and total cholesterol with total, cardiovascular, and cancer mortality in a 7-year prospective study of 10 000 men. *Lancet* 1981 May 9;1(8228):1011-5.

49 Blumenthal RS, Michos ED. The HALTS trial--halting atherosclerosis or halted too early? *N Engl J Med* 2009 November 26;361(22):2178-80.

50 Taylor AJ, Villines TC, Stanek EJ et al. Extended-release niacin or ezetimibe and carotid intima-media thickness. *N Engl J Med* 2009 November 26;361(22):2113-22.

51 Gurfinkel R, Joy TR. Anacetrapib: hope for CETP inhibitors? *Cardiovasc Ther* 2011 October;29(5):327-39.

52 van der Hoorn JW, de HW, Berbee JF et al. Niacin increases HDL by reducing hepatic expression and plasma levels of cholesteryl ester transfer protein in APOE*3Leiden.CETP mice. *Arterioscler Thromb Vasc Biol* 2008 November;28(11):2016-22.

53 Ginsberg HN. New perspectives on atherogenesis: role of abnormal triglyceride-rich lipoprotein metabolism. *Circulation* 2002 October 15;106(16):2137-42.

54 Bansal S, Buring JE, Rifai N, Mora S, Sacks FM, Ridker PM. Fasting compared with nonfasting triglycerides and risk of cardiovascular events in women. *JAMA* 2007 July 18;298(3):309-16.

55 Miller M, Stone NJ, Ballantyne C et al. Triglycerides and cardiovascular disease: a scientific statement from the American Heart Association. *Circulation* 2011 May 24;123(20):2292-333.

56 Sarwar N, Danesh J, Eiriksdottir G et al. Triglycerides and the risk of coronary heart disease: 10,158 incident cases among 262,525 participants in 29 Western prospective studies. *Circulation* 2007 January 30;115(4):450-8.

57 Hokanson JE, Austin MA. Plasma triglyceride level is a risk factor for cardiovascular disease independent of high-density lipoprotein cholesterol level: a meta-analysis of population-based prospective studies. *J Cardiovasc Risk* 1996 April;3(2):213-9.

58 Slawik M, Vidal-Puig AJ. Adipose tissue expandability and the metabolic syndrome. *Genes Nutr* 2007 October;2(1):41-5.

59 Schaffer JE. Lipotoxicity: when tissues overeat. *Curr Opin Lipidol* 2003 June;14(3):281-7.

60 Sakurai M, Takamura T, Ota T et al. Liver steatosis, but not fibrosis, is associated with insulin resistance in nonalcoholic fatty liver disease. *J Gastroenterol* 2007 April;42(4):312-7.

61 Unger RH, Orci L. Lipotoxic diseases of nonadipose tissues in obesity. *Int J Obes Relat Metab Disord* 2000 November;24 Suppl 4:S28-S32.

62 Hotamisligil GS. Inflammation and metabolic disorders. *Nature* 2006 December 14;444(7121):860-7.

63 Olefsky JM, Glass CK. Macrophages, inflammation, and insulin resistance. *Annu Rev Physiol* 2010;72:219-46.

64 Cai D, Yuan M, Frantz DF et al. Local and systemic insulin resistance resulting from hepatic activation of IKK-beta and NF-kappaB. *Nat Med* 2005 February;11(2):183-90.

65 Peng Y, Rideout D, Rakita S, Lee J, Murr M. Diet-induced obesity associated with steatosis, oxidative stress, and inflammation in liver. *Surg Obes Relat Dis* 2012 January;8(1):73-81.

66 Curtiss LK, Tobias PS. Emerging role of Toll-like receptors in atherosclerosis. *J Lipid Res* 2009 April;50 Suppl:S340-S345.

67 Ehses JA, Meier DT, Wueest S et al. Toll-like receptor 2-deficient mice are protected from insulin resistance and beta cell dysfunction induced by a high-fat diet. *Diabetologia* 2010 August;53(8):1795-806.

68 Tsukumo DM, Carvalho-Filho MA, Carvalheira JB et al. Loss-of-function mutation in Toll-like receptor 4 prevents diet-induced obesity and insulin resistance. *Diabetes* 2007 August;56(8):1986-98.

69 Kawai T, Akira S. Toll-like receptors and their crosstalk with other innate receptors in infection and immunity. *Immunity* 2011 May 27;34(5):637-50.

70 Medzhitov R. Toll-like receptors and innate immunity. *Nat Rev Immunol* 2001 November;1(2):135-45.

71 Kawai T, Akira S. TLR signaling. *Cell Death Differ* 2006 May;13(5):816-25.

72 Nguyen MT, Favelyukis S, Nguyen AK et al. A subpopulation of macrophages infiltrates hypertrophic adipose tissue and is activated by free fatty acids via Toll-like receptors 2 and 4 and JNK-dependent pathways. *J Biol Chem* 2007 November 30;282(48):35279-92.

73 Shi H, Kokoeva MV, Inouye K, Tzameli I, Yin H, Flier JS. TLR4 links innate immunity and fatty acid-induced insulin resistance. *J Clin Invest* 2006 November;116(11):3015-25.

74 Abe Y, Kawakami A, Osaka M et al. Apolipoprotein CIII induces monocyte chemoattractant protein-1 and interleukin 6 expression via Toll-like receptor 2 pathway in mouse adipocytes. *Arterioscler Thromb Vasc Biol* 2010 November;30(11):2242-8.

75 Hansson GK, Libby P. The immune response in atherosclerosis: a double-edged sword. *Nat Rev Immunol* 2006 July;6(7):508-19.

76 Schaeffler A, Gross P, Buettner R et al. Fatty acid-induced induction of Toll-like receptor-4/nuclear factor-kappaB pathway in adipocytes links nutritional signalling with innate immunity. *Immunology* 2009 February;126(2):233-45.

77 Davis JE, Gabler NK, Walker-Daniels J, Spurlock ME. Tlr-4 deficiency selectively protects against obesity induced by diets high in saturated fat. *Obesity* (Silver Spring) 2008 June;16(6):1248-55.

78 Kuo LH, Tsai PJ, Jiang MJ et al. Toll-like receptor 2 deficiency improves insulin sensitivity and hepatic insulin signalling in the mouse. *Diabetologia* 2011 January;54(1):168-79.

79 Himes RW, Smith CW. Tlr2 is critical for diet-induced metabolic syndrome in a murine model. *FASEB J* 2010 March;24(3):731-9.

80 Michelsen KS, Wong MH, Shah PK et al. Lack of Toll-like receptor 4 or myeloid differentiation factor 88 reduces atherosclerosis and alters plaque phenotype in mice deficient in apolipoprotein E. *Proc Natl Acad Sci U S A* 2004 July 20;101(29):10679-84.

81 Mullick AE, Tobias PS, Curtiss LK. Modulation of atherosclerosis in mice by Toll-like receptor 2. *J Clin Invest* 2005 November;115(11):3149-56.

CHAPTER 2

Gender-dependent effects of high-fat lard diet on cardiac function in C57Bl/6J mice

Appl. Physiol. Nutr. Metab. 37: 214–224 (2012)

Mieke C. Louwe[1], José W.A. van der Hoorn[5], Sjoerd A.A. van den Berg[2], J. Wouter Jukema[3], Johannes A. Romijn[1], Ko Willems van Dijk[2], Patrick C.N. Rensen[1], Johannes W.A. Smit[1] and Paul Steendijk[3]

Dept. of [1]General Internal Medicine, Endocrinology and Metabolic Diseases, [2]Human Genetics, [3]Cardiology, Leiden University Medical Center, Leiden, the Netherlands [5]TNO-Metabolic Health Research, Gaubius Laboratory, Leiden, the Netherlands

Gender-dependent effects of high-fat lard diet on cardiac function in C57Bl/6J mice

Abstract

Increased availability of fatty acids released from insulin-resistant adipose tissue may lead to excess fatty acid uptake in nonadipose organs, including the heart. Accumulation of toxic fatty acid intermediates may affect cardiac function. Our aim was to identify to which extent high-fat diet feeding leads to alterations in cardiac function and whether this depends on gender and/or duration of high-fat diet feeding.

Male and female C57Bl/6J mice (n = 8 per group) of 12 to 16 weeks old were fed a low-fat (10% energy) or high-fat (45% energy) lard diet for 6 or 12 weeks. Plasma lipid levels, echocardiography, and left ventricular pressure–volume relationships were obtained at 2, 1, and 0 weeks before termination, respectively.

In both male and female mice, the high-fat diet increased body weight and plasma lipid content. At 10 weeks, significant increases were observed for plasma total cholesterol (males: +44%; females: +86%), phospholipids (+16% and +34%), and triglycerides (+27% and +53%) (all $p < 0.001$). In male mice, but not in female mice, the high-fat diet significantly affected cardiac function at 12 weeks with increased end-systolic volume (25.4 ± 6.2 vs. 17.0 ± 6.7 μL, $p < 0.05$), increased end-systolic pressure (72.1 ± 6.9 vs. 63.6 ± 6.9 mm Hg, $p < 0.01$), and decreased ejection fraction ($61.2\% \pm 4.5\%$ vs. $68.1\% \pm 3.7\%$, $p < 0.01$), indicating reduced systolic function. Multiple linear regression analysis indicated a significant diet–gender interaction for end-systolic volume and ejection fraction.

In conclusion, high-fat diet feeding increased body weight and plasma lipid levels in male and in female mice, but resulted in impairment of cardiac function only in males.

Introduction

A drastic increase in caloric intake combined with lifestyle changes and immobilizing technical innovations have caused an unprecedented epidemic of obesity in the western world. It is assumed that obesity-related heart disease, in combination with diabetes, is predominantly related to coexisting disorders such as coronary artery disease and hypertension.[1, 2] However, studies suggest that increased myocardial lipid deposition, resulting from fatty acid (FA) overload of cardiac myocytes, is directly associated with cardiac dysfunction.[3, 4]

Oxidation of long-chain FAs by mitochondrial β-oxidation supplies most of the energy for the heart under normal conditions.[5] However, the uptake of FAs by the heart in relation to FA oxidation is not always tightly controlled, which may lead to excessive storage of FAs as triglycerides in cardiac myocytes. These myocardial triglyceride stores *per se* are probably inert, but triglycerides are involved in hydrolysis-reesterification cycles, yielding FAs, fatty acyl coenzyme A esters, and diacylglycerol as intermediates. Accumulated cardiac FAs and metabolites are described in several diseases like diabetes and obesity [6-9], as well as in the ischemic and hypertrophic heart [10, 11], and can result in cardiac dysfunction and cell damage.

In humans, gender-dependent differences in myocardial function are reported in certain conditions. For instance, following ischemia, males as compared with females have decreased diastolic function, cardiac contractility, and an increased mortality risk.[12] Furthermore, evidence is accumulating that gender differences also influence metabolic changes of the heart in presence of obesity, insulin resistance, and the related lipotoxicity and cardiac steatosis. Likewise, in animal models of myocardial infarction and hypertension, males are more prone to develop heart failure [13] and detrimental effects of lipotoxicity were shown in rodent models[14].w However, the impact of gender on the effect of lipotoxicity is not fully understood. Earlier, large gender differences have been observed in mice lacking the PPARα receptor, a nuclear receptor controlling lipid utilization. A combination of PPARα-deficiency and pharmacological carnitine palmitoyltransferase (CPT1) inhibition resulted in extreme myocardial lipid accumulation leading to death in 100% of the males but only in 25% of the females.[15] Despite the fact that gender effects are relevant in studies on cardiac pathophysiology, little is known about the effect of gender on the relationship between diet-induced obesity, lipid metabolism, and cardiac function.

Therefore, the aim of our study was to investigate to what extent high-fat diet (HFD) feeding as compared with low-fat diet (LFD) feeding leads to alterations in cardiac function in a widely used C57Bl/6J mouse model, and whether this depends on gender and/or duration of HFD feeding. We used pressure-volume (PV) conductance catheters to obtain accurate assessment of left ventricular performance. This PV-loop method is the gold standard for assessing intrinsic myocardial function in humans and animals.[16] Our data indicate a gender-specific effect of HFD feeding on cardiac function: in particular we observed a more pronounced effect on systolic function in male vs. female mice, despite less pronounced effects on plasma lipids.

Materials and methods

Animals and study protocol

The experiments were performed in 12- to 16-week-old male and female C57Bl/6J mice (Charles River, Maastricht, the Netherlands). Mice were housed in a temperature and humidity-controlled room on a 12-h light / 12-h dark cycle with ad libitum access to water and food. In all animals, the specific diets were started in week 0 and continued throughout the protocol. Body weights were measured weekly. The experimental protocol to study the effects of gender, dietary fat content, and diet duration is shown schematically in figure 1. Briefly, we studied 8 groups of mice (8 animals each). Measurements of plasma lipids, echocardiography, and PV-loops were performed in weeks 4, 5, and 6 (groups 1–4) and in weeks 10, 11, and 12 (groups 5–8), respectively. At the end of the experiments the animals were sacrificed. The protocol was approved by the Animal Ethics Committee from the Leiden University Medical Center and conformed to the Guide for Care and Use of Laboratory Animals (NIH publication no. 85–23, revised 1996).

Diets

Starting in week 0, all animals received either a lard-based LFD or HFD for 6, 10, or 12 weeks. The diets were obtained from Research Diets Inc. (Wijk bij Duurstede, the Netherlands) and supplied ad libitum. As a percentage of the total energy, the LFD contained 10% fat (4.5% lard and 5.5% soy bean oil) and 70% carbohydrate (34.5% energy from sucrose, 32% from corn starch, and 3.5% from maltodextrin). The HFD contained 45% energy from fat (39.5% lard and 5.5% soy bean oil) and 35% carbohydrate (17% energy from sucrose, 8% from corn starch and 10% from maltodextrin).

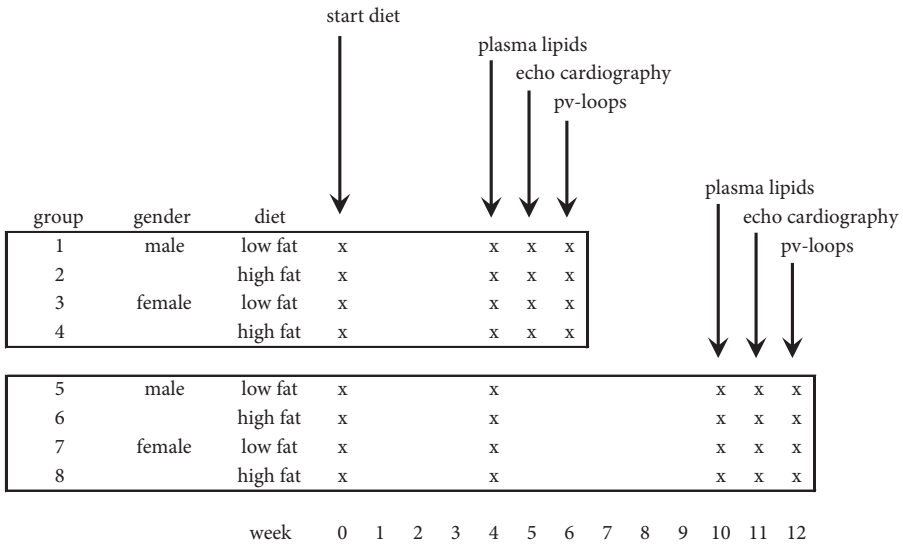

Figure 1 **Schematic study protocol.** See materials and methods for explanation.

Plasma analysis

Blood was sampled after a 4-h fast (09.00 to 13.00 h) via tail vein bleeding and was collected in potassium EDTA coated plastic tubes (Starstedt, Nümbrecht, Germany). Total plasma levels of cholesterol, triglyceride, phospholipid, and glucose were measured by using commercially available kits and standards according to the instructions of the manufacturer (kit no. 1489232, 11488872, and 101140; Roche Diagnostics, Mannheim, Germany; and 2942 Instruchemie, Delfzijl, the Netherlands). Plasma insulin concentrations were determined by ELISA (Crystal Chem Inc., Downers Grove, Ill., USA).

Echocardiography

Transthoracic echocardiography was performed using a VisualSonics Vevo 770 with a 30 MHz ultrasound transducer (VisualSonics, Toronto, Ont., Canada). During examination, mice were anesthetized with 2% inhaled isoflurane and placed on a temperature-controlled platform. Electrocardiogram, heart rate (HR), and respiratory rate were monitored continuously and recorded during the imaging process. Parasternal long axis and short axis images were recorded in all animals. Analysis of the data was performed with software provided by VisualSonics. Briefly, left ventricle (LV) internal diameters at end-diastole and end-systole (D_{ED}, D_{ES}) were obtained from short-axis M-mode images as average of 3 consecutive cardiac cycles. M-mode derived end-diastolic volume (EDV) and end-systolic volume (ESV) were estimated as [17]:

$$EDV = ((7.0 / (2.4 + D_{ED})) \times D_{ED}^3$$

$$ESV = ((7.0 / (2.4 + D_{ES})) \times D_{ES}^3$$

Ejection fraction (EF) and cardiac output (CO) were calculated as:

$$EF = 100\% \times (EDV - ESV) / EDV$$

$$CO = HR \times (EDV - ESV)$$

Left ventricular PV-loops

Hemodynamics and LV function indices were assessed by invasive PV-loops. Mice were anesthetized with an intraperitoneally injected mix of 6.25 $mg \cdot kg^{-1}$ body weight Ventranquil (Ceva Sante Animale, Naaldwijk, the Netherlands), 6.25 $mg \cdot kg^{-1}$ body weight Midazolam (Actavis, Hafnarfjordur, Iceland), and 0.3125 $mg \cdot kg^{-1}$ body weight Fentanyl (Hameln Pharmaceuticals, Hameln, Germany) diluted in sterile water. Thereafter the mice were placed supine under a surgical microscope on a temperature-controlled warming pad to maintain a normal body temperature. Via the right carotid artery a 1.2F PV catheter (FTS-1212B-4518, Scisense Inc., London, Ont., Canada) was placed into the LV. The catheter was connected to a Scisense ADV signal processor (Scisense Inc.) to generate high-fidelity pressure and volume signals. Positioning of the catheter was guided by online pressure and volume signals. On-line display and acquisition of the signals (2000 $samples \cdot s^{-1}$) was performed with a PowerLab 8/30 data acquisition system and LabChart Pro software (AD Instruments GmbH, Spechbach, Germany). Off-line data analysis was performed with custom-made software (CircLab, P. Steendijk). Raw LV volume signals obtained by conductance were calibrated by matching EF and CO with corresponding echocardiographic values. PV signals were acquired in steady state to obtain general hemodynamics via HR, stroke volume (SV), CO, and stroke work (SW). Effective arterial elastance (E_A) was calculated as the

ratio of end-systolic pressure (ESP) and SV.[18] Systolic LV function was quantified by ESP, ESV, EF, and maximal rate of pressure increase (dP/dt_{MAX}). In addition, we determined end-systolic elastance (E_{ES}) as a load-independent index of intrinsic LV function, using a validated single-beat approach.[19] Ventricular-arterial coupling was quantified as E_{ES}/E_A.[20] Diastolic LV function was assessed by end-diastolic pressure (EDP), EDV, relaxation time constant τ, and the maximal rate of pressure decline ($-dP/dt_{MIN}$). Intrinsic LV diastolic function was quantified by end-diastolic stiffness (E_{ED}) (1/compliance) and the diastolic stiffness constant (K_{ED}). Thus, all presented hemodynamic data were obtained from invasive PV loops and echocardiographic volumes were used to calibrate the conductance-derived volumes.

Statistical analyses

Results for body weight, plasma lipids, insulin and glucose levels, and cardiac function are shown as means ± SD and were compared using unpaired t-tests and DEXA scan data followed by a Tukey's multiple comparison test (SPSS for windows 17.0, SPSS Inc., Chicago, IL, USA).

To investigate the effects of gender, and type and duration (time) of the diet intervention, and in particular the interaction between these factors, the data were submitted to a multiple linear regression model:

$$Y = A_O + A_G \times G + A_D \times D + A_T \times T + A_{GD} \times G \times D + A_{GT} \times G \times T + A_{TD} \times T \times D$$

In this model, Y represents the independent measurement variable, G codes the gender (female: G = –1, male: G = 1), D the type of diet (LFD: D = –1, HFD: D = 1), and T codes the diet intervention duration (6 weeks: T = –1, 12 weeks: T = 1). By using effects coding, coefficient A_O provides the overall mean value of Y; A_G, A_D, and A_T are the magnitude of the main effects; and A_{GD}, A_{GT}, and A_{DT} are the magnitude of the corresponding interactive effects.[21] The p values of the various coefficients indicate whether the corresponding effects are statistically significant. Grubb's test for detecting outliers was used to identify and exclude outliers. $p < 0.05$ was considered significant. All data are presented as means ± SD.

Results

HFD feeding increases body weight in males and females

To determine the effect of duration of HFD feeding on cardiac function, male and female mice underwent diet intervention for 6 or 12 weeks. All male and all female groups had similar body weights at the start of the study (figure 2). Weekly monitoring of body weight showed that HFD feeding gradually increased body weight as compared with LFD feeding, the difference reached statistical significance from 5 weeks onwards for males and from 4 weeks onwards for females (not shown) and remained significant until the end of the study. After 6 weeks, body weight was increased for males by 19% ± 8% in the HFD group vs. 5% ± 2% in the LFD group ($p < 0.01$), which was similar to the females with increases of 18% ± 12% vs. 2% ± 5%, respectively ($p < 0.05$). After 12 weeks the difference between the HFD and LFD groups was more pronounced with 32% ±

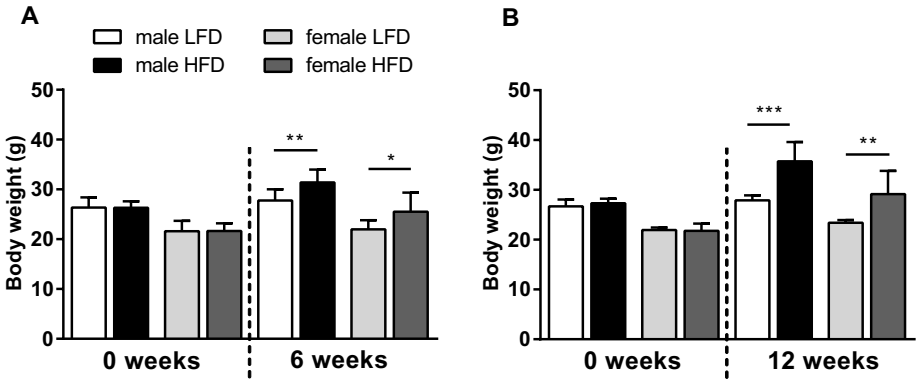

Figure 2 **Effect of diet intervention on body weight.** Male and female C57Bl/6J mice were fed a low-fat diet (LFD) or high-fat diet (HFD) for 6 weeks (A) or 12 weeks (B). Body weight was measured at baseline and at the end of dietary intervention. Values represent means ± SD (n=8 per group). *p<0.05, **p<0.01, ***p<0.001, compared to the corresponding LFD group.

10% vs. 5% ± 3% for the males (p< 0.001) and 32% ± 15% vs. 7% ± 2% for the females, respectively (p< 0.01). HFD-induced body weight gain was not significantly different between males and females after 6 and 12 weeks of diet intervention.

HFD feeding increases plasma lipids in males and females

After 4 and 10 weeks, blood samples were obtained and plasma levels of total cholesterol, phospholipid, and triglyceride levels were determined (figure 3). After 4 weeks of HFD feeding, total cholesterol levels were significantly increased in males (+31%, p< 0.05) and females (+55%, p< 0.001) as compared with the LFD groups. Furthermore, after 4 weeks of HFD feeding, phospholipid levels were increased in females only (+20%, p< 0.01) as compared with the LFD group, whereas HFD feeding did not affect triglyceride levels in

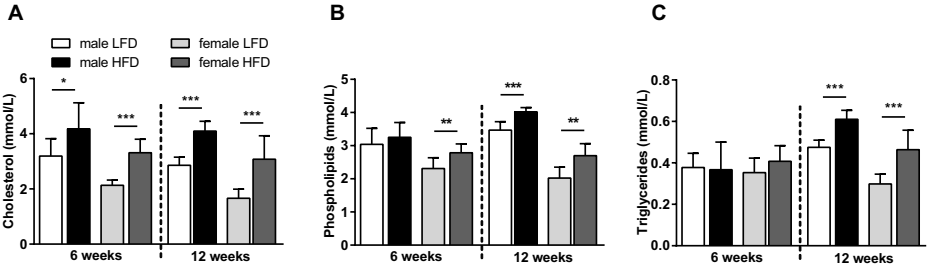

Figure 3 **Effect of diet intervention on plasma lipids.** Male and female C57Bl/6J mice were fed a low-fat diet (LFD) or high-fat diet (HFD) for 6 weeks or 12 weeks. Plasma levels of cholesterol (A), phospholipids (B) and triglycerides (C) were measured at 4 and 10 weeks, respectively. Values represent means ± SD (n=7-8 per group). *p<0.05, **p<0.01, ***p<0.001, compared to the corresponding LFD group.

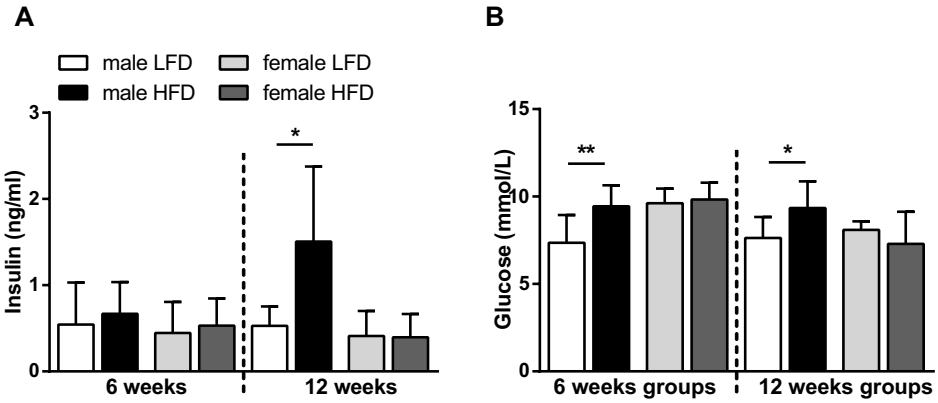

Figure 4 **Effect of diet intervention on plasma insulin and glucose levels.** Male and female C57Bl/6J mice were fed a low-fat diet (LFD) or high-fat diet (HFD) for 6 weeks or 12 weeks. Plasma levels of insulin (A) and glucose (B) were measured at 4 and 10 weeks, respectively. Values represent means ± SD (n=7-8 per group). *p<0.05, **p=0.01, compared to the corresponding LFD group.

both genders. After 10 weeks, all plasma lipid parameters for both males and females were significantly increased in the HFD group in comparison with the corresponding LFD group: total cholesterol (males: +44%, p< 0.001; females: +86%, p< 0.001), phospholipids (males: +16%, p< 0.001; females: +34%, p< 0.01) and triglycerides (males: +27%, p< 0.001; females: +53%, p< 0.001).

HFD feeding increases insulin and glucose levels in males

To determine the effect of HFD feeding on glucose metabolism, insulin and glucose levels were measured in plasma. As compared with the LFD group, 4 weeks of HFD feeding did not increase plasma insulin levels in males and females, whereas glucose levels were mildly increased in only male mice (+28%, p=0.01) (figure 4). After 10 weeks of HFD feeding, insulin (+186%, p< 0.05) as well as glucose levels (+22%, p< 0.05) were significantly increased in males, while the levels for females fed a LFD and HFD were not different.

HFD feeding selectively impairs cardiac function in males

Cardiac function measurements, obtained by combined echocardiography and PV-loops, are summarized in table 1. Based on the mean values for end-diastolic and end-systolic pressures and volumes, schematic PV-loops were created for all groups and corresponding end-systolic and end-diastolic PV-relations were added, based on mean E_{ES} and E_{ED} values (figure 5).

When compared with LFD, in male mice, but not in female mice, the HFD significantly affected cardiac function at 6 weeks with increased EDV (58.0 ± 12.2 vs. 39.9 ± 15.4 μL,

Table 1 **Effect of diet intervention on cardiac function.**

	Male		Female		Male		Female	
	6 weeks LFD	6 weeks HFD	6 weeks LFD	6 weeks HFD	12 weeks LFD	12 weeks HFD	12 weeks LFD	12 weeks HFD
General								
HR (beats/min)	378 ± 38	369 ± 36	377 ± 125	421 ± 125	414 ± 63	384 ± 66	317 ± 94	328 ± 63
SV (μL)	28.1 ± 7.3	38.7 ± 9.7	35.6 ± 6.1	35.1 ± 1.8	40.2 ± 8.0	39.7 ± 6.0	27.5 ± 6.9	33.9 ± 9.8
CO (mL/min)	10.6 ± 3.6	14.4 ± 4.1	12.9 ± 2.8	13.7 ± 4.5	17.2 ± 3.7	15.3 ± 3.7	8.5 ± 2.7	10.8 ± 2.5
SW (mm Hg.μL)	1854 ± 541	2504 ± 635	2436 ± 312	2232 ± 620	2650 ± 523	2847 ± 361	1725 ± 509	2298 ± 745
E_A (mm Hg/μL)	2.60 ± 0.84	1.84 ± 0.37	2.39 ± 0.85	2.21 ± 0.60	1.69 ± 0.38	1.87 ± 0.35	2.69 ± 0.91	2.27 ± 0.59
Ees/Ea	1.37 ± 0.18	1.43 ± 0.19	1.48 ± 0.31	1.21 ± 0.35	1.19 ± 0.24	1.25 ± 0.19	1.36 ± 0.37	1.40 ± 0.21
Systolic								
ESP (mm Hg)	67.1 ± 5.7	66.0 ± 4.1	78.1 ± 14.1	69.3 ± 13.7	63.6 ± 4.2	72.1 ± 6.9**	70.8 ± 4.0	71.8 ± 5.5
ESV (μL)	11.8 ± 8.7	19.3 ± 4.8	15.0 ± 6.6	14.3 ± 5.3	17.0 ± 6.2	25.4 ± 6.2*	15.1 ± 6.9	15.4 ± 4.7
EF (%)	74.2 ± 11.7	66.5 ± 7.0	71.6 ± 9.1	70.6 ± 6.0	68.1 ± 3.1	61.2 ± 4.5**	65.6 ± 11.5	68.7 ± 6.6
dP/dt_{MAX} (mm Hg/ms)	5.7 ± 2.0	5.4 ± 0.5	6.6 ± 3.0	6.1 ± 2.7	5.9 ± 0.4	6.0 ± 1.2	4.8 ± 2.1	5.3 ± 0.8
E_{ES} (mm Hg/μL)	3.53 ± 1.11	2.63 ± 0.77	3.27 ± 0.47	2.63 ± 0.82	2.04 ± 0.71	2.29 ± 0.32	3.85 ± 2.02	3.10 ± 0.60
Diastolic								
EDP (mm Hg)	4.29 ± 1.57	3.15 ± 1.01	7.73 ± 3.11	5.49 ± 4.65	4.03 ± 1.49	5.01 ± 2.10	6.07 ± 3.24	6.11 ± 3.70
EDV (μL)	39.9 ± 15.4	58.0 ± 12.2*	50.6 ± 10.9	47.3 ± 9.2	57.2 ± 13.0	65.1 ± 11.1	42.5 ± 11.2	49.4 ± 13.0
Tau (ms)	14.4 ± 3.8	14.4 ± 1.8	14.4 ± 4.4	14.8 ± 5.3	11.1 ± 1.2	12.7 ± 1.8	18.0 ± 5.7	16.0 ± 2.4
$-dP/dt_{MIN}$ (mm Hg/ms)	3.6 ± 0.9	3.5 ± 0.3	4.7 ±2.0	4.0 ± 1.8	4.3 ± 0.3	4.2 ± 0.8	3.1 ± 1.2	3.4 ± 0.7
E_{ED} (mm Hg/μL)	0.160 ± 0.06	0.139 ± 0.05	0.200 ±0.06	0.170 ± 0.11	0.144 ± 0.06	0.183 ± 0.08	0.220 ± 0.09	0.234 ± 0.14
K_{ED} (1/μL)	0.051 ± 0.02	0.061 ± 0.03	0.068 ± 0.03	0.066 ± 0.02	0.043 ± 0.02	0.061 ± 0.02	0.051 ± 0.01	0.066 ± 0.02

Male and female C57Bl/6J mice were fed a low-fat diet (LFD) or high-fat diet (HFD) for 6 weeks or 12 weeks, and cardiac function was determined. Left ventricle (LV) volume signals obtained by conductance catheter were calibrated by matching EF and CO with corresponding echocardiographic values obtained by measurements four days earlier. Values represent means ± SD (n=8 per group). *p<0.05, **p<0.01 as compared to LFD group. HR, heart rate; SV, stroke volume; CO, cardiac output; SW, stroke work; E_A, arterial elastance (afterload); E_{ES}/E_A, ventricular arterial coupling; ESP, end-systolic pressure; ESV, end-systolic volume; EF, ejection fraction; dP/dt_{MAX}, maximal rate of pressure increase; E_{ES}, end-systolic elastance; EDP, end-diastolic pressure; EDV, end-diastolic volume; Tau, relaxation time constant; $-dP/dt_{MIN}$, maximal rate op pressure decline; E_{ED}, diastolic stiffness; K_{ED}, diastolic stiffness constant.

p< 0.05) and at 12 weeks with increased ESV (at 12 weeks: 25.4 ± 6.2 vs. 17.0 ± 6.7 μL, p< 0.05), increased ESP (72.1 ± 6.9 vs. 63.6 ± 6.9 mm Hg, p< 0.01), and decreased EF (61.2 ± 4.5 vs. 68.1 ± 3.7%, p< 0.01), indicating reduced systolic function after 12 weeks of HFD feeding (table 1).

Subsequently, we used a multiple linear regression model to test whether the gender, the type of diet, or the duration of the diet interventions had significant effects on the various hemodynamic indices. In addition to these main effects, this approach was used to statistically analyze possible interactive effects, in particular to investigate if the diet effects were statistically different for male and female mice. The statistical analyses are presented in table 2.

To explain the results of the multiple linear regression model, ESV is taken as an example. The coefficient A_0 (16.66) yields the mean value of ESV averaged over all mice. Since p_F, reflecting the overall significance of the model, was significant (p = 0.004), the investigated effects (gender, diet, and/or time) apparently significantly affected ESV. A significant effect was observed for gender (p = 0.032): the positive value of A_G (1.72) indicates that the average ESV in male mice (G = 1) was higher (16.66 + 1.72 mL) than in females (G = –1, thus 16.66 – 1.72 mL). The significant (p = 0.017) coefficient A_D indicates that average ESV in mice subjected to HFD (D = 1) was 1.94 mL higher than the overall mean, and for mice with a LFD (D = –1) ESV was 1.94 mL lower. Finally, the coefficient A_{GD} indicates a significant (p = 0.012) gender-diet interaction (thus, the diet effect is different between males and females) with an additional 2.03 mL increase in ESV for males with HFD (and corresponding interactive effects in the other groups).

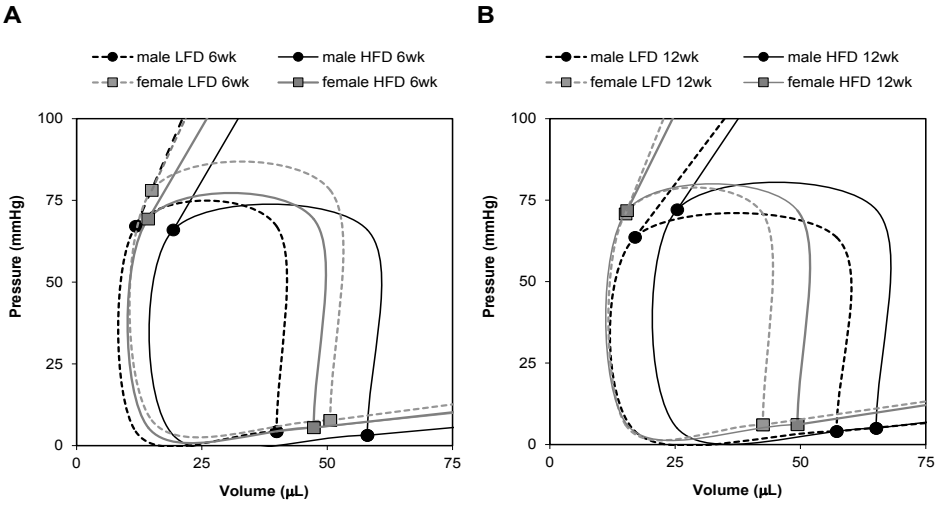

Figure 5 **Effect of diet intervention on pressure-volume loops and pressure-volume relations.** Male and female C57Bl/6J mice were fed a low-fat diet (LFD) or high-fat diet (HFD) for 6 weeks (A) or 12 weeks (B). Pressure-volume loops were recorded in each mouse, and average pressure-volume loops are shown per group.

Table 2 **Effects of diet intervention on cardiac function (multiple linear regression model)**

	Intercept		Main Effects						Interactive Effects					
	A_0	(p_F)	A_G	(p)	A_D	(p)	A_T	(p)	A_{GD}	(p)	A_{GT}	(p)	A_{DT}	(p)
General														
HR	373.54	(0.226)	12.82	(0.245)	2.12	(0.847)	-12.76	(0.247)	-11.80	(0.284)	25.37	(0.024)	-6.66	(0.544)
SV	34.85	(0.003)	1.82	(0.052)	2.00	(0.033)	0.47	(0.609)	0.53	(0.565)	2.79	(0.004)	-0.50	(0.587)
CO	12.93	(0.000)	1.44	(0.002)	0.64	(0.152)	0.04	(0.925)	-0.16	(0.722)	1.85	(0.000)	-0.53	(0.234)
SW	2318.3	(0.002)	145.6	(0.038)	152.0	(0.030)	61.7	(0.371)	59.9	(0.385)	223.0	(0.002)	40.5	(0.557)
E_A	2.19	(0.024)	-0.20	(0.019)	-0.15	(0.074)	-0.06	(0.430)	0.00	(0.983)	-0.15	(0.063)	0.09	(0.295)
E_{ES}/E_A	1.34	(0.267)	-0.03	(0.439)	-0.01	(0.677)	-0.03	(0.308)	0.04	(0.199)	-0.05	(0.104)	0.04	(0.221)
Systolic														
ESP	69.85	(0.036)	-2.66	(0.013)	-0.06	(0.957)	-0.29	(0.781)	1.89	(0.072)	0.92	(0.377)	2.45	(0.022)
ESV	16.66	(0.004)	1.72	(0.032)	1.94	(0.017)	1.55	(0.053)	2.03	(0.012)	1.26	(0.116)	0.24	(0.759)
EF	68.28	(0.069)	-0.81	(0.418)	-1.57	(0.122)	-2.42	(0.019)	-2.09	(0.041)	-0.43	(0.670)	0.61	(0.541)
dP/dt_{MAX}	5.711	(0.635)	0.021	(0.928)	-0.033	(0.886)	-0.221	(0.342)	-0.038	(0.871)	0.426	(0.070)	0.191	(0.412)
E_{ES}	2.92	(0.006)	-0.29	(0.020)	-0.26	(0.043)	-0.10	(0.423)	0.09	(0.457)	-0.36	(0.005)	0.13	(0.298)
Diastolic														
EDP	5.23	(0.068)	-1.12	(0.003)	-0.29	(0.416)	0.07	(0.845)	0.26	(0.478)	0.33	(0.361)	0.55	(0.130)
EDV	51.26	(0.002)	3.80	(0.015)	3.69	(0.018)	2.28	(0.138)	2.82	(0.068)	3.79	(0.015)	-0.01	(0.997)
Tau	14.49	(0.026)	-1.33	(0.005)	0.02	(0.964)	-0.02	(0.970)	0.41	(0.371)	-1.22	(0.010)	-0.10	(0.823)
$-dP/dt_{MIN}$	3.853	(0.124)	0.060	(0.683)	-0.068	(0.642)	-0.106	(0.471)	-0.024	(0.867)	-0.447	(0.003)	-0.140	(0.338)
E_{ED}	0.181	(0.232)	-0.025	(0.021)	0.000	(0.976)	0.014	(0.183)	0.004	(0.686)	-0.007	(0.500)	0.013	(0.216)
K_{ED}	0.058	(0.199)	-0.004	(0.110)	0.005	(0.052)	-0.003	(0.237)	0.002	(0.486)	0.001	(0.699)	0.003	(0.249)

All hemodynamic indices from table 1 were fitted to the multiple linear regression model: $Y = A_O + A_G \times G + A_D \times D + A_T \times T + A_{GD} \times G \times D + A_{GT} \times G \times T + A_{DT} \times D \times T$. In this model, Y represents the independent measurement variable, G codes the gender (female: G=-1, male: G=1), D codes the type of diet (low-fat: D=-1, high-fat: D=1), and T codes the diet intervention duration (6-week: T=-1, 12-week: T=1). With this coding, the coefficient A_0 gives the overall mean value of each index; A_G, A_D, and A_T indicate the magnitudes of the main effects; A_{GD}, A_{GT}, and A_{DT} the interactive effects. The significance of the model is given by p_F, the significance of each coefficient by the corresponding p-value shown in the same column. For abbreviations see legends of table 1.

First, calculations were made for the entire model fit for each hemodynamic index. The p values are presented in the Intercept block in table 2, reflecting the significance of this F test. The model showed significant effects for general hemodynamic function (SV, CO, SW, and E_A), for systolic function (ESP, ESV and E_{ES}), and diastolic function (EDV and τ).

Then, the effects of the separate factors, gender, type of diet, and duration of diet intervention were calculated for the affected indices. These calculations are presented in the main effects block in table 2. All these indices showed a significant gender effect (except SV, which just fell short of statistical significance at p = 0.052), with higher CO, SW, ESV, and EDV (indicated by the positive AG) and lower E_A, ESP, E_{ES}, and τ (negative A_G) in males (G = 1) compared with females (G = –1). The type of diet (coefficient A_D) had a significant main effect on SV, SW, E_A, (marginal, p=0.074) ESV, E_{ES}, and EDV. HFD feeding (D = 1) resulted in higher values for SV, SW, ESV, and EDV, and lower values for E_A and E_{ES}. For none of the indices, diet duration (reflected by coefficient A_T) had a significant main effect, indicating that for the full cohort (thus males and females on both LFD and HFD) there was no significant difference between 6 weeks and 12 weeks diet intervention.

Furthermore, the interaction of the different factors on the hemodynamic indices was calculated (interactive effects block, table 2). For several indices there was a significant interaction between gender and diet duration, indicating that either the effect of diet duration was different between males and females or the effect of gender was significantly different between the 6 and 12 weeks groups. This significant interaction was found for SV, CO, SW, E_{ES}, EDV, and τ. Furthermore, a significant interactive diet duration–diet type effect was found for ESP, whereas interaction between gender and diet type was present for ESV, EF, ESP, and EDV, the latter being only marginally significant.

Discussion

The present study was designed to investigate to what extent high-fat feeding leads to alterations in cardiac function in C57Bl/6J mice and whether this depends on gender and/or durations of high-fat feeding. The data obtained from both echocardiography and conductance catheter indicates that in male mice cardiac function was significantly altered by prolonged HFD feeding. HFD feeding also increased the insulin and glucose levels in males, implying an impaired glucose tolerance. These effects were absent in female mice despite their more pronounced elevation of plasma lipid levels, indicating the relevance of gender in this mouse model of obesity-related cardiac disease.

Previous studies have provided strong evidence that excessive accumulation of triglycerides in cardiac myocytes of obese animals results in impaired cardiac function, as characterized by an increase in LV end-diastolic diameter and a significant reduction in cardiac contraction.[4,22] In addition, increased triglyceride stores are found in cardiac myocytes of streptozotocin-induced diabetic rats [23,24] and cholesterol-fed hyperlipidemic

rats [25]. However, in these experiments it has never been investigated whether there is a difference in cardiac function between male and female mice, and thus whether gender choice of the animal model is of importance in future research of obesity-induced cardiac disease.

We have now showed that 12 weeks of intervention with HFD induced obesity and increased plasma lipid levels in both male and female mice. However, insulin and glucose levels, as well as the effects on cardiac function, were only affected in males. The difference in heart function was observed by comparing the HFD fed animals to the corresponding LFD group, revealing that only in males systolic function was attenuated by feeding HFD for 12 weeks. This was evidenced by increased ESP and ESV and a reduced EF. The most pronounced effect of the diet is seen in males after 12 weeks as compared with 6 weeks of HFD feeding, which explains that a longer exposure results in a stronger effect. In females the HFD did not affect any cardiac function parameter after 6 or 12 weeks.

We further quantified the contributions of the separate factors and their interactions in a multiple linear regression model. This analysis (table 2) showed that gender had the most prominent effects on cardiac function. Also, these gender effects were not confined to a sole parameter, but were observed in most parameters for general, systolic, and diastolic indices. Fully consistent with previous studies in humans [26, 27], the males showed higher ventricular volumes and cardiac output and lower pressures, whereas E_{ES} and E_A, representing intrinsic systolic function and afterload, respectively, were also both lower in males. Thus, lower systolic function is more prominent in males and is compensated by lower afterload resulting in maintained, or even higher, cardiac output compared with females.

The multiple linear regression model further showed significant main effects of the diet intervention on cardiac function as indicated by increased volumes and a decreased E_{ES}. This is in line with studies in humans, which show an association between obesity and impaired cardiac function.[1, 28] However, to our knowledge no studies investigated possible differences between men and women on this association. In our study, the overall effects of diet did not reach significance in all individual groups (table 1). In particular, the females showed limited or no changes in volume, whereas the changes were much more pronounced in males. This differential effect was indeed reflected by (nearly) significant interactive gender–diet effects on ESV ($p= 0.012$) and EVD ($p= 0.068$). With regard to E_{ES}, the overall significant decrease with HFD feeding was reflected by clear trends for a decrease in all individual groups, except for males after 12 weeks on HFD (table 1). This is interesting since in this particular group ESP and ESV both increased significantly, but E_{ES} remained unchanged. However, given the E_{ES} of approximately 2 mm Hg·μL^{-1}, the observed increase in ESV (8.4 μL) could not be explained merely by the higher ESP (8.5 mm Hg). Thus, in this group the end-systolic pressure-volume relation apparently showed a more or less parallel rightward shift (as shown in figure 5B), which is also associated with a decreased contractile state.[29, 30]

Furthermore, while in our study HFD feeding resulted in a reduced systolic function, it had only minor effects on diastolic function. This is in contrast with earlier findings in

literature, which showed that in obese patients mainly the diastolic function seemed to be affected.[31,32] Although this discrepancy could be due to species differences, additional factors are likely to play a role. In particular, we studied the effect of a single isolated factor, the lard diet, whereas previous studies in humans are clearly multifactorial.

A possible explanation for the different response in cardiac function between males and females may be a difference in susceptibility to obesity. Unpublished data from our group (S.A.A. van den Berg 2008, unpublished data) showed that sex hormones are the main contributing factors to obesity. We observed that HFD fed males compared with HFD fed females have a similar lean body mass, while males have an excessive increase in fat mass, which is not observed in females. Furthermore, ovariectomized females fed a HFD showed similar weight gain as males fed a HFD, which is explained by an increase in body fat. Conversely, male mice treated with estrogen fed a HFD showed a largely decreased weight gain, similar to HFD fed females, which is explained by a largely reduced body fat (supplementary figure S1). Collectively, these data indicate that sex hormones greatly influence HFD-induced increase in fat mass.

Besides the effect of estrogen on obesity, differences in sex hormones in males and females themselves can also influence heart function. Cardiac protection by estrogen is reported in several studies in different species. Studies with gene-targeted mouse strains revealed protection against hypertrophy in females.[33, 34] Also in male rats an accelerated progression to heart failure is reported after hypertension.[35] Additionally, comparable results are observed in humans: in postmenopausal women estrogen replacement reduced the risk of cardiovascular events.[36] Similarly, the survival rate after ischemic heart failure is higher in females compared with males.[37] Thus, it can be speculated that gender differences in sex hormones and fat content may contribute to the alterations in cardiac function we observed in our study.

Several limitation of our study should be mentioned. The number of animals investigated was relatively small (8 mice per group). Thus, potential group differences that currently showed clear trends could have reached significance with larger sample sizes. Assessment of PV relations was based on a single-beat estimates rather than load interventions. This approach has been validated, but its accuracy remains debated. We quantified afterload by effective E_A based on ventricular parameters, rather than a more detailed but complex aortic impedance analysis based on aortic pressure and flow data. However, the present study was mainly focused on ventricular function and E_A has been shown useful parameter to study ventricular-arterial coupling.[38] Calibration of the conductance catheter was based on echocardiographic data obtained 4 days earlier, thus using a non-simultaneous reference method. However, the same protocol was followed in all animals so this approach is unlikely to have influenced the observed effects or comparisons between groups.

In conclusion, the present study indicates that high-fat feeding gradually increases body weights and plasma lipids levels in C57Bl/6J mice independent of gender. However, at 12 weeks cardiac function is impaired in male mice, but not in female mice. These results indicate a gender-specific effect of high-fat feeding on cardiac function in mice, independent of increased plasma lipids. This was confirmed by additional statistical

analyses, calculating the impact of the separate factors and their interactions. We thus propose that male mice are the preferred model to investigate effects of ischemia and drug treatments on cardiac function in a setting of diet induced obesity.

Acknowledgements

We thank C.J.A. van der Wee-Pals for her excellent technical assistance. This research was performed within the framework of CTMM, the Center for Translational Molecular Medicine (www.ctmm.nl), project PREDICCt (grant 01C-104), and was supported by the Netherlands Heart Foundation, Dutch Diabetes Research Foundation and Dutch Kidney Foundation. PCN Rensen is an Established Investigator of the Netherlands Heart Foundation (grant 2009T038).

References

1 Abbasi F, Brown BW, Jr., Lamendola C, McLaughlin T, Reaven GM. Relationship between obesity, insulin resistance, and coronary heart disease risk. *J Am Coll Cardiol* 2002 September 4;40(5):937-43.

2 Sorof J, Daniels S. Obesity hypertension in children: a problem of epidemic proportions. *Hypertension* 2002 October;40(4):441-7.

3 McGavock JM, Victor RG, Unger RH, Szczepaniak LS. Adiposity of the heart, revisited. *Ann Intern Med* 2006 April 4;144(7):517-24.

4 Zhou YT, Grayburn P, Karim A et al. Lipotoxic heart disease in obese rats: implications for human obesity. *Proc Natl Acad Sci U S A* 2000 February 15;97(4):1784-9.

5 Stanley WC, Recchia FA, Lopaschuk GD. Myocardial substrate metabolism in the normal and failing heart. *Physiol Rev* 2005 July;85(3):1093-129.

6 Lopaschuk GD, Tsang H. Metabolism of palmitate in isolated working hearts from spontaneously diabetic "BB" Wistar rats. *Circ Res* 1987 December;61(6):853-8.

7 Rodrigues B, Cam MC, McNeill JH. Metabolic disturbances in diabetic cardiomyopathy. *Mol Cell Biochem* 1998 March;180(1-2):53-7.

8 Unger RH, Zhou YT, Orci L. Regulation of fatty acid homeostasis in cells: novel role of leptin. *Proc Natl Acad Sci U S A* 1999 March 2;96(5):2327-32.

9 Unger RH, Orci L. Lipotoxic diseases of nonadipose tissues in obesity. *Int J Obes Relat Metab Disord* 2000 November;24 Suppl 4:S28-S32.

10 Jeppesen J, Hein HO, Suadicani P, Gyntelberg F. High triglycerides/low high-density lipoprotein cholesterol, ischemic electrocardiogram changes, and risk of ischemic heart disease. *Am Heart J* 2003 January;145(1):103-8.

11 Szczepaniak LS, Victor RG, Orci L, Unger RH. Forgotten but not gone: the rediscovery of fatty heart, the most common unrecognized disease in America. *Circ Res* 2007 October 12;101(8):759-67.

12 Luczak ED, Leinwand LA. Sex-based cardiac physiology. *Annu Rev Physiol* 2009;71:1-18.

13 Jain M, Liao R, Podesser BK, Ngoy S, Apstein CS, Eberli FR. Influence of gender on the response to hemodynamic overload after myocardial infarction. *Am J Physiol Heart Circ Physiol* 2002 December;283(6):H2544-H2550.

14 Wende AR, Abel ED. Lipotoxicity in the heart. *Biochim Biophys Acta* 2010 March;1801(3):311-9.

15 Djouadi F, Weinheimer CJ, Saffitz JE et al. A gender-related defect in lipid metabolism and glucose homeostasis in peroxisome proliferator- activated receptor alpha- deficient mice. *J Clin Invest* 1998 September 15;102(6):1083-91.

16 Georgakopoulos D, Mitzner WA, Chen CH et al. In vivo murine left ventricular pressure-volume relations by miniaturized conductance micromanometry. *Am J Physiol* 1998 April;274(4 Pt 2):H1416-H1422.

17 Teichholz LE, Kreulen T, Herman MV, Gorlin R. Problems in echocardiographic volume determinations: echocardiographic-angiographic correlations in the presence of absence of asynergy. *Am J Cardiol* 1976 January;37(1):7-11.

18 Kelly RP, Ting CT, Yang TM et al. Effective arterial elastance as index of arterial vascular load in humans. *Circulation* 1992 August;86(2):513-21.

19 Ten Brinke EA, Klautz RJ, Verwey HF, van der Wall EE, Dion RA, Steendijk P. Single-beat estimation of the left ventricular end-systolic pressure-volume relationship in patients with heart failure. *Acta Physiol* (Oxf) 2010 January;198(1):37-46.

20 Chantler PD, Lakatta EG, Najjar SS. Arterial-ventricular coupling: mechanistic insights into cardiovascular performance at rest and during exercise. *J Appl Physiol* 2008 October;105(4):1342-51.

21 Slinker BK, Glantz SA. Multiple regression for physiological data analysis: the problem of multicollinearity. *Am J Physiol* 1985 July;249(1 Pt 2):R1-12.

22 Christoffersen C, Bollano E, Lindegaard ML et al. Cardiac lipid accumulation associated with diastolic dysfunction in obese mice. *Endocrinology* 2003 August;144(8):3483-90.

23 Heyliger CE, Scarim AL, Eymer VP, Skau KA, Powell DM. Characteristics of the myocardial PM-FABP: effect of diabetes mellitus. *Mol Cell Biochem* 1997 November;176(1-2):281-6.

24 Myrmel T, Forsdahl K, Larsen TS. Triacylglycerol metabolism in hypoxic, glucose-deprived rat cardiomyocytes. *J Mol Cell Cardiol* 1992 August;24(8):855-68.

25 Hexeberg S, Willumsen N, Rotevatn S, Hexeberg E, Berge RK. Cholesterol induced lipid accumulation in myocardial cells of rats. *Cardiovasc Res* 1993 March;27(3):442-6.

26 Celentano A, Palmieri V, Arezzi E et al. Gender differences in left ventricular chamber and midwall systolic function in normotensive and hypertensive adults. *J Hypertens* 2003 July;21(7):1415-23.

27 Hayward CS, Kalnins WV, Kelly RP. Gender-related differences in left ventricular chamber function. *Cardiovasc Res* 2001 February 1;49(2):340-50.

28 Vasan RS. Cardiac function and obesity. *Heart* 2003 October;89(10):1127-9.

29 Burkhoff D, Mirsky I, Suga H. Assessment of systolic and diastolic ventricular properties via pressure-volume analysis: a guide for clinical, translational, and basic researchers. *Am J Physiol Heart Circ Physiol* 2005 August;289(2):H501-H512.

30 Steendijk P, Baan J, Jr., Van der Velde ET, Baan J. Effects of critical coronary stenosis on global systolic left ventricular function quantified by pressure-volume relations during dobutamine stress in the canine heart. *J Am Coll Cardiol* 1998 September;32(3):816-26.

31 Fischer M, Baessler A, Hense HW et al. Prevalence of left ventricular diastolic dysfunction in the community. Results from a Doppler echocardiographic-based survey of a population sample. *Eur Heart J* 2003 February;24(4):320-8.

32 Powell BD, Redfield MM, Bybee KA, Freeman WK, Rihal CS. Association of obesity with left ventricular remodeling and diastolic dysfunction in patients without coronary artery disease. *Am J Cardiol* 2006 July 1;98(1):116-20.

33 van Eickels M, Grohe C, Cleutjens JP, Janssen BJ, Wellens HJ, Doevendans PA. 17beta-estradiol attenuates the development of pressure-overload hypertrophy. *Circulation* 2001 September 18;104(12):1419-23.

34 Xin HB, Senbonmatsu T, Cheng DS et al. Oestrogen protects FKBP12.6 null mice from cardiac hypertrophy. *Nature* 2002 March 21;416(6878):334-8.

35 Wallen WJ, Cserti C, Belanger MP, Wittnich C. Gender-differences in myocardial adaptation to afterload in normotensive and hypertensive rats. *Hypertension* 2000 November;36(5):774-9.

36 Adams KF, Jr., Dunlap SH, Sueta CA et al. Relation between gender, etiology and survival in patients with symptomatic heart failure. *J Am Coll Cardiol* 1996 December;28(7):1781-8.

37 Nabulsi AA, Folsom AR, White A et al. Association of hormone-replacement therapy with various cardiovascular risk factors in postmenopausal women. The Atherosclerosis Risk in Communities Study Investigators. *N Engl J Med* 1993 April 15;328(15):1069-75.

38 Kass DA. Age-related changes in venticular-arterial coupling: pathophysiologic implications. *Heart Fail Rev* 2002 January;7(1):51-62.

Supplemental data

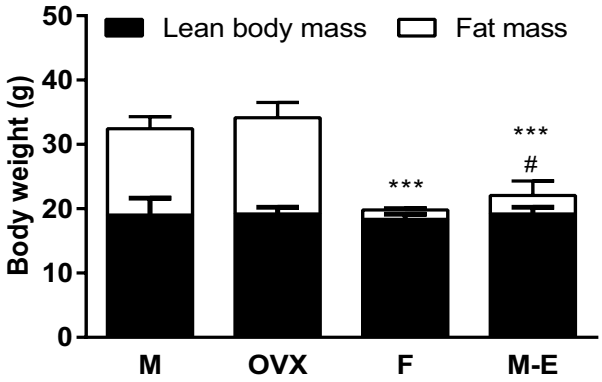

Supplemental figure S1 **Effect of sex hormones on lean body mass and fat mass.** Male and female C57Bl/6J mice were fed a high-fat diet (HFD) for 10 weeks. M= male, OVX= ovariectomy, F= female, M-E= male treated with estrogen. Values represent means ± SD (n=5-6 per group). ***p<0.001, compared both with males and OVX females for fat mass; #p<0.05, compared with females for lean body mass.

CHAPTER 3

High-fat diet does not aggravate cardiac function after a myocardial infarction in C57Bl/6J mice

Submitted for publication

Mieke C. Louwe[1,2], Saskia Maas[3], José W.A. van der Hoorn[6], Daniela Salvatori[3], Patrick C.N. Rensen[1,2], Ko Willems van Dijk[1,2,4], Paul Steendijk[5] and Johannes W.A. Smit[1]

[1]Dept. of Endocrinology and Metabolic Diseases, [2]Einthoven Laboratory for Experimental Vascular Medicine, [3]Laboratory Animal Facility, [4]Dept. of Human Genetics, [5]Dept. of Cardiology, Leiden University Medical Center, Leiden, the Netherlands [6]TNO - Metabolic Health Research, Leiden, the Netherlands

High-fat diet does not aggravate cardiac function after a myocardial infarction in C57Bl/6J mice

Abstract

Obesity is accompanied by a low-grade systemic inflammation and associated with increased risk of cardiovascular diseases (CVD) including myocardial infarction (MI). We studied whether high-fat diet (HFD) feeding results in aggravated cardiac dysfunction after an MI, due to an increased inflammatory response.

C57Bl/6J male mice were fed a low-fat diet (LFD) or HFD for 14 weeks. Lipid levels were measured 10 weeks after the start of diet feeding. At 12 weeks mice were subjected to MI induction or a sham procedure, and cardiac function was measured 2 weeks later (at week 14) by echocardiography and invasive pressure-volume loop measurements. Subsequently, mice were sacrificed for histological analyses and determination of infarct sizes.

Prior to MI induction, HFD fed mice had increased body weights (+31%, $p<0.001$) and increased plasma levels of total cholesterol (+51%, $p<0.01$) and phospholipids (+20%, $p<0.001$), whereas triglyceride levels were not different compared to LFD fed mice. Two weeks after MI induction, MI size was not different between LFD and HFD groups. Cardiac function measurements showed that HFD feeding *per se* induced mild cardiac dysfunction, although HFD did not lead to a more pronounced cardiac dysfunction compared to LFD after MI. Interestingly, HFD fed MI mice showed a tendency towards more macrophages in the infarcted area compared to LFD fed MI mice (+327%, $p=0.07$).

HFD does not aggravate cardiac dysfunction after MI compared to LFD fed mice, despite a tendency towards an increased presence of macrophages in the infarcted area.

Introduction

Obesity is a rapid developing epidemic which is caused by a disturbed energy balance due to decreased physical activity and excess consumption of high energy foods. In Western countries, where obesity is most prevalent, cardiovascular diseases due to myocardial infarctions (MI) are a leading cause of death. The pathogenesis of obesity-related disorders is complex and involves multiple pathways, including lipotoxicity and inflammation associated with disturbed lipid and adipose tissue metabolism. In humans, high-fat diets (HFD) rapidly increase plasma triglycerides (TG)[1], increase hepatic TG content[2] and cause insulin resistance.[3] In addition, HFDs also increase intramyocellular TG content in skeletal muscle and the myocardium, which is associated with alterations in myocardial function.[4, 5]

An important hallmark of obesity is systemic inflammation that contributes to obesity-related complications, including atherosclerosis and cardiac dysfunction.[6, 7] It is known that inflammation in the heart, for example by local macrophage accumulation, impairs heart function.[8, 9] Interestingly, saturated fatty acids (FA) have been shown to cause inflammatory responses via Toll-like receptors (TLR) on macrophages.[10, 11] In addition, excessive FA influx in macrophages, due to absence of Angptl4, causes massive macrophage activation.[12] Altogether, these data indicate that HFDs activate macrophages which may lead to deleterious effects on heart function.

Therefore, this study was designed to test the hypothesis that increased FA intake associated with HFD feeding results in more severe cardiac dysfunction *per se* and after an MI due to an increased inflammatory response as compared to normal FA intake associated with low-fat diet (LFD) feeding. We fed C57Bl/6J mice a HFD for 12 weeks and induced MI by permanent ligation of the left anterior descending (LAD) coronary artery. Two weeks after MI, extensive hemodynamic measurements were performed and we found that HFD fed mice had no aggravated cardiac dysfunction compared to LFD-fed mice, despite a clear tendency towards increased macrophage infiltration in the infarcted area.

Materials and methods

Animals, diets, and experimental design

Twelve week old C57Bl/6J male mice (Charles River, Maastricht, the Netherlands) received either a lard-based LFD or HFD for 14 weeks. These diets were obtained from Research Diets Inc. (Wijk bij Duurstede, the Netherlands) and supplied *ad libitum*. As percentage of the total energy, the LFD contained 10% fat (4.5% lard and 5.5% soy bean oil) and 70% carbohydrate (34.5% energy from sucrose, 32% from corn starch and 3.5% from maltodextrin). The HFD contained 45% energy from fat (39.5% lard and 5.5% soy bean oil) and 35% carbohydrate (17% energy from sucrose, 8% from corn starch and 10% from maltodextrin).

Mice were housed in a temperature and humidity-controlled room on a 12:12 h light-dark cycle with *ad libitum* access to water and food. Body weights (BW) were measured weekly. After 10 weeks blood was drawn to measure plasma lipids. At 12 weeks, mice were subjected to either sham surgery or MI induction by coronary ligation (see below, LFD sham (n=8), LFD MI (n=26), HFD sham (n=8) and HFD MI (n=27) mice. Heart function was assessed using echocardiography and pressure-volume loops (PV-loops), 10 days and 14 days post MI, respectively (see below). At the end of the experiment mice were sacrificed and hearts were isolated for further examination. Mice that died before the completion of the entire study protocol were excluded from analysis. The protocol was approved by the Animal Ethics Committee from the Leiden University Medical Center and was conform to the *Guide for Care and Use of Laboratory Animals* (NIH publication No.85-23, Revised 1996).

Plasma lipids

After 4 hour fasting (9.00-13.00 h), blood was collected via tail vein bleeding in potassium EDTA-coated plastic tubes (Starstedt, Germany). Plasma total cholesterol, TGs and phospholipids were determined individually using commercially available kits (kit no. 1489232; 11488872 and 101140, Roche Diagnostics Mannheim, Germany) in 96-wells plates (Greiner Bio-One), according to the manufacturer's protocols.

Induction of myocardial infarctions

Mice were anesthetized by intraperitoneal injection of a mixture of Dormicum (0.7 mg/kg BW), Dexdomitor (7.2 mg/kg BW), and Fentanyl (0.07 mg/kg BW). Body temperature was maintained at 37°C by using a temperature controlled, automatic heating pad. Mice were artificially ventilated using a dedicated mouse ventilator (model 845, Harvard apparatus, Holliston, MA, USA). The LAD was ligated with a 7-0 Ethilon suture (Johnson and Johnson, New Brunswick, NJ, USA) just distal to the left atrial appendix. Ischemia was confirmed by bleaching of the left ventricle (LV). The thorax was closed and the mice subcutaneously received Anexate (0.5 mg/kg BW) Antisedan (2.5 mg/kg BW) and Naloxon (1.2 mg/kg BW) and 50 µL Temgesic/MilliQ (1.5 µg/50 mL MilliQ). The mice were allowed to recover on a temperature-controlled heating pad. The operation procedure was similar in sham mice, except for the ligation of the LAD.

Hemodynamic measurements

Ten days after induction of the MI transthoracic echocardiography was performed using a VisualSonics Vevo 770 with a 30 MHz ultrasound transducer (VisualSonics, Toronto, Canada) as described earlier.[13] The following parameters were obtained: heart rate (HR), stroke volume (SV), cardiac output (CO), end-diastolic volume (EDV) end-systolic volume (ESV), ejection fraction (EF), fractional area change (FAC) and area change. Briefly, mice were anesthetized with a starting dose of 4% isoflurane (in 1:1 (v/v) oxygen:air) and a maintenance dose of 1.5% isoflurane (in 1:1 (v/v) oxygen:air) and placed on a temperature controlled platform. Parasternal long axis and short axis images were recorded in all animals. Analysis of the data was performed with software provided by VisualSonics. Four days later (14 days post MI), LV function was assessed by invasive PV-loops as described earlier.[13] Briefly, mice were anesthetized with a starting dose of 4% isoflurane (in 1:1 oxygen:air) and a maintenance dose of 1.5% isoflurane (in 1:1 oxygen:air). After intubation mice were ventilated and the jugular vein was cannulated for infusion of hypertonic saline to determine parallel conductance. Via the right carotid artery a 1.2F PV catheter (FTS-1212B-4518,

Scisense Inc., London, Ontario, Canada) was placed into the LV. The catheter was connected to a Scisense ADV signal processor (Scisense Inc) to generate high-fidelity pressure and volume signals. Positioning of the catheter was guided by online pressure and volume signals. On-line display and acquisition of the signals (2000 samples/s) was performed with a PowerLab 8/30 data acquisition system and LabChart Pro software (AD Instruments GmbH, Spechbach, Germany). Off-line data analysis was performed with custom-made software (CircLab, P. Steendijk).

The following parameters were measured: HR, SV, CO, EDV, ESV, EF, end-diastolic pressure (EDP) and end-systolic pressure (ESP). Stroke work (SW) was determined as the area of the PV-loop and the maximal and minimal rate of LV pressure change, dP/dt_{MAX} and dP/dt_{MIN} were obtained. Raw LV volume signals, obtained by conductance, were calibrated by matching EF and CO with corresponding echocardiographic values and data from PV-loop measurements are presented.

Infarct size and (immuno)histochemistry

Hearts were fixed overnight in paraformaldehyde and cut into five 1 mm-thick slices, perpendicular to the long axis of the heart. These slices were flat embedded in paraffin and 5 µm-thick sections were prepared. To delineate LV area and MI area sections, the lower 3 sections were stained histochemically for collagen with Sirius Red. Total LV wall area (including septum) and infarct area were measured with cell^D imaging software (Olympus Soft Imaging Solutions). The infarct area was expressed as percentage (v/v) of the LV wall area.

Additionally, sections were immunohistochemically stained for macrophages (F4/80, 1:10; kindly provided by Dr. P.J. Nijweide, Dept. of Molecular Cell Biology, Leiden University Medical Center, the Netherlands). Three specific regions of the myocardium were distinguished based on the Sirius Red staining: the infarcted area, the border zone and the remote 'undamaged/healthy' myocardium. For each region, the macrophage content was quantified as percentage of the total cardiac tissue area using ImageJ software package (http://rsb.info.nih.gov/ij). To this end, the area of F4/80 staining within the cardiac tissue was measured within a representative image (200x magnification). The chosen threshold for quantification had a maximum staining within the macrophage and minimal (unspecific) staining of other cells.

Statistical analysis

Significance of differences between groups was calculated non-parametrically using a Kruskal-Wallis test followed by a Mann-Whitney U-test. P-values ≤ 0.05 were considered statistically significant. SPSS 20.0 for Windows (IBM SPSS, Armonk, NY, USA) was used for statistical analysis. Values are presented as means ± SD.

Results

HFD feeding increases body weight and induces dyslipidemia

At 12 weeks, the HFD fed mice had a higher body weight compared to the LFD-fed control mice (LFD: 29.4±1.8 g versus HFD: 38.6±2.7 g, p<0.001). Body weights between sham and MI groups were comparable. Immediately after MI, all groups lost weight. However, they recovered quickly and 1 week post-MI an increase in body weight was observed. At termination of the study, body weight in HFD sham and HFD MI groups was higher compared to both LFD fed groups (figure 1). In addition, LFD sham mice were slightly, but significantly, heavier compared to LFD MI mice (sham: 28.9±1.5 g versus MI: 27.6±1.2 g; p<0.05).

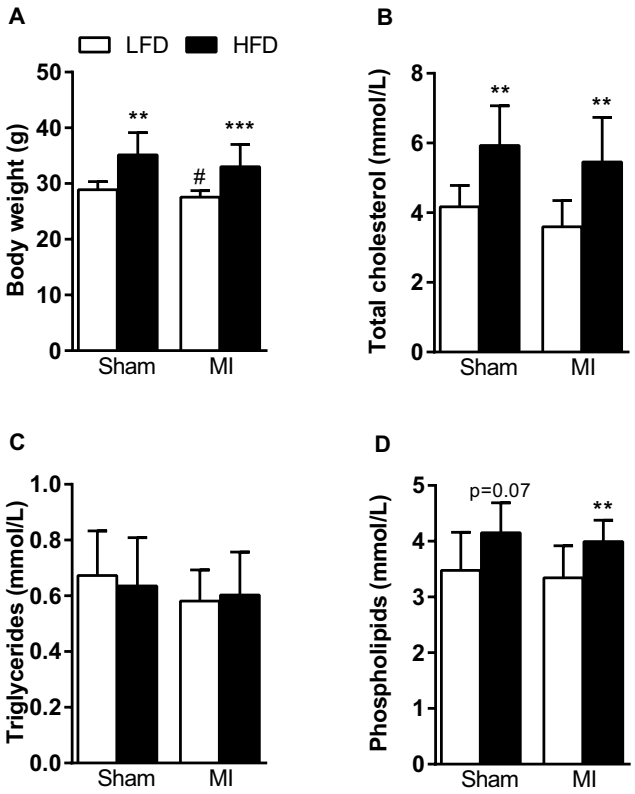

Figure 1 **Effect of LFD and HFD feeding on body weight and plasma lipids.** Male C57Bl/6J mice were fed a low-fat diet (LFD) or a high-fat diet (HFD) for 14 weeks. Body weight results at 14 weeks of diet feeding (A). Plasma total cholesterol (B) triglycerides (C) and phospholipids (D) were measured after 10 weeks of diet feeding. Values are means ± SD (n≥8 per group). ** p<0.01, *** p<0.001 versus LFD fed group, # p<0.05 versus sham group.

After 10 weeks (2 weeks prior to MI induction), plasma lipid levels were determined after a 4 hour fast. Compared to the LFD group, total cholesterol levels were increased in HFD fed mice (HFD sham: +43% versus HFD MI: +52%; both $p<0.01$) as well as phospholipids levels (HFD sham +20% $p=0.07$, HFD MI: +19% $p<0.01$). TG levels were not affected by the HFD feeding.

HFD feeding does not result in a higher mortality rate after a myocardial infarction

Sham surgeries and MI inductions were performed after 12 weeks of diet feeding. Surgical mortality for the sham animals was 0% (0/8 mice) in both LFD and HFD fed groups. HFD feeding in combination with an MI resulted in a mortality rate of 60% (16/27 mice). This was comparable to the mortality rate after LFD feeding and MI 54% (14/26 mice), indicating that HFD feeding *per se* did not influence the mortality after MI induction.

HFD feeding does not lead to aggravation of cardiac function after a myocardial infarction

To investigate whether HFD feeding influences cardiac function after MI, 14 days post MI PV-loops were recorded in each mouse and results are summarized in table 1. We confirmed that HFD feeding *per se* induced mild cardiac dysfunction compared to LFD feeding as reflected by changes of several parameters, including increased end-systolic volume (+21%, $p=0.05$) and relaxation constant tau (+17%, $p<0.05$). As

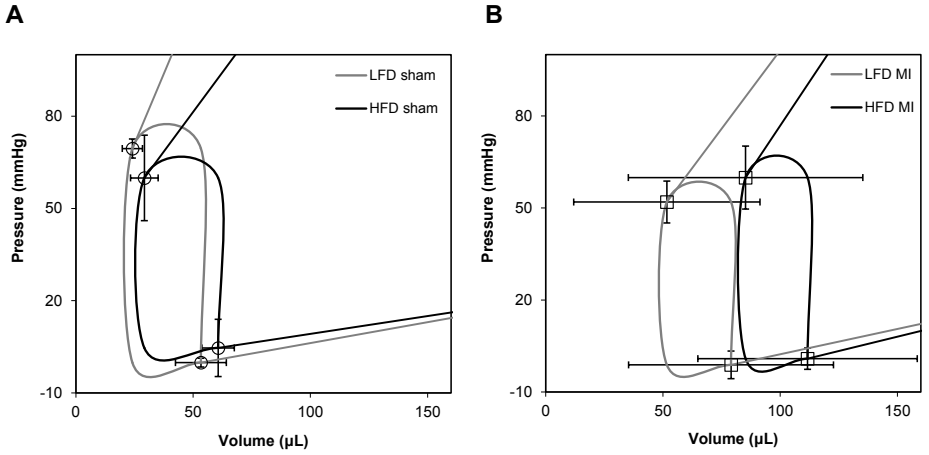

Figure 2 **Effect of LFD and HFD feeding on PV-loops and PV-relations without (sham) and with an MI.** Male C57Bl6/J mice were fed a low-fat diet (LFD) or a high-fat diet (HFD) for 14 weeks. Two weeks after induction of a myocardial infarction (MI), pressure-volume loops (PV-loops)were measured in each mouse and average PV-loops are shown for the sham group (A) and the MI group (B). Values are means ± SD for end-diastolic and end-systolic volumes and pressures ($n\geq8$ per group).

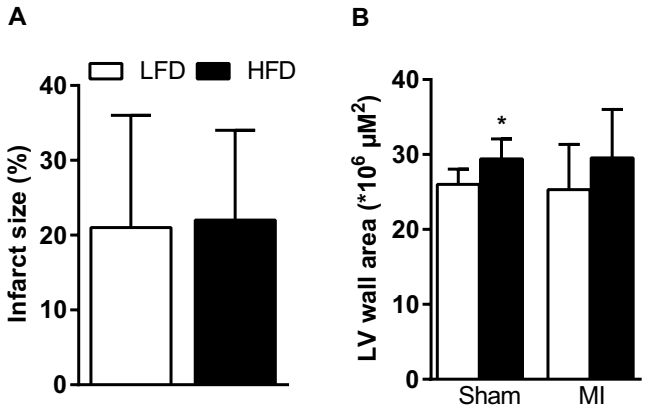

Figure 3 **Effect of LFD and HFD feeding on infarct size and LV wall area.** Male C57Bl/6J mice were fed a low-fat diet (LFD) or a high-fat diet (HFD) for 14 weeks. Two weeks after induction of a myocardial infarction (MI), infarct size was determined (A), total left ventricular (LV) wall area was measured to determine heart size (B). Values are means ± SD (n≥8 per group). * p<0.05 versus LFD fed group.

expected, induction of an MI also compromised cardiac dysfunction by a decreased ejection fraction (-32% LFD versus -43% HFD; both p<0.01) and increased end-systolic volume (LFD MI: +115% versus HFD MI: +192%; both p<0.05) both compared to their respective sham group.

Based on the mean values for end-diastolic and end-systolic volumes, average PV-loops for LFD and HFD MI groups were generated and corresponding end-diastolic and end-systolic PV-relations were calculated (figure 2). Cardiac function measurements revealed that HFD feeding did not lead to a more pronounced LV cardiac dysfunction after an MI compared to LFD fed mice with an MI.

HFD feeding does not lead to differences in infarct size

Differences is MI size may influence cardiac function. For this reason hearts were isolated directly after PV-loop measurements. Infarct area of the LV was determined by staining for collagen using Sirius red. Figure 3 shows that infarct size did not differ between LFD and HFD fed mice (LFD: 20±15% versus HFD: 22±12%; p=0.50). Hearts were unaffected in both sham operated groups (data not shown). Furthermore, total LV wall area was measured, and was found to be slightly elevated in the HFD fed groups. After correction for increased body weights in the HFD groups, no differences were found in LV wall area per gram body weight between all the groups (data not shown).

HFD feeding increases macrophages in the infarcted area of the myocardium

To study the effect of HFD feeding and MI induction on macrophage infiltration in the myocardial tissue, macrophage content in three specific areas of the myocardium was analyzed; the remote 'undamaged/healthy' myocardium, the zone adjacent to the infarcted area (border zone) and the infarcted zone. The macrophage area (as percentage of the total area) stained in the undamaged or healthy area of the sham as well as the

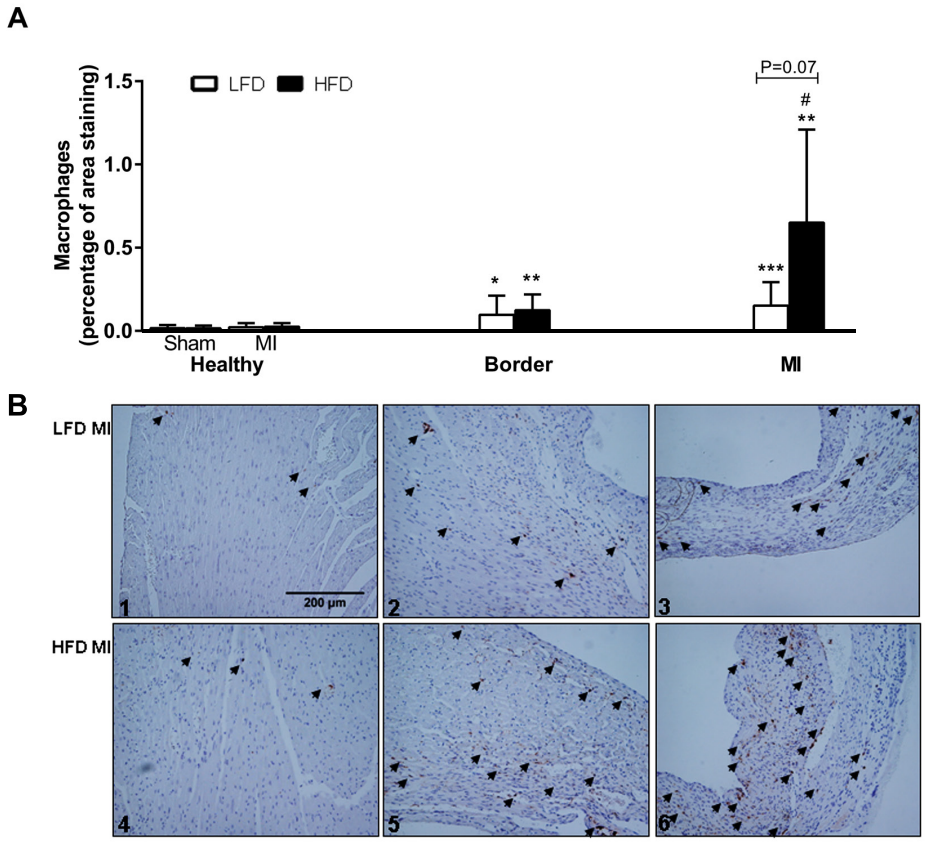

Figure 4 **Effect of LFD and HFD feeding on macrophages after an MI.** Male C57Bl/6J mice were fed a low-fat diet (LFD) or a high-fat diet (HFD) for 14 weeks. Two weeks after induction of a myocardial infarction (MI) macrophages were stained in the ventricles. (A) Percentage of macrophage stained for F4/80 per photograph for healthy myocardium, myocardium adjacent to the infarcted area (border) and the infarcted area. Values are means ± SD (n≥6 per group). * $p<0.05$ versus healthy, *** $p<0.001$ versus healthy; # $p<0.05$ versus border. (B) The upper panels show macrophage staining in LFD fed mice with a section from the healthy myocardium remotely from the infarcted area (1), the border zone (2), and the infarcted area (3). The lower panels show macrophage staining in a HFD fed mice with a section from the healthy myocardium remotely from the infarcted area (4), the border zone (5), and the infarcted area (6). Magnification 200x.

MI groups was very low and did not differ between the four groups (figure 4A). In the border zone a higher percentage of macrophage staining was detected compared to the undamaged zones (LFD MI: +346%, $p<0.05$ and HFD MI: +383%, $p<0.05$), although no differences were observed between the LFD and HFD MI groups. In the infarcted area of the LFD fed group the percentage of macrophages was comparable to the border zone. Interestingly, the percentage of macrophages in the infarcted area in the HFD groups tended to be higher than the LFD fed group (+327%, $p=0.07$). Furthermore, in the infarcted area of the HFD mice the percentage of macrophages was significantly higher compared to the macrophages in the border zone of HFD fed mice (+424%, $p=0.05$). Figure 4B shows representative images of macrophage infiltration in the three selected areas of the myocardium in both LFD and HFD fed mice after MI induction.

Discussion

We tested the hypothesis that HFD feeding, as compared to LFD feeding, aggravates cardiac dysfunction after MI. Although we found that HFD *per se* leads to small deleterious changes in cardiac function, no differences in MI size and cardiac function after MI induction were observed between LFD and HFD fed mice. However macrophage infiltration in infarcted areas of HFD fed mice was more prominent.

As mentioned before, we found that HFD *per se* leads to cardiac dysfunction prior to the MI as indicated by e.g. a tendency towards reduction of end-systolic pressure, a reduction in contractility marker dP/dt_{MAX} and an increase in end-systolic volume. These results are in agreement with a previous study from our group showing that HFD feeding leads to cardiac dysfunction.[13] However, our data are not in agreement with the study of Berthiaume *et al.* who described a cardio-protective role of high saturated fat diet feeding subsequent to an MI in rats.[14] Although, their study was performed in another species and HFD feeding was initiated *after* MI, whereas in our study HFD was started 12 weeks *before* MI. This could indicate that the timing of HFD is important for the effect on cardiac dysfunction after MI induction and this aspect requires further investigation.

We did not observe a difference in mortality rate between LFD fed and HFD fed mice after MI. This is in contrast with findings in clinical studies where an 'obesity paradox' is observed among patients hospitalized for an acute MI. It is shown that patients with higher body mass indices (BMI) are associated with lower long-term mortality.[15, 16] Although some investigators suggest that patient demographics like age, gender and smoking might be confounding factors in these studies[15], others observed this effect to be independent of patient characteristics.[16] One of the proposed mechanisms of the latter findings is an increased awareness of the risk of having an MI for obese people and due to earlier presentation these patients have less severe LV dysfunction. Furthermore, patients with a low BMI might have a worse prognosis after MI due to a lack of a metabolic reserve that may lead to unfavorable hemodynamic changes.[17] Since in our experiment all mice were treated similarly, the first explanation is not relevant in this research setting. Although the LFD MI group had a lower body weight gain compared

Table 1 **Effect of diet intervention on cardiac function after MI.**

	LFD sham	HFD sham	LFD MI	HFD MI
General				
HR (beats/min)	564±31	534±86	521±56	550±49
SV (μL)	29±9	31±9	27±5	26±9
CO (mL/min)	16±5	17±7	14±4	15±5
SW (mm Hg.μL)	1958±739	1647±566	1024±349#	1186±388
E_A (mm Hg/μL)	2.6±0.9	2.1±0.7	2.1±0.4	2.4±3.3
PHT (ms)	5.1±0.8	7.2±2.8 p=0.07	5.8±1.4	6.0±1.0
Systolic				
ESP (mm Hg)	69±3	60±14 p=0.09	52±7###	60±10
ESV (μL)	24±4	29±6*	52±40#	85±50#
EF (%)	57±10	52±11	39±13#	29±17#
dP/dt_{MAX} (mmHg/ms)	5907±1341	4487±1130*	3965±1132#	4519±961
$SB\text{-}E_{ES}$(mm Hg/μL)	1.8±0.5	1.0±0.5*	1.0±0.7#	1.1±0.4
Diastolic				
EDP (mm Hg)	-0.1±1.4	4.6±9.3	-1.2±4.5	0.9±3.5
EDV (μL)	53±11	61±7	79±44	112±47#
Tau (ms)	10.4±1.7	12.2±1.0	12.2±2.1	12.1±1.6
$-dP/dt_{MIN}$ (mm Hg/ms)	-5173±1141	-3589±911**	-3255±902#	-3716±862
$SB\text{-}E_{ED}$ (mm Hg/μL)	0.14±0.05	0.12±0.08	0.17±0.11	0.19±0.11

Mice were fed a low-fat diet (LFD) or a high-fat diet (HFD) for 14 weeks, after 12 weeks the left anterior descending aorta was ligated to induce a myocardial infarction (MI). Two weeks post-MI cardiac function was determined. Left ventricular volume signals obtained by conductance catheter were calibrated by matching EF and CO with corresponding echocardiographic values obtained by measurements four days earlier. Values represent means ± SD (n≥7 per group). * $p<0.05$; ** $p<0.01$ as compared to corresponding LFD group; # $p<0.05$, ### $p<0.001$ as compared to corresponding sham group. HR, heart rate; SV, stroke volume; CO, cardiac output; SW, stroke work; E_A, arterial elastance (afterload); PHT, pressure half time; ESP, end-systolic pressure; ESV, end-systolic volume; EF, ejection fraction; dP/dt_{MAX}, maximal rate of pressure increase; $SB\text{-}E_{ES}$, end-systolic elastance; EDP, end-diastolic pressure; EDV, end-diastolic volume; Tau, relaxation time constant; $-dP/dt_{MIN}$, minimal rate of pressure decline; $SB\text{-}E_{ED}$, end-diastolic elastance (diastolic stiffness).

to the LFD sham group we did not observe differences in cardiac function. Therefore we cannot rule out that severe cardiac dysfunction in lean individuals play a role in the higher mortality observed in the clinical situation.

Apart from the effects of HFD on cardiac function post-MI, inflammation in the heart by for example local macrophage accumulation can also contribute to cardiac malfunctioning. Macrophages are not only involved in clearance of cellular debris post-MI, but also secrete cytokines and growth factors like TGF-β which stimulate fibroblast activation eventually resulting in LV remodeling.[18] Although the increased presence of macrophages at this time point did not lead to differences in cardiac function, we cannot exclude that, in the long-term, secondary effects might cause such differences.

We are confident that study design and hemodynamic measurements are appropriate to conclude that cardiac dysfunction after MI does not differ significantly between LFD and HFD fed mice.

First, HFD feeding resulted in an anticipated increase in body weight, total cholesterol and phospholipids levels. In addition, ligation of the coronary arteries resulted in an expected dilation of the LV, contractile dysfunction and a subsequent remodeling which are all considered to be hallmarks of heart failure.[19-21]

Second, induction of MI was successful as relevant infarctions were observed at histology. Although literature reports about both similar infarct sizes[22, 23] as well as increased infarct sizes[21, 24] in obese rodents, we observed no differences in infarct sizes between LFD and HFD groups. This discrepancy might be due to the fact that in studies that found a different infarct size transgenic mice and rats were used, while we used C57Bl/6J mice on a HFD. This also suggests that HFD feeding *per se* could be of importance as in studies that did not observe infarct size differences, including our study, diets were fed for a minimum of 8 weeks.

Third, as cardiac remodeling is a prolonged process, one could suggest that the time course of our study was too short to observe significant differences in cardiac function between HFD and LFD. However, studies in chow fed mice with a follow-up period up to 6 months post-MI demonstrated that the most prominent decline in LV function occurs 7-14 days after MI.[25, 26] Therefore if HFD leads to deteriorated cardiac function, this would have been observed in our study.

In summary, we tested the hypothesis that HFD feeding affects cardiac function 14 days post-MI. We found that HFD feeding leads to mild cardiac dysfunction, but does not influence infarct size and cardiac dysfunction after MI.

Acknowledgements

We thank Lianne van der Wee-Pals and Erik Offerman for their excellent technical assistance. The F4/80 monoclonal antibody was a kind gift from Dr. P.J. Nijweide (Dept. of Molecular Cell Biology, Leiden University Medical Centre, the Netherlands).

This research was performed within the framework of CTMM, the Center for Translational Molecular Medicine (www.ctmm.nl), project PREDICCt (grant 01C-104), and supported by the Netherlands Heart Foundation, Dutch Diabetes Research Foundation and Dutch Kidney Foundation and Netherlands Consortium for Systems Biology. PCNR is an Established Investigator of the Netherlands Heart Foundation (2009T038).

References

1 Reingold JS, McGavock JM, Kaka S, Tillery T, Victor RG, Szczepaniak LS. Determination of triglyceride in the human myocardium by magnetic resonance spectroscopy: reproducibility and sensitivity of the method. *Am J Physiol Endocrinol Metab* 2005 November;289(5):E935-E939.

2 van der Meer RW, Hammer S, Lamb HJ et al. Effects of short-term high-fat, high-energy diet on hepatic and myocardial triglyceride content in healthy men. *J Clin Endocrinol Metab* 2008 July;93(7):2702-8.

3 Bachmann OP, Dahl DB, Brechtel K et al. Effects of intravenous and dietary lipid challenge on intramyocellular lipid content and the relation with insulin sensitivity in humans. *Diabetes* 2001 November;50(11):2579-84.

4 Schrauwen-Hinderling VB, Kooi ME, Hesselink MK et al. Intramyocellular lipid content and molecular adaptations in response to a 1-week high-fat diet. *Obes Res* 2005 December;13(12):2088-94.

5 McGavock JM, Lingvay I, Zib I et al. Cardiac steatosis in diabetes mellitus: a 1H-magnetic resonance spectroscopy study. *Circulation* 2007 September 4;116(10):1170-5.

6 Eckel RH. Obesity and heart disease: a statement for healthcare professionals from the Nutrition Committee, American Heart Association. *Circulation* 1997 November 4;96(9):3248-50.

7 Kenchaiah S, Evans JC, Levy D et al. Obesity and the risk of heart failure. *N Engl J Med* 2002 August 1;347(5):305-13.

8 Schilling JD, Machkovech HM, Kim AH, Schwedwener R, Schaffer JE. Macrophages modulate cardiac function in lipotoxic cardiomyopathy. *Am J Physiol Heart Circ Physiol* 2012 December;303(11):H1366-H1373.

9 Simms MG, Walley KR. Activated macrophages decrease rat cardiac myocyte contractility: importance of ICAM-1-dependent adhesion. *Am J Physiol* 1999 July;277(1 Pt 2):H253-H260.

10 Shi H, Kokoeva MV, Inouye K, Tzameli I, Yin H, Flier JS. TLR4 links innate immunity and fatty acid-induced insulin resistance. *J Clin Invest* 2006 November;116(11):3015-25.

11 Schwartz EA, Zhang WY, Karnik SK et al. Nutrient modification of the innate immune response: a novel mechanism by which saturated fatty acids greatly amplify monocyte inflammation. *Arterioscler Thromb Vasc Biol* 2010 April;30(4):802-8.

12 Lichtenstein L, Mattijssen F, de Wit NJ et al. Angptl4 protects against severe proinflammatory effects of saturated fat by inhibiting fatty acid uptake into mesenteric lymph node macrophages. *Cell Metab* 2010 December 1;12(6):580-92.

13 Louwe MC, van der Hoorn JW, van den Berg SA et al. Gender-dependent effects of high-fat lard diet on cardiac function in C57Bl/6J mice. *Appl Physiol Nutr Metab* 2012 April;37(2):214-24.

14 Berthiaume JM, Young ME, Chen X, McElfresh TA, Yu X, Chandler MP. Normalizing the metabolic phenotype after myocardial infarction: impact of subchronic high fat feeding. *J Mol Cell Cardiol* 2012 July;53(1):125-33.

15 Mehta L, Devlin W, McCullough PA et al. Impact of body mass index on outcomes after percutaneous coronary intervention in patients with acute myocardial infarction. *Am J Cardiol* 2007 April 1;99(7):906-10.

16 Bucholz EM, Rathore SS, Reid KJ et al. Body mass index and mortality in acute myocardial infarction patients. *Am J Med* 2012 August;125(8):796-803.

17 Steinberg BA, Cannon CP, Hernandez AF, Pan W, Peterson ED, Fonarow GC. Medical therapies and invasive treatments for coronary artery disease by body mass: the "obesity paradox" in the Get With The Guidelines database. *Am J Cardiol* 2007 November 1;100(9):1331-5.

18 Frangogiannis NG. The mechanistic basis of infarct healing. *Antioxid Redox Signal* 2006 November;8(11-12):1907-39.

19 Kehat I, Molkentin JD. Molecular pathways underlying cardiac remodeling during pathophysiological stimulation. *Circulation* 2010 December 21;122(25):2727-35.

20 Thakker GD, Frangogiannis NG, Bujak M et al. Effects of diet-induced obesity on inflammation and remodeling after myocardial infarction. *Am J Physiol Heart Circ Physiol* 2006 November;291(5):H2504-H2514.

21 Greer JJ, Ware DP, Lefer DJ. Myocardial infarction and heart failure in the db/db diabetic mouse. *Am J Physiol Heart Circ Physiol* 2006 January;290(1):H146-H153.

22 Thim T, Bentzon JF, Kristiansen SB et al. Size of myocardial infarction induced by ischaemia/reperfusion is unaltered in rats with metabolic syndrome. *Clin Sci (Lond)* 2006 June;110(6):665-71.

23 Lim SY, Davidson SM, Yellon DM, Smith CC. The cannabinoid CB1 receptor antagonist, rimonabant, protects against acute myocardial infarction. *Basic Res Cardiol* 2009 November;104(6):781-92.

24 Katakam PV, Jordan JE, Snipes JA, Tulbert CD, Miller AW, Busija DW. Myocardial preconditioning against ischemia-reperfusion injury is abolished in Zucker obese rats with insulin resistance. *Am J Physiol Regul Integr Comp Physiol* 2007 February;292(2):R920-R926.

25 Gao XM, Dart AM, Dewar E, Jennings G, Du XJ. Serial echocardiographic assessment of left ventricular dimensions and function after myocardial infarction in mice. *Cardiovasc Res* 2000 January 14;45(2):330-8.

26 Yang F, Liu YH, Yang XP, Xu J, Kapke A, Carretero OA. Myocardial infarction and cardiac remodelling in mice. *Exp Physiol* 2002 September;87(5):547-55.

CHAPTER 4

ABCA1 deficiency protects the heart against injury following myocardial infarction

Manuscript in preparation

Mieke C. Louwe[*1,2], Bart Lammers*[*3], Miguel A. Frias[4], Amanda C. Foks[3], Reeni B. Hildebrand[3], Johan Kuiper[3], Johannes W.A. Smit[1], Theo J.C. Van Berkel[3], Richard W. James[4], Patrick C.N. Rensen[1,2] and Miranda van Eck[3]. * These authors contributed equally to the manuscript*

Dept. of [1]Endocrinology and Metabolic Diseases, [2]Einthoven Laboratory for Experimental Vascular Medicine, Leiden University Medical Center, Leiden, the Netherlands [3]Division of Biopharmaceutics, Leiden Academic Centre for Drug Research, Gorlaeus Laboratories, Leiden University, Leiden, the Netherlands [4]Dept. of Internal Medicine, Endocrinology, Diabetology and Nutrition, University of Geneva, Geneva, Switzerland

ABCA1 deficiency protects the heart against injury following myocardial infarction

Abstract

ATP-binding cassette transporter A1 (ABCA1) exerts anti-atherogenic functions in the pathogenesis of atherosclerosis. We aimed to explore the role of ABCA1 after acute myocardial infarct (MI) induction.

In ABCA1 knockout (KO) mice, wild-type (WT) controls and in WT mice transplanted with ABCA1 KO or WT bone marrow an MI was induced and mice were allowed to recover for two weeks. In addition, isolated hearts from ABCA1 KO and WT mice were subjected to MI induction in a Langendorff perfusion system.

MI size was reduced in both ABCA1 KO mice (-59%, p=0.03) and WT mice transplanted with ABCA1 KO bone marrow (-43%, p=0.12) both compared to their WT controls. MI induction in isolated hearts by Langendorff perfusion showed no effect of ABCA1 deficiency on infarct size. The smaller infarct size *in vivo* in ABCA1 KO mice is thus likely not due to a direct effect of ABCA1 deficiency on myocyte function. Interestingly, after MI, ABCA1 KO mice compared to WT controls, showed higher levels of $CD19^+$ B-lymphocytes (+300%, p=0.02) and $CD3^+$ T-lymphocytes (+420%, p=0.002). Both $CD4^+$ and $CD8^+$ lymphocytes (+460% and +370%; both p=0.002) contributed to the observed increase in $CD3^+$ T-lymphocytes. There were no differences in leukocyte numbers after bone marrow transplantation. However, white blood cell counts were increased 2-7 fold compared to the first experiment.

Although ABCA1 has a protective role in atherosclerosis, it exerts detrimental effects on cardiac function after MI, possibly caused by a reduced activation status of immune cells resulting in less efficient repair after MI.

Introduction

Tangier Disease (TD), resulting in extreme HDL deficiency, is caused by detrimental mutations in the ABCA1 gene.[1-3] Since HDL plays a key protective role in atherosclerosis, by exerting several cardioprotective functions, including anti-oxidative, anti-inflammatory and vasomotor activities[4], the mechanism of action of ABCA1 and its regulation have been investigated extensively.[5-8] Mice deficient for ABCA1 exhibit low plasma HDL levels as well as cholesterol accumulation in peripheral macrophages, a phenotype similar to that of TD patients.[9] Although atherosclerosis-prone mouse models deficient for ABCA1 display impaired cellular cholesterol efflux[10], atherosclerotic lesion development does not increase in these mice[11], probably due to a less atherogenic lipid profile despite the almost complete absence of protective HDL. Deletion of ABCA1 in bone marrow-derived cells, however, did increase atherosclerotic lesion development, coinciding with increased numbers of peritoneal foam cells and impaired cholesterol efflux from macrophages towards apoA-I and HDL, indicating a pronounced anti-atherosclerotic effect of leukocyte ABCA1.[12, 13] In humans, low HDL levels have been correlated to an increased risk of MI; an acute cardiovascular event, often resulting from rupture of advanced atherosclerotic lesions and superimposed thrombus formation.[14]

Inflammatory responses are a critical factor in the balance between adverse ventricular remodeling induced by MI on the one hand[15, 16], and cardiac repair on the other hand.[17] Ischemia induces the Janus kinase 2/signal transducer and activator of transcription 3 (JAK2/STAT3) pathway, an important regulator of cytokine signaling, which plays a vital role in cardioprotection by inducing cytoprotective and survival signals in infarcted hearts.[18] Interestingly, ABCA1 acts as an anti-inflammatory mediator in baby hamster kidney (BHK) cells by inducing signaling through the JAK2/STAT3 pathway in response to binding of lipid-poor apoA-I.[19] Furthermore, ABCA1 exerts important anti-inflammatory properties, due to its key role in modulating the cholesterol content of the plasma membrane and within intracellular compartments.[20, 21] ABCA1 is thus anticipated to be cardioprotective during MI, indirectly by generating HDL as well as directly by its anti-inflammatory effects through JAK2/STAT3 signaling. The actual role of ABCA1 during MI, however, is currently unknown.

In order to investigate the importance of ABCA1 with respect to MI, we performed permanent coronary artery ligation experiments in ABCA1 KO and WT control mice as well as in WT mice transplanted with ABCA1 KO or WT bone marrow. Our results evidently show that ABCA1 has unanticipated unfavorable cardiac effects after MI.

Materials and methods

Animals and bone marrow transplantation

Female WT mice (C57Bl/6J background) and ABCA1 KO mice (kindly provided by Dr. G. Chimini, Centre d'Immunologie de Marseille-Luminy; more than 7 times backcrossed onto a C57Bl/6J background) were used.

To generate mice that specifically lack ABCA1 in bone marrow-derived cells, bone marrow from WT mice and ABCA1 KO mice was transplanted into WT mice as previously described.[22] Briefly, irradiated WT recipients received 5×10^6 bone marrow cells by intravenous injection into the tail vein. After 8 weeks, myocardial infarctions were induced or mice were subjected to a sham operation.

All animals had *ad libitum* access to food and water. At the end of each experiment the mice were sacrificed and hearts and/or blood were isolated for further examination. Animal experiments were approved by the Ethics Committee for Animal Experiments of Leiden University and performed at the Gorlaeus Laboratories of the Leiden Academic Centre for Drug Research in accordance with the National Laws.

Induction of myocardial infarctions

Mice were anesthetized by intraperitoneal injection of a mixture of dormicum (0.7 mg/kg b.w.), dexdomitor (7.2 mg/kg b.w.), and fentanyl (0.07 mg/kg b.w.). Body temperature was maintained at 37°C with an automatic heating pad. Mice were artificially ventilated using a dedicated rodent ventilator (model 845, Harvard Apparatus, Holliston, MA). The left anterior descending (LAD) coronary artery was ligated with a 7-0 Ethilon suture (Johnson and Johnson, New Brunswick, NJ, USA), just distal to the left atrial appendix. All mice that had ischemia, confirmed by bleaching of the left ventricle (LV), and the emergence of arrhythmias, were included in the study. The thorax was closed and the mice received a subcutaneous injection of Anexate (0.5 mg/kg b.w.), Antisedan (2.5 mg/kg b.w.), Naloxon (1.2 mg/kg b.w.), and 50 µL Temgesic/PBS (1.5 µg/50 mL PBS). Thereafter, the mice were allowed to recover on a temperature-controlled heating pad. Mice received another 50 µL Temgesic/PBS (1.5 µg/50 mL PBS) at 24 h after surgery.

Infarct size and immunohistochemistry

Two weeks after MI induction, mice were sacrificed and the arterial tree was perfused *in situ* with PBS (100 mm Hg) for 10 min via a cannula in LV apex. Subsequently, hearts were isolated and cut into four equal 1-2 mm thick slices, perpendicular to the long axis of the heart. The two lower slices, from the middle of the heart to the apex, represent the infarcted area, and were used for infarct quantification. These slices were flat embedded and serial sections (10 µm) were cut using a Leica CM3050S cryostat. To delineate the LV area and infarct area, sections were stained immunohistochemically with Sirius red for collagen. Total LV wall area (including septum) and infarct area were measured with cell^D imaging software (Olympus Soft Imaging Solutions, Tokyo, Japan). Infarct areas were normalized to total LV areas and averaged for individual hearts.

Leukocyte content and flow cytometry

Upon sacrifice, 2 weeks after MI, blood was collected by retro-orbital venous plexus puncture. Leukocyte content was analyzed using an automated Sysmex XT-2000iV Veterinary Hematology analyzer (Sysmex Corporation, Kobe, Japan). For fluorescent activated cell sorting (FACS) analysis, erythrocytes were lysed using erythrocyte lysis buffer (0.15 M NH_4Cl, 10 mM $NaHCO_3$, 0.1 mM EDTA, pH 7.3). Blood cells were subsequent stained (0.25 µg Ab/200,000 cells) for T-lymphocytes (CD3, CD4, and CD8), B-lymphocytes (CD19), monocytes/macrophages (F4/80) and dendritic cells (DC; CD11c). Antibodies were purchased from eBioscience (Vienna, Austria). FACS analyses were performed on a FACS Canto II (BD Biosciences, Mountain View, CA, USA). Data were analyzed using FACSDiva software (BD Biosciences).

Ex vivo Langendorff perfusion

To isolate the heart for Langendorff perfusion, the chest was opened excising the sternum and attached costal cartilages to give adequate access to the mediastinum. The heart was rapidly removed and placed in ice cold (4°C) Krebs–Henseleit buffer and the aorta cannulated. Hearts were then perfused with a Krebs–Henseleit buffer (118.0 mM NaCl; 24.0 mM $NaHCO_3$; 4.0 mM KCl; 1.0 mM NaH_2PO_4; 2.5 mM $CaCl_2$; 1.2 mM $MgCl_2$; 0.5 mM EDTA.Na_2; 10 mM glucose, pH 7.4; gassed with 95% O_2/5% CO_2 at 37°C) in a retrograde fashion with a constant pressure of 110 cm H_2O. The coronary flow rate was measured by timed collection of the perfusate. The hearts were stabilized for 20 min and subsequently exposed to 35 min of no-flow global ischemia followed by 45 min of reperfusion. At the end of the reperfusion period, the heart was immediately frozen. Frozen hearts were cut into 6-7 slices, perpendicular to the long axis of the heart, and incubated with triphenyltetrazolium chloride (TTC) to stain viable myocardium. Total myocardium and infarcted areas were measured from computed images using NIH Image software.

Statistical analysis

Statistically significant differences among the means of the different populations were tested using the unpaired Student's t-test (GraphPad InStat and Prism 4 software). The probability level (alpha) for statistical significance was set at 0.05. Results are expressed as mean ± SEM.

Results

ABCA1 KO mice show decreased coronary artery ligation-induced myocardial infarction

To investigate the effects of ABCA1 deficiency on MI-induced damage in vivo, we subjected ABCA1 KO and WT mice to LAD coronary artery ligation. Two weeks after induction of MI, infarct size was quantified. Surprisingly, despite the anticipated cardioprotective functions of ABCA1, ABCA1 KO mice displayed a substantial 59% reduction in MI size as compared to WT mice (p=0.03; figure 1, left panel). No differences in total LV wall area were found (figure 1, right panel), indicating that the observed reduction in MI did not result from alterations in LV size.

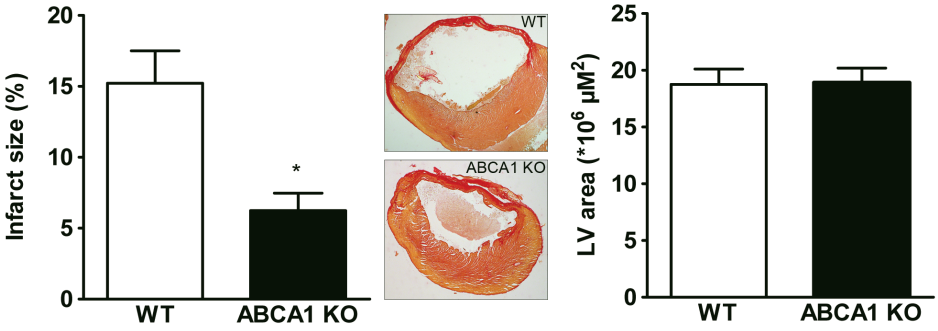

Figure 1 **Reduced myocardial infarct size in ABCA1 KO mice after coronary artery ligation.** Two weeks after induction of myocardial infarction (MI) by ligation of the left anterior descending (LAD) coronary artery, infarct size was determined (left panel). Representative cross sections are shown, stained with Sirius red to visualize the collagen-rich infarcted area (middle panels). Total left ventricle (LV) wall area was determined as a general indicator of heart size (right panel). Values are means ± SEM (n≥4 per group). *p<0.05

ABCA1 KO mice have higher circulating white blood cell and lymphocyte numbers after coronary artery ligation-induced myocardial infarction

Before MI induction, no differences in leukocyte subsets were observed between ABCA1 KO and WT mice (data not shown). Two weeks after MI, however, total leukocyte counts were 2.9-fold higher in ABCA1 KO mice (p<0.05; figure 2), which was primarily the result of augmented numbers of circulating lymphocytes (4.6-fold; p=0.002). To further investigate the increased lymphocyte population in the circulation of ABCA1 KO mice after MI, blood cells were subjected to FACS analysis (figure 3). Before MI, no differences

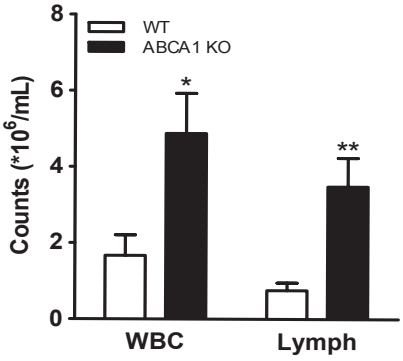

Figure 2 **Increased WBC and lymphocytes in ABCA1 KO mice after MI induction by coronary artery ligation.** Two weeks after induction of a myocardial infarction (MI), total white blood cells (WBC) and lymphocytes in plasma were determined with a hematology analyzer. Values are means ± SEM (n≥4 mice per group). *p<0.05, **p<0.01

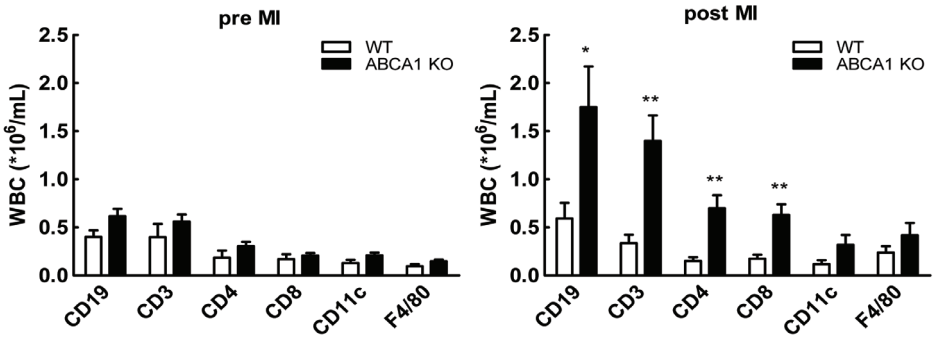

Figure 3 **Increased circulating T- and B-cells in ABCA1 KO mice after MI induction by coronary artery ligation *in vivo*.** Isolated white blood cells (WBC) were stained for T-cells (CD3+, CD4+, and CD8+), B-cells (CD19+), monocytes/macrophages (F4/80+) and dendritic cells (CD11c+) and analyzed by flow cytometry before (left panel) and after myocardial infarction (MI) (right panel). Values are means ± SEM (n≥4 mice per group). *p<0.05, **p<0.01

in T-lymphocytes ($CD3^+$, $CD4^+$, and $CD8^+$), B-lymphocytes ($CD19^+$), dendritic cells ($CD11c^+$) or monocytes/macrophages ($F4/80^+$) were observed between both genotypes (figure 3 left panel). After MI, however, $CD3^+$ T-lymphocytes increased a striking 4.2-fold (p=0.002; figure 3 right panel). $CD4^+$ T-helper lymphocytes (4.6-fold increase; p=0.002) and $CD8^+$ cytotoxic T-lymphocytes (3.7-fold increase; p=0.002) both contributed to this phenomenon. In addition, ABCA1 KO mice displayed a clear 3.0-fold increase (p=0.02) in $CD19^+$ B-lymphocytes after MI. In contrast, monocytes/macrophages ($F4/80^+$) and dendritic cells ($CD11c^+$) did not change between both genotypes upon MI. This indicates that the induction of MI in ABCA1 KO mice primarily induced common lymphoid progenitor (CLP)-derived cells, such as T- and B-lymphocytes, rather than common myeloid progenitor (CMP)-derived cells including monocytes/macrophages and dendritic cells.

ABCA1 KO hearts show unaltered myocardial infarction in a Langendorff perfusion system *ex vivo*

ABCA1 KO mice have been shown to develop cardiomegaly.[23] To determine the direct effects of ABCA1 deficiency on myocyte function during ischemia, MI was induced *ex vivo* in isolated hearts from ABCA1 KO mice and WT controls using the Langendorff perfusion method. After 35 minutes of no-flow global ischemia followed by 45 minutes of reperfusion, only a tendency towards a 15% decrease (p=0.47; figure 4) in infarct size was observed in hearts from ABCA1 KO mice. These data thus indicate that ABCA1-deficiency in cardiomyocytes is not contributing to the smaller infarct size observed in ABCA1 KO mice after coronary artery ligation.

Hematopoietic deficiency for ABCA1 tends to reduce coronary artery ligation-induced myocardial infarction

Next, we investigated if the observed decrease in MI in ABCA1 KO mice results from ABCA1-deficiency in bone marrow-derived cells that may be involved in MI-induced cardiac remodeling. Hereto, we induced MI in WT mice, transplanted with bone marrow from ABCA1 KO vs WT mice. Quantification of infarct size two weeks after MI induction showed a strong trend towards a reduction in MI size (-43%; p=0.12) (figure 5, left panel) without an effect on LV wall area (figure 5, right panel) in mice transplanted with ABCA1 KO as compared to WT bone marrow.

Hematopoietic deficiency for ABCA1 does not affect circulating white blood cell numbers after coronary artery ligation-induced myocardial infarction

Two weeks after MI induction, blood cells were subjected to FACS analysis to investigate the numbers of circulating lymphocytes (figure 6). No difference in T-lymphocytes ($CD3^+$, $CD4^+$, and $CD8^+$), B-lymphocytes ($CD19^+$), dendritic cells ($CD11c^+$) or monocytes/macrophages ($F4/80^+$) were observed between mice transplanted with ABCA1 KO vs WT bone marrow. Strikingly, the number of white blood cell (WBC) counts *per se* was 2-7 fold higher in mice transplanted with WT bone marrow compared to the WT mice in the first *in vivo* experiment. Since a WT control group without bone marrow transplantation in the second experiment also did not show an increase in WBC counts (data not shown) this indicates that the observed increase in WBC counts is induced by the transplantation procedure, combined with MI induction.

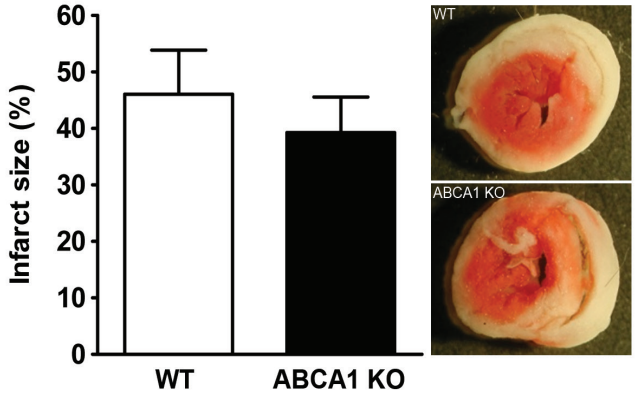

Figure 4 **Unaltered infarcted area of isolated hearts from ABCA1 KO mice subjected to ischemia/reperfusion *ex vivo*.** Isolated hearts were stabilized for 20 minutes in a Langendorff perfusion system, followed by 35 minutes of no-flow global ischemia, and 45 minutes of reperfusion. Infarct size was measured with cell^D imaging software. Infarct areas were normalized to total left ventricular areas and averaged for individual hearts (left panel). Values are means ± SEM (n≥5 mice per group). Representative cross sections are shown, stained with TTC to determine viable myocardium (red staining; right panels).

Discussion

In the current study we show for the first time that mice lacking ABCA1, thereby having reduced HDL levels, are protected against cardiac damage after permanent coronary artery ligation. At first sight, this is remarkable as several studies have revealed protective effects of HDL after MI.[24, 25] HDL protects against MI by inhibiting ischemia-induced cardiomyocyte apoptosis and by reducing the recruitment of inflammatory neutrophils into the infarcted area.[25] In addition, intravenous injection of apoA-I before the onset of reperfusion after MI reduced TNF-α and IL-6 expression in the heart, as well as suppressed ICAM-1 expression in the heart, thereby diminishing neutrophil adherence and subsequent reduced myocyte injury.[24] On the other hand, mice lacking the HDL receptor scavenger receptor BI (SR-BI), have high levels of HDL but spontaneously develop MI.[26, 27] Deficiency of ABCA1 not only results in the lack of HDL, but also highly attenuates total cholesterol levels.[28] Although cholesterol levels are positively correlated with MI risk in humans[29], differential results have been obtained in murine MI models.[30-32]

Interestingly, induction of MI in ABCA1 KO mice resulted in a substantial increase in circulating leukocytes due to higher numbers of circulating B- and T-lymphocytes. No differences in leukocyte numbers or subsets were found prior to coronary artery ligation. Therefore, the increased inflammatory environment, caused by the induction of MI, might have attributed to induce this phenotype in ABCA1 KO mice. Proliferation of LSK stem cells and committed CMPs is regulated by cholesterol efflux mechanisms, whereby HDL suppresses proliferation by facilitating cellular cholesterol efflux via the ABC-transporters ABCA1 and ABCG1.[33] However, mice lacking ABCA1 and ABCG1 did not show an increase in CLP cells that give rise to B-and T-lymphocytes.[33]

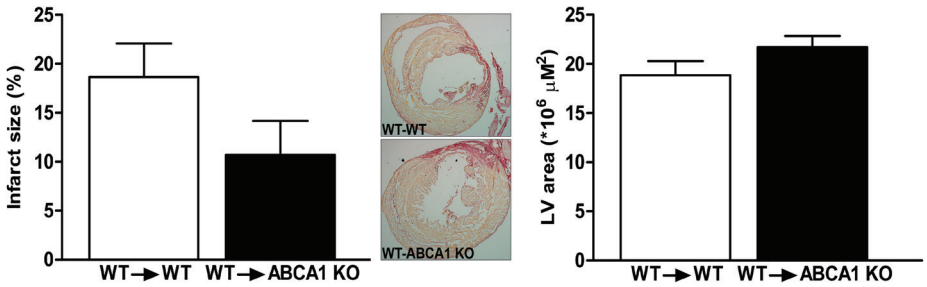

Figure 5 **MI size tends to be lower in WT mice transplanted with ABCA1 KO bone marrow.** WT mice were transplanted with bone marrow from WT or ABCA1 KO mice. After 8 weeks, myocardial infarction (MI) was induced by ligation of the LAD coronary artery. Two weeks later, infarct size was determined (left panel). Representative cross sections are shown, stained with Sirius red to visualize the collagen-rich infarcted area (middle panels). Total left ventricle (LV) wall area was determined as a general indicator of heart size (right panel). WT->WT, WT mice transplanted with WT bone marrow, ABCA1 KO->WT, WT mice transplanted with ABCA1 KO bone marrow. Values are means ± SEM (n≥4 per group).

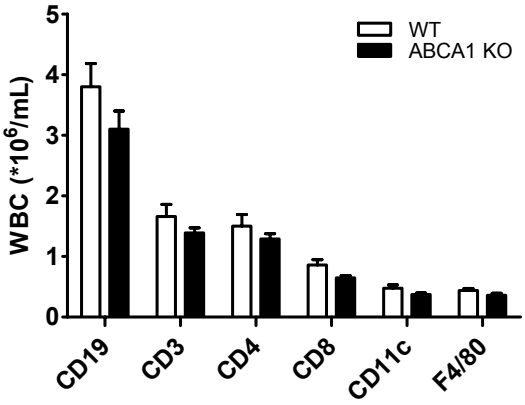

Figure 6 **Comparable circulating T- and B-lymphocytes in WT mice transplanted with ABCA1 KO and WT bone marrow after MI induction by coronary artery ligation *in vivo*.** Isolated white blood cells (WBC) were stained for T-cells (CD3+, CD4+, and CD8+), B-cells (CD19+), monocytes/macrophages (F4/80+) and dendritic cells (CD11c+) and analyzed by flow cytometry after MI. Values are means ± SEM (n≥4 mice per group).

Importantly, we have previously shown that deficiency of leukocyte ABCA1 increases circulating lymphocytes upon induction of atherosclerosis[12], similarly as observed in the current study upon coronary artery ligation. Since the infarct size in ABCA1 KO mice was drastically attenuated, the higher number of circulating lymphocytes might have been mediating tissue repair. This hypothesis is strengthened by the fact that studying the effect of ischemia on isolated hearts from ABCA1 KO and WT mice, thus in absence of blood cells, did not show differences in infarct size using the Langendorff perfusion system.

T-lymphocytes rapidly accumulate in the heart after ischemia/reperfusion injury. Specifically, $CD4^+$ T-lymphocytes were identified as protective mediators of myocardial perfusion injury after MI.[33,34] Recently, Wara *et al.* showed that LSK-derived CMPs, but not CLPs, can differentiate into proangiogenic cells, thereby promoting neovascularization.[34] Instead, $CD4^+$ lymphocytes modulate the influx of among others monocytes, which is a prerequisite for proper myocardial wound healing.[35, 36] Moreover, intramyocardial injection of B-lymphocytes into early post-ischemic myocardium has been shown to preserve cardiac function[37], emphasizing the protective roles of B- and T-lymphocytes upon MI.

The most pronounced lipid phenotype of ABCA1 deficiency is the near absence of HDL cholesterol in the circulation.[23] It is therefore plausible that the absence of HDL, at least in part, promoted the observed secondary effects on lymphocyte numbers upon MI. In agreement, Wilhelm *et al.* observed increased circulating lymphocytes in Western-type diet fed LDLr KO mice lacking apoA-I.[38] ApoA-I KO mice, like ABCA1 KO mice, have virtually no circulating HDL. To provide definitive proof for the distinct importance of ABCA1 and HDL, MI should be induced in apoA-I KO mice, which express ABCA1, but have virtually no HDL.

To elucidate the effect of ABCA1-deficiency in leukocytes on MI, bone marrow was transplanted from ABCA1 KO and WT mice to WT mice, after which MI was induced by coronary artery ligation. A strong trend was observed towards a reduction in MI size (-43%), which just did not reach statistical significance because of large interindividual variation. However, these data strongly suggest that hematopoietic ABCA1 deficiency underlies the difference in MI size observed in the first experiment. No differences were observed in CLP- nor in CMP-derived cells after bone marrow transplantation. However, it should be noted that WBC numbers were dramatically higher in both transplanted groups compared to the non-transplanted animals in the first experiment. Hofmann *et al.* previously showed that the mere presence of CD4+ T-lymphocytes was not sufficient for proper wound healing and that T-cell receptor activation by released cardiac autoantigens after MI is a prerequisite.[35] Furthermore, Wilhelm *et al.* was the first to show that not only monocytes/macrophages become cholesterol enriched but also T- and B-lymphocytes and this cholesterol enrichment seems to be the stimulus that initiates T-lymphocyte activation.[38, 39] One could hypothesize that the inability of immune cells to efflux cholesterol could enhance the activation status of these cells towards more efficient repair of damage induced by MI. However, it remains to be determined how ABCA1 expressing leukocytes exactly exert their detrimental effects during cardiac wound healing.

In conclusion, despite its protective effects regarding the development of atherosclerosis, ABCA1 has adverse effects on cardiac function after MI, which is possibly related to an increased activation status, rather than an increase in the absolute numbers of B- and T-lymphocytes. Importantly, although ABCA1 is considered a potential therapeutic target to treat atherosclerosis, strategies aiming at upregulation of ABCA1 function should be pursued with care in the light of potential adverse effects on cardiac remodeling following MI.

Acknowledgements

This work was supported by the Netherlands Heart Foundation (Established Investigator Grants 2007T056 (B.L. and M.V.E.) and 2009T038 (P.C.N.R.). Additional support was obtained from CTMM, the Center for Translational Molecular Medicine (www.ctmm.nl), project PREDICCt (grant 01C-104), the Dutch Diabetes Research Foundation, and the Dutch Kidney Foundation.

References

1 Bodzioch M, Orso E, Klucken J et al. The gene encoding ATP-binding cassette transporter 1 is mutated in Tangier disease. *Nat Genet* 1999 August;22(4):347-51.

2 Brooks-Wilson A, Marcil M, Clee SM et al. Mutations in ABC1 in Tangier disease and familial high-density lipoprotein deficiency. *Nat Genet* 1999 August;22(4):336-45.

3 Rust S, Rosier M, Funke H et al. Tangier disease is caused by mutations in the gene encoding ATP-binding cassette transporter 1. *Nat Genet* 1999 August;22(4):352-5.

4 Assmann G, Gotto AM, Jr. HDL cholesterol and protective factors in atherosclerosis. *Circulation* 2004 June 15;109(23 Suppl 1):III8-14.

5 Attie AD, Kastelein JP, Hayden MR. Pivotal role of ABCA1 in reverse cholesterol transport influencing HDL levels and susceptibility to atherosclerosis. *J Lipid Res* 2001 November;42(11):1717-26.

6 Brunham LR, Singaraja RR, Hayden MR. Variations on a gene: rare and common variants in ABCA1 and their impact on HDL cholesterol levels and atherosclerosis. *Annu Rev Nutr* 2006;26:105-29.

7 Oram JF. HDL apolipoproteins and ABCA1: partners in the removal of excess cellular cholesterol. *Arterioscler Thromb Vasc Biol* 2003 May 1;23(5):720-7.

8 Ye D, Lammers B, Zhao Y, Meurs I, Van Berkel TJ, van Eck M. ATP-binding cassette transporters A1 and G1, HDL metabolism, cholesterol efflux, and inflammation: important targets for the treatment of atherosclerosis. *Curr Drug Targets* 2011 May;12(5):647-60.

9 McNeish J, Aiello RJ, Guyot D et al. High density lipoprotein deficiency and foam cell accumulation in mice with targeted disruption of ATP-binding cassette transporter-1. *Proc Natl Acad Sci U S A* 2000 April 11;97(8):4245-50.

10 Schmitz G, Kaminski WE, Orso E. ABC transporters in cellular lipid trafficking. *Curr Opin Lipidol* 2000 October;11(5):493-501.

11 Aiello RJ, Brees D, Bourassa PA et al. Increased atherosclerosis in hyperlipidemic mice with inactivation of ABCA1 in macrophages. *Arterioscler Thromb Vasc Biol* 2002 April 1;22(4):630-7.

12 van Eck M, Bos IS, Kaminski WE et al. Leukocyte ABCA1 controls susceptibility to atherosclerosis and macrophage recruitment into tissues. *Proc Natl Acad Sci U S A* 2002 April 30;99(9):6298-303.

13 Zhao Y, Pennings M, Vrins CL et al. Hypocholesterolemia, foam cell accumulation, but no atherosclerosis in mice lacking ABC-transporter A1 and scavenger receptor BI. *Atherosclerosis* 2011 October;218(2):314-22.

14 Duffy D, Holmes DN, Roe MT, Peterson ED. The impact of high-density lipoprotein cholesterol levels on long-term outcomes after non-ST-elevation myocardial infarction. *Am Heart J* 2012 April;163(4):705-13.

15 Frangogiannis NG, Smith CW, Entman ML. The inflammatory response in myocardial infarction. *Cardiovasc Res* 2002 January;53(1):31-47.

16 Nian M, Lee P, Khaper N, Liu P. Inflammatory cytokines and postmyocardial infarction remodeling. *Circ Res* 2004 June 25;94(12):1543-53.

17 Frangogiannis NG. Regulation of the inflammatory response in cardiac repair. *Circ Res* 2012 January 6;110(1):159-73.

18 Boengler K, Hilfiker-Kleiner D, Drexler H, Heusch G, Schulz R. The myocardial JAK/STAT pathway: from protection to failure. *Pharmacol Ther* 2008 November;120(2):172-85.

19 Tang C, Liu Y, Kessler PS, Vaughan AM, Oram JF. The macrophage cholesterol exporter ABCA1 functions as an anti-inflammatory receptor. *J Biol Chem* 2009 November 20;284(47):32336-43.

20 Jahangiri A, de Beer MC, Noffsinger V et al. HDL remodeling during the acute phase response. *Arterioscler Thromb Vasc Biol* 2009 February;29(2):261-7.

21 McGillicuddy FC, de la Llera MM, Hinkle CC et al. Inflammation impairs reverse cholesterol transport in vivo. *Circulation* 2009 March 3;119(8):1135-45.

22 Out R, Hoekstra M, Hildebrand RB et al. Macrophage ABCG1 deletion disrupts lipid homeostasis in alveolar macrophages and moderately influences atherosclerotic lesion development in LDL receptor-deficient mice. *Arterioscler Thromb Vasc Biol* 2006 October;26(10):2295-300.

23 Christiansen-Weber TA, Voland JR, Wu Y et al. Functional loss of ABCA1 in mice causes severe placental malformation, aberrant lipid distribution, and kidney glomerulonephritis as well as high-density lipoprotein cholesterol deficiency. *Am J Pathol* 2000 September;157(3):1017-29.

24 Gu SS, Shi N, Wu MP. The protective effect of ApolipoproteinA-I on myocardial ischemia-reperfusion injury in rats. *Life Sci* 2007 August 9;81(9):702-9.

25 Theilmeier G, Schmidt C, Herrmann J et al. High-density lipoproteins and their constituent, sphingosine-1-phosphate, directly protect the heart against ischemia/reperfusion injury in vivo via the S1P3 lysophospholipid receptor. *Circulation* 2006 September 26;114(13):1403-9.

26 Braun A, Trigatti BL, Post MJ et al. Loss of SR-BI expression leads to the early onset of occlusive atherosclerotic coronary artery disease, spontaneous myocardial infarctions, severe cardiac dysfunction, and premature death in apolipoprotein E-deficient mice. *Circ Res* 2002 February 22;90(3):270-6.

27 Zhang S, Picard MH, Vasile E et al. Diet-induced occlusive coronary atherosclerosis, myocardial infarction, cardiac dysfunction, and premature death in scavenger receptor class B type I-deficient, hypomorphic apolipoprotein ER61 mice. *Circulation* 2005 June 28;111(25):3457-64.

28 Drobnik W, Lindenthal B, Lieser B et al. ATP-binding cassette transporter A1 (ABCA1) affects total body sterol metabolism. *Gastroenterology* 2001 April;120(5):1203-11.

29 Castelli WP, Garrison RJ, Wilson PW, Abbott RD, Kalousdian S, Kannel WB. Incidence of coronary heart disease and lipoprotein cholesterol levels. The Framingham Study. *JAMA* 1986 November 28;256(20):2835-8.

30 Girod WG, Jones SP, Sieber N, Aw TY, Lefer DJ. Effects of hypercholesterolemia on myocardial ischemia-reperfusion injury in LDL receptor-deficient mice. *Arterioscler Thromb Vasc Biol* 1999 November;19(11):2776-81.

31 Jones SP, Girod WG, Marotti KR, Aw TY, Lefer DJ. Acute exposure to a high cholesterol diet attenuates myocardial ischemia-reperfusion injury in cholesteryl ester transfer protein mice. *Coron Artery Dis* 2001 February;12(1):37-44.

32 Van Craeyveld E, Jacobs F, Gordts SC, De Geest B. Low-density lipoprotein receptor gene transfer in hypercholesterolemic mice improves cardiac function after myocardial infarction. *Gene Ther* 2012 August;19(8):860-71.

33 Yvan-Charvet L, Pagler T, Gautier EL et al. ATP-binding cassette transporters and HDL suppress hematopoietic stem cell proliferation. *Science* 2010 June 25;328(5986):1689-93.

34 Wara AK, Croce K, Foo S et al. Bone marrow-derived CMPs and GMPs represent highly functional proangiogenic cells: implications for ischemic cardiovascular disease. *Blood* 2011 December 8;118(24):6461-4.

35 Hofmann U, Beyersdorf N, Weirather J et al. Activation of CD4+ T lymphocytes improves wound healing and survival after experimental myocardial infarction in mice. *Circulation* 2012 April 3;125(13):1652-63.

36 Nahrendorf M, Swirski FK, Aikawa E et al. The healing myocardium sequentially mobilizes two monocyte subsets with divergent and complementary functions. *J Exp Med* 2007 November 26;204(12):3037-47.

37 Goodchild TT, Robinson KA, Pang W et al. Bone marrow-derived B cells preserve ventricular function after acute myocardial infarction. *JACC Cardiovasc Interv* 2009 October;2(10):1005-16.

38 Wilhelm AJ, Zabalawi M, Grayson JM et al. Apolipoprotein A-I and its role in lymphocyte cholesterol homeostasis and autoimmunity. *Arterioscler Thromb Vasc Biol* 2009 June;29(6):843-9.

39 Wilhelm AJ, Zabalawi M, Owen JS et al. Apolipoprotein A-I modulates regulatory T cells in autoimmune LDLr-/-, ApoA-I-/- mice. *J Biol Chem* 2010 November 12;285(46):36158-69.

CHAPTER 5

RP105 deficiency aggravates cardiac dysfunction after myocardial infarction in mice

Submitted for publication

Mieke C. Louwe[*1,3], Jacco C. Karper*[*2,3], Margreet R. de Vries[2,3], Antonius J.N.M. Bastiaansen[2,3], José W.A. van der Hoorn[6], Ko Willems van Dijk[1,4], Patrick C.N. Rensen[1,3], Paul Steendijk[5], Johannes W.A. Smit[1] and Paul H.A. Quax[2,3]. * These authors contributed equally to the manuscript*

[1]Dept. of Endocrinology and Metabolic Diseases, [2]Dept. of Vascular Surgery, [3]Einthoven Laboratory for Experimental Vascular Medicine, [4]Dept. of Human Genetics, [5]Dept. of Cardiology; Leiden University Medical Center, Leiden, the Netherlands [6]TNO - Metabolic Health Research, Leiden, the Netherlands

RP105 deficiency aggravates cardiac dysfunction after myocardial infarction in mice

Abstract

Toll-like receptor 4 (TLR4), a receptor of the innate immune system, is suggested to have detrimental effects on cardiac function after myocardial infarction (MI). RP105 (CD180) is a TLR4 homolog lacking the intracellular signalling domain that competitively inhibits TLR4-signalling. Thus, we hypothesized that RP105 deficiency, by amplifying TLR4 signalling, would lead to aggravated cardiac dysfunction after MI.

First, whole blood from RP105$^{-/-}$ and wild-type (WT) male C57Bl/6N mice was stimulated with LPS, which induced a strong inflammatory TNFα response in RP105$^{-/-}$ mice. Then, baseline heart function was assessed by left ventricular pressure-volume relationships which were not different between RP105$^{-/-}$ and WT mice. Permanent ligation of the left anterior descending coronary artery was performed to induce MI. Infarct sizes were analysed by (immuno)histology and did not differ. Fifteen days post MI heart function was assessed and RP105$^{-/-}$ mice had significantly higher heart rate (+21%, $p<0.01$), end-systolic volume index (+57%, $p<0.05$), end-systolic pressure (+22%, $p<0.05$) and lower relaxation time constant Tau (-12%, $p<0.05$), and a tendency for increased end-diastolic volume index (+42%, $p<0.06$), compared to WT mice. In the area adjacent to the infarct zone, compared to the healthy myocardium, levels of RP105, TLR4 and the endogenous TLR4 ligand fibronectin-EDA were increased as well as the number of macrophages, however this was not different between both groups.

Deficiency of the endogenous TLR4 inhibitor RP105 leads to an enhanced inflammatory status and more pronounced cardiac dilatation after induction of MI, underscoring the role of the TLR4 pathway in post-infarction remodelling.

Introduction

Cardiovascular diseases remain the leading cause of death in the western countries, which is mainly accounted for by the high incidence of myocardial infarction (MI). Although survival after MI has improved significantly due to novel medical strategies and interventions, the incidence and prevalence of MI related morbidity is increasing which is mainly due to development of congestive heart failure (CHF).[1, 2] CHF is the result of a remodelling response of the ventricle upon reduced contraction capacity after cardiac damage such as MI.[2] During the last decades the immune system was demonstrated to a play major role in myocardial repair and remodelling. Evidence accumulates that prolongation of the post-infarction inflammatory response leads to increased remodelling and thereby CHF progression.[3-5] Therefore, new strategies to intervene in the pathogenesis of CHF may be worthwhile, which can be achieved by immediate anticipation and tackling of the inflammatory- and matrix degeneration processes that have been initiated by the immune system.[6]

Toll like receptors (TLR) are part of the innate immune system and are capable of recognizing Pathogen Associated Molecular Patterns (PAMPs) as well as Damage Associated Molecular Patterns (DAMPs). PAMPs are parts of exogenous pathogens such as bacteria while DAMPs, like fibronectin-extra domain-A (EDA) or Heat Shock Protein, may become available after cell stress or tissue damage/injury without the involvement of exogenous pathogens.[7] They have been widely associated with atherosclerotic plaque formation, restenosis and vein graft failure; all processes that may initiate ischemia or MI, resulting in cardiac remodelling.[8-10] One of the most studied TLRs is TLR4, which is present on circulating cells and cardiomyocytes. Cardiac expression of TLR4 was shown to be upregulated in cardiomyopathy.[11] In preclinical studies TLR4 was shown to

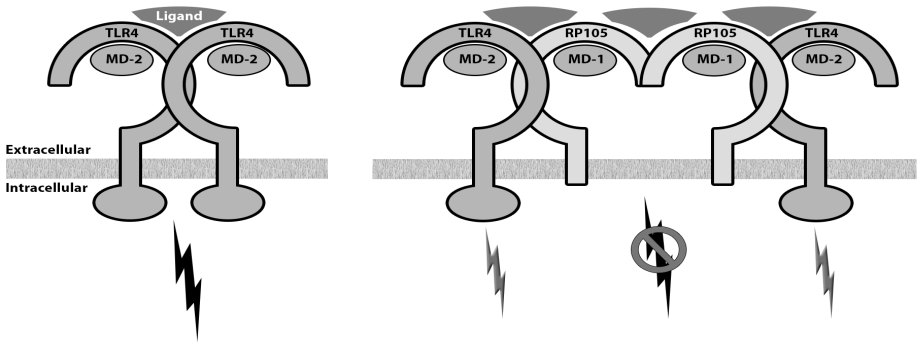

Figure 1 **Schematic model of the TLR4-MD2 and RP105-MD1 complex.** Activation of the TLR4-MD2 heterodimer by ligand binding results in activation of the intracellular signaling domain thereby initiating a downstream signaling cascade (left panel). The formation of the unusual 2:2 homodimer by TLR4-MD2 and RP105-MD1 alters the TLR4 signaling cascade, whereas RP105 dimerization by itself has no signaling capacity at all as it lacks the intracellular Toll Interleukin Receptor (TIR) domain (right panel). Adapted from Otho *et al.*[25]

play an important role in MI healing, left ventricular (LV) remodelling and functional impairment following MI.[12] Additionally, intervention with a specific TLR4 antagonist Eritoran was demonstrated to be protective against remodelling.[13]

TLR-signalling is mainly regulated by accessory molecules[14], and no role for these accessory molecules in cardiac remodelling has been defined yet. RP105, one of these molecules, resides on the cell surface and has a high extracellular structural similarity to TLR4 (figure 1).[15] In addition, like TLR4, whose signalling depends on association with the extracellular accessory protein MD-2, RP105 surface expression depends on co-expression of the MD-2 homolog: MD-1. However, in contrast to TLR4, RP105 lacks the intracellular Toll Interleukin Receptor (TIR) domain that is essential to initiate cellular activation. As such RP105 is an inhibitor of the TLR4 signaling pathway.[16, 17] Whereas no direct ligands have been found for RP105, strong indications exist that it can bind TLR4 ligands, thereby influencing TLR4 signalling and dampening the inflammatory responses induced by TLR4 activation.

As TLR4 activation has been shown to enhance cardiac remodelling after MI, we hypothesized that RP105 deficiency would aggravate these effects, through reduced inhibition (thus by stimulation) of TLR4 signalling. In this study we demonstrate that RP105 deficiency indeed has a functional role in cardiac remodeling, since systolic and diastolic cardiac function indices are affected after MI.

Materials and methods

Animals and experimental design

Studies were performed with 10-12 week old, male RP105-deficient ($RP105^{-/-}$) mice bred in our animal facility and wild-type (WT) mice (Charles River, Maastricht, the Netherlands), both on a C57Bl/6N background. Animals were housed in a temperature and humidity controlled room on a 12:12-h light-dark cycle with *ad libitum* access to water and normal chow diet. Body weights were measured weekly. MI was induced by coronary ligation (see below) at day 0 in $RP105^{-/-}$ (n=12) and WT (n=12) mice. Subsequently, cardiac function assessments by pressure-volume loops (PV-loops) were performed at day 15. To obtain baseline cardiac function, additional PV-loop measurements were performed in a separate group of animals ($RP105^{-/-}$, n=4; WT, n=4) without MI. After PV-loop measurements the mice were sacrificed and hearts were isolated for further examination. The protocol was approved by the Animal Ethics Committee from the Leiden University Medical Center and was conform to the *Guide for Care and Use of Laboratory Animals* (NIH publication No.85-23, Revised 1996).

Whole blood TNFα stimulation assay

In order to investigate the inflammatory response at baseline of the different groups, venous blood via a tail vein cut was collected and suspended 1:25 with RPMI 1640 (Gibco 52400-025, Paisley, UK) supplemented with non-essential amino acids (PAA M11-003, Pasching, Austria)

and glutamax (Gibco 35050). Blood from both WT and RP105$^{-/-}$ mice was incubated overnight at 37°C in absence and presence of LPS in the concentrations 25 ng/mL and 50 ng/mL. Subsequently, TNFα levels were measured by ELISA (BD Biosciences).

Induction of myocardial infarctions

Mice were anesthetized by an intraperitoneal injection of a mixture of dormicum (0.7 mg/kg BW), dexdomitor (7.2 mg/kg BW) and fentanyl (0.07 mg/kg BW). Body temperature was maintained at 37°C using a temperature controlled, automatic heating pad. Mice were artificially ventilated using a dedicated mouse ventilator (model 845, Harvard Apparatus, Holliston, MA). The left anterior descending coronary artery (LAD) was ligated with a 7-0 ethilon suture (Johnson and Johnson, New Brunswick, NJ, USA), just distal to the left atrial appendage. Ischemia was visually confirmed by bleaching of the LV. The thorax was closed and the mice received an intraperitoneal injection of anexate (0.5 mg/kg BW), antisedan (2.5 mg/kg BW), naloxon (1.2 mg/kg BW) to antagonize the anesthesia. Analgesic temgesic (1.5 μg in 50 μL PBS) was administered subcutaneously. Thereafter, the mice were allowed to recover on a temperature controlled heating pad.

Hemodynamic measurements

Thirteen days after induction of the MI, transthoracic, cardiac echocardiography was performed using a VisualSonics Vevo 770 with a 30 MHz ultrasound transducer (VisualSonics, Toronto, Canada) as described earlier.[18] The following parameters were obtained: heart rate (HR), stroke volume (SV), cardiac output (CO), end-diastolic volume (EDV) end-systolic volume (ESV), ejection fraction (EF), fractional area change (FAC) and area change. Briefly, mice were anesthetized with 3% isoflurane, and placed supine on a temperature-controlled animal platform. Parasternal long axis and short axis images were recorded in all animals. Analysis of the data was performed with software provided by VisualSonics. Subsequently, 2 days later (at day 15 post MI), LV function was assessed by invasive PV-loops as described earlier.[18] Mice were anesthetized with a starting dose of 4% isoflurane and a maintenance dose of 1.5% isoflurane. After intubation mice were ventilated and the jugular vein was cannulated for infusion of hypertonic saline to determine parallel conductance. Via the right carotid artery a 1.2F PV catheter (FTS-1212B-4518, Scisense Inc., London, Ontario, Canada) was placed into the LV. The catheter was connected to a Scisense ADV signal processor (Scisense Inc) to generate high-fidelity pressure and volume signals. Positioning of the catheter was guided by online pressure and volume signals. On-line display and acquisition of the signals (2000 samples/s) was performed with a PowerLab 8/30 data acquisition system and LabChart Pro software (AD Instruments GmbH, Spechbach, Germany). Off-line data analysis was performed with custom-made software (CircLab, P. Steendijk). The following parameters were measured: heart rate (HR), stroke volume (SV), cardiac output (CO), end-diastolic volume (EDV) end-systolic volume (ESV), ejection fraction (EF), end-diastolic pressure (EDP) and end-systolic pressure (ESP). Stroke work (SW) was determined as the area of the PV-loop and the maximal and minimal rate of LV pressure change, dP/dt_{MAX} and dP/dt_{MIN} were obtained. Effective arterial elastance (E_A) was calculated as ESP/SV. Relaxation time tau was calculated as the time-constant of mono-exponential pressure decay during isovolumic relaxation.

Myocardial (immuno)histochemistry

Hearts were fixed overnight in paraformaldehyde and cut into five 1 mm-thick slices, perpendicular to the long axis of the heart. These slices were flat embedded in paraffin and 5 μm-thick sections

were prepared. To delineate LV area and infarct area the lower 3 sections were stained for collagen with Sirius Red. Total LV wall area (including septum) and infarct area were measured with cell^D imaging software (Olympus Soft Imaging Solutions, Tokyo, Japan). The infarct area was expressed as percentage (v/v) of the LV wall volume.

Additionally, sections were immunohistochemically stained for macrophages (rat anti-mouse MAC-3, 1:200; BD Biosciences, Erembodegem, Belgium) to count the infiltrating macrophages into the myocardium, TLR4 (rabbit anti-human TLR4, 1:150 SantaCruz, Heidelberg, Germany) to observe presence of TLR4 in the different areas of the myocardium, RP105 (rabbit anti-human, 1:250 SantaCruz) to verify the presence of the accessory molecule in WT mice, and fibronectin-EDA (mouse anti-human 1:800, Abcam, Cambridge, United Kingdom) whose presence precedes that of collagen and serves as an endogenous ligand for TLR4, which is frequently induced upon tissue injury and is known to play a role in cardiac remodeling. Images were scored by an observer blinded for the study groups. Per image three specific areas of the myocardium were distinguished: the infarcted area, the border zone and the remote, undamaged, healthy myocardium. MAC-3 staining was analyzed by counting the number of macrophages in three consecutive fields of view per specific area. For TLR4, RP105 and fibronectin-EDA stainings were scored in a semi-quantitative manner, using zero staining as grade 0, mild to moderate staining as grade 1 and a profound staining as grade 2.

Statistical methods

Significance of differences between the groups was calculated non-parametrically using a Mann-Whitney U-test. Difference in survival rate after MI was calculated using a chi-squared test. P-values <0.05 were considered statistically significant. SPSS 17.0 for Windows (SPSS, Chicago, IL, USA) was used for statistical analysis. Values are presented as means ± SD.

Results

Increased inflammatory response in RP105$^{-/-}$ mice after TLR4 stimulation by LPS

To demonstrate whether an increased TLR4 mediated inflammatory response is present in RP105$^{-/-}$ mice as compared to WT mice, an *ex vivo* whole blood stimulation assay was performed in the presence and absence of LPS. After an overnight LPS stimulation with 25 ng/mL and 50 ng/mL LPS, TNFα levels were markedly increased in RP105$^{-/-}$ mice compared to WT mice for both concentrations, whereas no significant difference was observed under non-stimulated conditions (table 1).

RP105 deficiency does not affect baseline cardiac function

To determine possible differences in baseline cardiac function between WT and RP105$^{-/-}$ mice, echocardiography and PV-loops were measured in animals without MI. Since body weight differed between the groups (25.7 ± 0.7 g in WT vs. 28.9 ± 2.7 g in RP105$^{-/-}$,

Table 1 **Effect of RP105 deficiency TLR4 mediated inflammatory response.**

	TNFα (ng/mL) WT	TNFα (ng/mL) RP105$^{-/-}$
LPS dose (ng/mL)		
25	**20.0±4.1 ng/mL**	**108±24 ng/mL**
50	**28.7±7.0 ng/mL**	**128±25 ng/mL**

Blood samples of WT and RP105$^{-/-}$ mice were diluted 1:25 with RPMI 1640, and incubated overnight with 25 or 50 ng/mL LPS. Subsequently TNFα levels were measured and expressed as ng/mL. Values represent means ± SD; n=5 per group.

p=0.036) all volumetric parameters were corrected for body weight. Results for the main PV-loop derived parameters show no significant differences between the WT and the RP105$^{-/-}$ mice (see supplemental table 1). These findings indicate that RP105 deficiency *per se* does not influence basal cardiac function.

RP105 deficiency promotes cardiac dilatation after myocardial infarction

To investigate whether RP105 deficiency influences cardiac function after MI, the LAD was permanently ligated in 12 WT and 12 RP105$^{-/-}$ mice. No significant difference in survival rates was observed (92% in WT vs. 75% in RP105$^{-/-}$, p=0.273), suggesting that both strains were equally able to cope with the severe cardiac damage.

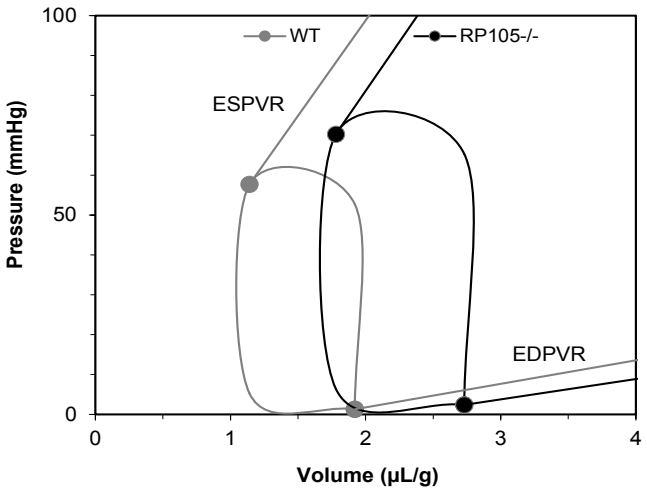

Figure 2 **PV-loops after MI.** WT and RP105$^{-/-}$ mice underwent ligation of the LAD, and 15 days post myocardial infarction (MI) pressure-volume loops (PV-loops) were recorded in each mouse. Average PV-loops and PV-relations, corrected for body weight, are shown per group. n=8 per group. ESPVR, end-systolic pressure volume relation; EDPVR, end-diastolic pressure volume relation.

Table 2 **Effect of RP105 deficiency on cardiac function after an MI.**

	WT	RP105$^{-/-}$	P-value
General			
HR (beats/min)	446±19	538±44	**0.003**
SV (µL/g)	0.8±0.3	0.9±0.4	0.490
CO ((mL/g)/min)	0.4±0.1	0.5±0.2	0.300
SW (mmHg.(µL/g))	42±14	57±44	0.916
E_A (mmHg/(µL/g))	0.2±0.1	0.1±0.1	0.223
E_{ES}/E_A	0.7±0.3	0.6±0.3	0.395
Systolic			
ESP (mmHg)	58±9	70±9	**0.021**
ESV (µL/g)	1.1±0.7	1.8±0.7	**0.038**
EF (%)	43±16	35±10	0.372
dP/dt_{MAX} (mmHg/ms)	5±2	6±2	0.462
E_{ES} (mmHg/(µL/g))	48±10	49±27	0.955
Diastolic			
EDP (mmHg)	1±2	2±2	0.293
EDV (µL/g)	1.9±0.6	2.7±0.9	0.058
Tau (ms)	11.9±0.9	10.4±1.5	**0.046**
$-dP/dt_{MIN}$ (mmHg/ms)	4±0.8	5±2	0.093
E_{ED} (mmHg/(µL/g))	6±4	5±3	0.721
K_{ED} (1/(µL/g))	0.2±0.1	0.1±0.0	0.114

HR, heart rate; SV, stroke volume; CO, cardiac output; SW, stroke work; E_A, arterial elastance (afterload); E_{ES}/E_A, ventricular arterial coupling; ESP, end-systolic pressure; ESV, end-systolic volume; EF, ejection fraction; dP/dt_{MAX}, maximal rate of pressure increase; E_{ES}, end-systolic elastance (slope of ESPVR); EDP, end-diastolic pressure; EDV, end-diastolic volume; Tau, relaxation time constant; $-dP/dt_{MIN}$, maximal rate op pressure decline; E_{ED}, end-diastolic stiffness (slope of EDPVR); K_{ED}, diastolic stiffness constant. Values represent means ± SD; n=8 per group.

Fifteen days after induction of the MI, functional parameters were obtained by intraventricular PV-loop measurements. The results of these analyses are summarized in table 2. Based on mean values for end-diastolic and end-systolic pressures and volumes, average PV-loops were created for both groups (figure 2). Corresponding end-diastolic and end-systolic PV-relations were added, based on mean E_{ES} and E_{ED} values. These measurements revealed that RP105 deficiency significantly affected heart function after MI. Compared with WT mice, RP105$^{-/-}$ mice showed significantly higher heart rate (+21% p=0.003), ESV index (+42%, p=0.038), ESP (+22%, p=0.021) and lower Tau (-12%, p=0.046). Furthermore a clear tendency for a higher EDV (+35%, p=0.058) and higher $-dP/dt_{MIN}$ (+24%, p=0.093) was observed. Taken together, RP105$^{-/-}$ mice showed more prominent cardiac dilatation after MI, but general hemodynamics appeared to be relatively unaffected at this stage.

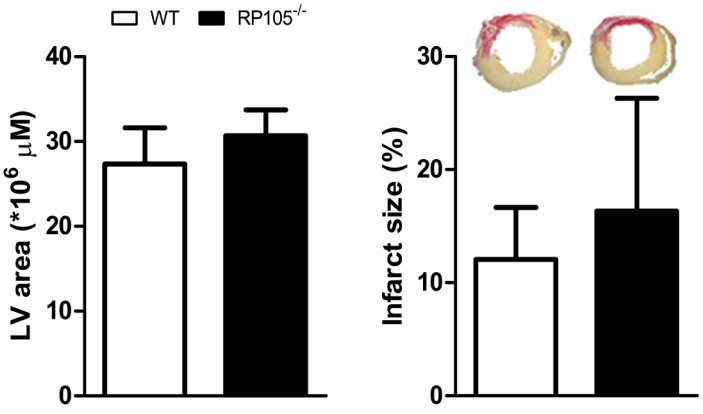

Figure 3 **Left ventricular area and myocardial infarct size in WT and RP105$^{-/-}$ mice.** Representative cross sections, after Sirius red staining, are shown above the corresponding bars for myocardial infarct size. Each bar represent mean ± SD; n= 8-10 per group.

RP105 deficiency does not influence infarct size

Then it was investigated whether the enhanced dilatation of the RP105$^{-/-}$ mice could be secondary to an increased myocardial infarct size. Directly after the PV-loop measurements, 15 days after MI, mice were sacrificed and hearts were isolated. Figure 3 shows representative Sirius red stained cross sections of the infarcted heart. No differences in total LV area were observed ($27*10^6 \pm 4*10^6$ µM in WT vs $31*10^6 \pm 3*10^6$ µM in RP105$^{-/-}$, p=0.11) whereas the infarct area comprised 12 ± 5% of the total LV in the WT animals versus 16 ± 10% in the RP105$^{-/-}$ mice (p=0.53). The infarct sizes in both groups were thus similar, which may suggest that the more pronounced dilatation in RP105$^{-/-}$ mice reflects that the remote 'healthy' myocardium of the RP105$^{-/-}$ mice is less able to maintain cardiac function after MI as compared to WT mice.

Structural analysis of the myocardium and infarct area

To investigate potential underlying mechanisms causing the observed differences in cardiac function after MI, (immuno)histochemical analyses on the myocardium of both groups were performed. We focused on inflammatory components in specific areas of the myocardium: the infarcted area, the border zone and the remote 'undamaged/ healthy' myocardium. Figure 4 shows representative images of the different stainings for Sirius red, TLR4, fibronectin-EDA, MAC-3 and RP105. All stainings showed little to no response in the undamaged myocardium remote from the infarct area. An upregulation of TLR4, fibronectin-EDA staining and the number of macrophages (figure 5) were observed in the area adjacent to the infarcted zone. As expected, the infarcted area consisted mainly of collagen (scar tissue) and macrophages. No differences in staining patterns were observed between WT and RP105$^{-/-}$ mice.

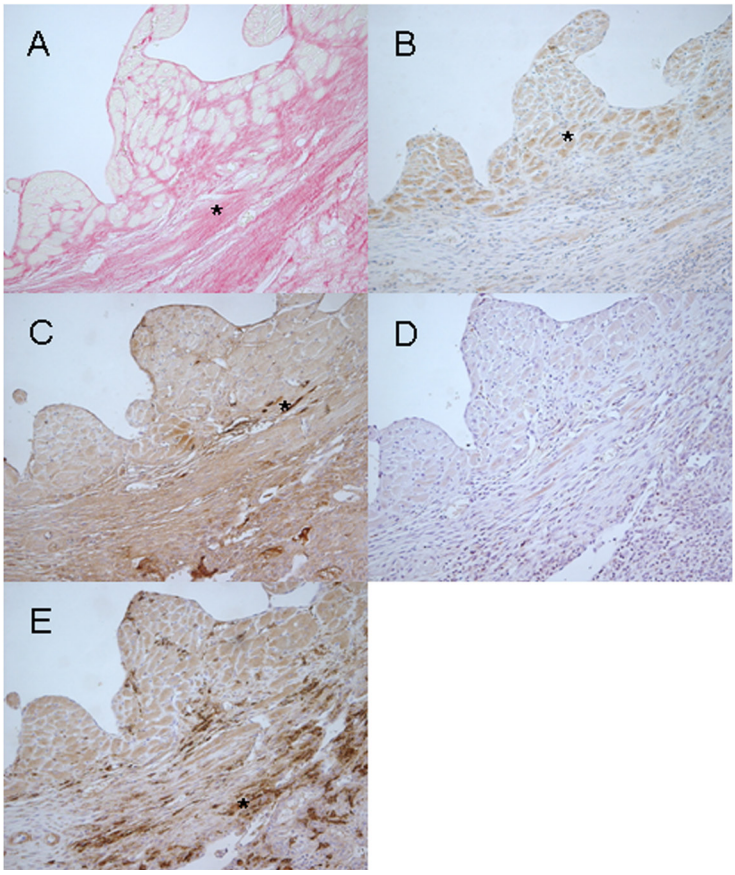

Figure 4 **Typical examples of (immuno)histological stainings**. Images are shown of (A) Sirius red staining indicating the collagen in the tissue adjacent to the infarcted area (*), (B) TLR4 staining in tissue adjacent to the infarcted area (*), (C) fibronectin-EDA staining in tissue adjacent to the infarcted area (*), (D) MAC-3 (macrophages) and (E) RP105 staining in tissue adjacent to the infarcted area (*). All images were photographed in sections adjacent to the infarcted area and this example is from a WT mouse. No differences were observed for Sirius red, TLR4, fibronectin-EDA or MAC-3 staining between the two groups. 200x magnification.

Discussion

The innate immune system, and especially TLRs, plays a pivotal role in the remodeling process that is initiated after an MI. Since the role of TLR accessory molecules and especially the negative regulator of TLR4, RP105, in cardiovascular disease is still largely unknown, we investigated its role in post MI cardiac function and remodeling. Our results show, for the first time, that deficiency of the TLR accessory molecule RP105, results in hampered post MI repair and subsequent loss of cardiac function. This causal involvement of RP105 in the post MI inflammatory processes provides new opportunities for therapeutic approaches to reduce cardiac remodeling and thereby improving cardiac function after a myocardial event.

RP105 was originally identified as a B-cell specific molecule, but turned out to be also present on myeloid cells including macrophages and dendritic cells.[16, 19] Since the expression of RP105 mirrors that of TLR4, and TLR4 is an important player in the pathophysiology of cardiovascular disease processes, we hypothesized that RP105 might be an essential regulator in cardiovascular diseases. In this study we demonstrate that after an MI, RP105 deficiency results in an increased ESV and EDV which is associated with a more dilated LV. Since infarct size was similar in both groups, this effect suggests that the unaffected healthy myocardium of RP105$^{-/-}$ mice is less able to preserve cardiac function after MI as compared to WT mice.

After MI, loss of function in the infarct zone may be compensated by the unaffected myocardium, for example by hypertrophy, or by invoking the Frank-Starling mechanism via cardiac dilatation. In addition, cardiac output may be maintained by increased heart rate. No significant differences in cardiac output were observed between the two groups, but the RP105$^{-/-}$ mice showed a more pronounced dilatation and higher heart rate. This suggests that the intrinsic myocardial function in the undamaged myocardium was less in these mice, requiring more pronounced compensatory responses.

This conclusion is supported by the results regarding the end-systolic pressure volume relation (ESPVR) as shown in figure 2. The figure illustrates that the differences between the groups do not merely reflect altered loading conditions, but changes in intrinsic LV function as well reflected by a rightward shift of the ESPRV. Interestingly, in contrast to the ESPVR which indicates a depressed systolic LV function, the downward shift of the end-diastolic pressure volume relation (EDPVR) points towards an improved diastolic function in line with the positive effects on Tau and dP/dt_{MIN}.

Although macrophages in the infarcted zone are essential for the removal of necrotic tissue [20], they may also contribute to cardiac dysfunction by adherence to cardiomyocytes.[21]

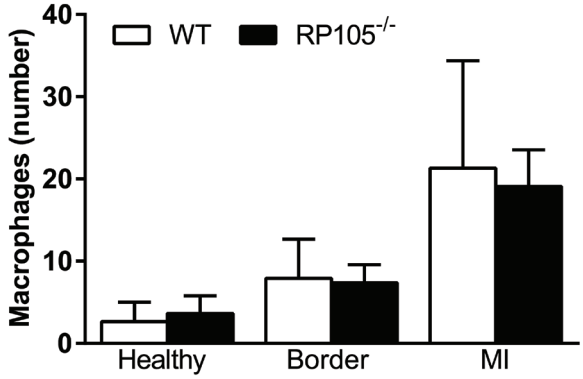

Figure 5 **Amount of macrophages per specific area of the myocardium in WT and RP105$^{-/-}$ mice.** the infarcted area, the border zone and the remote 'undamaged/healthy' myocardium Per image three specific areas of the myocardium were distinguished per image; the infarcted area, the border zone and the remote, undamaged, healthy myocardium. The number of macrophages was in three consecutive fields of view per specific area. Each bar represent mean ± SD; n= 8-10 per group.

However, as both WT and RP105$^{-/-}$ mice show a comparable density of macrophages in the border and infarcted areas, this cannot explain the differences in cardiac function.

Another factor that may contribute to the observed LV dilatation could be the availability of ligands for TLR4. Previously we showed presence of TLR4 and the endogenous TLR4 ligand fibronectin-EDA after MI resulting in deteriorating effects on cardiac remodeling.[12, 22] Similarly, in this study we observed an upregulation of fibronectin-EDA in WT mice when the damaged myocardium is compared to the undamaged myocardium. This was similar in the RP105 deficient mice showing equal fibronectin-EDA expression. We thereby demonstrated that RP105 does not influence local endogenous TLR ligand fibronectin-EDA expression.

In the current study we did not observe any effects of RP105 deficiency on histologic parameters. This could be explained by the lack of RP105 expression in the myocardium, since RP105 is known to be present on antigen presenting cells (APC)[16] but not on cardiomyocytes. APCs are well known to be involved in the cardiac remodeling process.

Alternatively it could be that RP105 has no direct signaling capacities. Since RP105 has no direct signaling function, but rather acts as a potent inhibitor of TLR4 signaling, it is more likely that the effects of RP105 deficiency are due to enhanced TLR4 signaling. In line with previously published results of Divanovic *et al.*[16, 23] we were able to demonstrate an enhanced inflammatory response in whole blood in RP105$^{-/-}$ mice. *Ex vivo* stimulation of whole blood samples of RP105$^{-/-}$ mice by the TLR4 ligand LPS resulted in strong upregulation of TNFα levels compared to the controls (table 1), a difference in TNFα levels that was not observed under unstimulated conditions. This supports the hypothesis that the TLR4 mediated inflammatory response is enhanced by RP105 deficiency.

RP105 alters TLR4 signaling via the RP105-MD1 complex which forms an unusual 2:2 homodimer. Two possible mechanisms for signaling inhibition effects on TLR4-MD2 were suggested previously; a lateral binding of TLR4-MD2 to the RP105-MD1 complex or the formation of TLR4-MD2/RP105-MD1 complexes reminiscent of the usual ligand-induced TLR homodimers.[24] Therefore the final effects of same amount of endogenous ligands activating TLR signaling, and thereby initiating cardiac remodeling, may have been increased due to the lack of RP105. While TLR4 expression in the myocardium was also comparable in both groups, this supports the hypothesis that RP105 does not cause its effects in remodeling directly via endogenous ligand or modulation of TLR4 receptor expression but probably via its previously described alternation of TLR4 signalling. By demonstrating that deficiency of the TLR accessory molecule RP105 affects the remodelling process, we reveal that a non-signalling extracellular receptor may be a potential target in the prevention of cardiac remodelling.

In summary, this study provides the first evidence that RP105 is involved in mechanisms underlying the TLR4 pathway induced post-infarction healing process. We show that RP105 deficiency has deleterious effects on cardiac function after an MI compared to WT mice with similar infarct size. These results underscore the role of the TLR4-pathway in post-infarction remodelling and as a result modulating RP105 may be an interesting new therapeutic strategy. To elucidate the exact mechanism further investigations are necessary.

Acknowledgements

This research was performed within the framework of CTMM, the Center for Translational Molecular Medicine (www.ctmm.nl), project PREDICCt (grant 01C-104), supported by the Netherlands Heart Foundation, Dutch Diabetes Research Foundation and Dutch Kidney Foundation and Netherlands Consortium for Systems Biology, as well as the framework of project D1–101 of the Dutch Top Institute Pharma. Furthermore, this study was performed with financial support from BioMedical Materials, Dutch Ministry of Economic Affairs, Agriculture and Innovation (BMM-PENT; P1.03). PCNR is an Established Investigator of the Netherlands Heart Foundation (NHS 2009T038).

References

1 Kannel WB, Sorlie P, McNamara PM. Prognosis after initial myocardial infarction: the Framingham study. *Am J Cardiol* 1979 July;44(1):53-9.

2 Lewis EF, Moye LA, Rouleau JL et al. Predictors of late development of heart failure in stable survivors of myocardial infarction: the CARE study. *J Am Coll Cardiol* 2003 October 15;42(8):1446-53.

3 Frangogiannis NG, Smith CW, Entman ML. The inflammatory response in myocardial infarction. *Cardiovasc Res* 2002 January;53(1):31-47.

4 Frangogiannis NG. The immune system and cardiac repair. *Pharmacol Res* 2008 August;58(2):88-111.

5 Frangogiannis NG. Regulation of the inflammatory response in cardiac repair. *Circ Res* 2012 January 6;110(1):159-73.

6 McMurray JJ, Adamopoulos S, Anker SD et al. ESC Guidelines for the diagnosis and treatment of acute and chronic heart failure 2012: The Task Force for the Diagnosis and Treatment of Acute and Chronic Heart Failure 2012 of the European Society of Cardiology. Developed in collaboration with the Heart Failure Association (HFA) of the ESC. *Eur Heart J* 2012 July;33(14):1787-847.

7 Kawai T, Akira S. The role of pattern-recognition receptors in innate immunity: update on Toll-like receptors. *Nat Immunol* 2010 May;11(5):373-84.

8 Hansson GK, Hermansson A. The immune system in atherosclerosis. *Nat Immunol* 2011 March;12(3):204-12.

9 Karper JC, De Vries MR, van den Brand BT et al. Toll-like receptor 4 is involved in human and mouse vein graft remodeling, and local gene silencing reduces vein graft disease in hypercholesterolemic APOE*3Leiden mice. *Arterioscler Thromb Vasc Biol* 2011 May;31(5):1033-40.

10 Vink A, Schoneveld AH, van der Meer JJ et al. In vivo evidence for a role of toll-like receptor 4 in the development of intimal lesions. *Circulation* 2002 October 8;106(15):1985-90.

11 Frantz S, Kobzik L, Kim YD et al. Toll4 (TLR4) expression in cardiac myocytes in normal and failing myocardium. *J Clin Invest* 1999 August;104(3):271-80.

12 Timmers L, Sluijter JP, van Keulen JK et al. Toll-like receptor 4 mediates maladaptive left ventricular remodeling and impairs cardiac function after myocardial infarction. *Circ Res* 2008 February 1;102(2):257-64.

13 Shimamoto A, Chong AJ, Yada M et al. Inhibition of Toll-like receptor 4 with eritoran attenuates myocardial ischemia-reperfusion injury. *Circulation* 2006 July 4;114(1 Suppl):I270-I274.

14 Akashi-Takamura S, Miyake K. TLR accessory molecules. *Curr Opin Immunol* 2008 August;20(4):420-5.

15 Miyake K, Yamashita Y, Ogata M, Sudo T, Kimoto M. RP105, a novel B cell surface molecule implicated in B cell activation, is a member of the leucine-rich repeat protein family. *J Immunol* 1995 April 1;154(7):3333-40.

16 Divanovic S, Trompette A, Atabani SF et al. Negative regulation of Toll-like receptor 4 signaling by the Toll-like receptor homolog RP105. *Nat Immunol* 2005 June;6(6):571-8.

17 Divanovic S, Trompette A, Petiniot LK et al. Regulation of TLR4 signaling and the host interface with pathogens and danger: the role of RP105. *J Leukoc Biol* 2007 August;82(2):265-71.

18 Louwe MC, van der Hoorn JW, van den Berg SA et al. Gender-dependent effects of high-fat lard diet on cardiac function in C57Bl/6J mice. *Appl Physiol Nutr Metab* 2012 April;37(2):214-24.

19 Miyake K, Yamashita Y, Hitoshi Y, Takatsu K, Kimoto M. Murine B cell proliferation and protection from apoptosis with an antibody against a 105-kD molecule: unresponsiveness of X-linked immunodeficient B cells. *J Exp Med* 1994 October 1;180(4):1217-24.

20 Lambert JM, Lopez EF, Lindsey ML. Macrophage roles following myocardial infarction. *Int J Cardiol* 2008 November 12;130(2):147-58.

21 Simms MG, Walley KR. Activated macrophages decrease rat cardiac myocyte contractility: importance of ICAM-1-dependent adhesion. *Am J Physiol* 1999 July;277(1 Pt 2):H253-H260.

22 Arslan F, Smeets MB, Riem Vis PW et al. Lack of fibronectin-EDA promotes survival and prevents adverse remodeling and heart function deterioration after myocardial infarction. *Circ Res* 2011 March 4;108(5):582-92.

23 Divanovic S, Trompette A, Atabani SF et al. Inhibition of TLR-4/MD-2 signaling by RP105/MD-1. *J Endotoxin Res* 2005;11(6):363-8.

24 Yoon SI, Hong M, Wilson IA. An unusual dimeric structure and assembly for TLR4 regulator RP105-MD-1. *Nat Struct Mol Biol* 2011 September;18(9):1028-35.

25 Ohto U, Miyake K, Shimizu T. Crystal structures of mouse and human RP105/MD-1 complexes reveal unique dimer organization of the toll-like receptor family. *J Mol Biol* 2011 November 4;413(4):815-25.

Supplemental data

Supplemental table 1 **Baseline cardiac function of WT and RP105$^{-/-}$ mice.**

	WT	RP105$^{-/-}$	P-value
General			
HR (beats/min)	587 ± 51	545 ± 79	1.000
SV (µL/g)	0.7±0.3	0.8±0.3	1.000
CO ((mL/g)/min)	0.4 ± 0.1	0.4 ± 0.2	0.886
SW (mmHg.(µL/g))	69±20	71±19	1.000
E_A (mmHg/(µL/g))	0.2±0.1	0.2±0.1	0.486
E_{ES}/E_A	1.0±0.1	0.9±0.1	0.343
Systolic			
ESP (mmHg)	96 ± 14	90 ± 17	0.686
ESV (µL/g)	1.0 ± 0.3	0.9 ± 02	0.686
EF (%)	42.3 ± 5.7	45 ± 10.4	0.686
dP/dt_{MAX} (mmHg/ms)	8.9±1.8	8.0±1.4	0.686
Ees (mmHg/(µL/g))	138±57	116±66	0.686
Diastolic			
EDP (mmHg)	6 ± 5	3 ± 3	0.686
EDV (µL/g)	1.7 ± 0.6	1.7 ± 0.4	1.000
Tau (ms)	10±3	9±1	1.000
$-dP/dt_{MIN}$ (mmHg/ms)	8±2	7±1	1.000
E_{ED} (mmHg/(µL/g))	6±1	8±4	1.000
K_{ED} (1/(µL/g))	0.16±0.03	0.09±0.0	0.500

HR, heart rate; SV, stroke volume; CO, cardiac output; SW, stroke work; E_A, arterial elastance (afterload); E_{ES}/E_A, ventricular arterial coupling; ESP, end-systolic pressure; ESV, end-systolic volume; EF, ejection fraction; dP/dt_{MAX}, maximal rate of pressure increase; E_{ES}, end-systolic elastance (slope of ESPVR); EDP, end-diastolic pressure; EDV, end-diastolic volume; Tau, relaxation time constant; $-dP/dt_{MIN}$, maximal rate op pressure decline; E_{ED}, end-diastolic stiffness (slope of EDPVR); K_{ED}, diastolic stiffness constant. Values represent means ± SD; n=4 per group.

CHAPTER 6

Toll-like receptor 2 and Toll-like receptor 4 deficiency modestly influence cardiac function in mice on a high-fat diet

Mieke C. Louwe[1,2], José W.A. van der Hoorn[5], Patrick C.N. Rensen[1,2], Ko Willems van Dijk[1,2,3], Paul Steendijk[4] and Johannes W.A. Smit[1]

[1]Dept. of Endocrinology and Metabolic Diseases, [2]Einthoven Laboratory for Experimental Vascular Medicine, [3]Dept. of Human Genetics, [4]Dept. of Cardiology, Leiden University Medical Center, Leiden, the Netherlands [5]TNO - Metabolic Health Research, Leiden, the Netherlands

Toll-like receptor 2 and Toll-like receptor 4 deficiency modestly influence cardiac function in mice on a high-fat diet

Abstract

High-fat diet (HFD) feeding is a potent trigger for the development of obesity and cardiovascular disease. In addition, we previously reported that HFD feeding modestly impairs cardiac function in mice. Toll-like receptors (TLR) 2 and TLR4, receptors of the innate immune system, are hypothesized to be activated by ligands associated with HFD exposure such as (modified) fatty acids. Although TLR2 and 4 are involved in inflammation in cardiac disease, a direct relationship between HFD, TLR activation and cardiac dysfunction has not been reported. We therefore investigated the role of TLR2 and TLR4 in the impairment of cardiac function after exposure to HFD.

Male TLR2-deficient ($TLR2^{-/-}$) mice, TLR4-deficient ($TLR4^{-/-}$) mice and their corresponding wild-type (WT) littermates were fed a HFD for 12 weeks. Body weights were measured weekly, plasma lipid levels were obtained at week 10, and left ventricular pressure-volume relationships were measured at week 12.

As compared to their respective WT littermates, $TLR2^{-/-}$ and $TLR4^{-/-}$ mice showed no difference in body weight, plasma phospholipid, total cholesterol and triglyceride levels. In $TLR2^{-/-}$ mice, an increased end-diastolic volume (51±12 versus 73±18 μL; p=0.03) was observed, whereas other parameters of cardiac function were not different from WT littermates. In $TLR4^{-/-}$ mice, we observed trends of a decreased pressure half time (5.3±1.0 versus 4.3±0.6 ms; p=0.06) and an increased end-systolic elastance (1.6± 0.6 versus 3.3±2.0 mm Hg/μL; p=0.07).

This study shows that deficiency for TLR2 or TLR4 only mildly impairs cardiac function in HFD fed mice, suggesting that TLR2 and TLR4 may play a modest protective role in HFD-induced cardiac dysfunction.

Introduction

Overweight and obesity are reaching epidemic proportions worldwide, due to reduced physical activity in combination with a calorie rich diet. Since adipose tissue has a limited capacity to store fat, excess fat may be stored in non-adipose tissue such as liver and muscle, contributing to the pathogenesis of type 2 diabetes and cardiovascular diseases (CVD).

Saturated fatty acids such as palmitate and stearate which are abundantly available in most HFDs induce the accumulation of lipids in non-adipose tissues which is thought to give rise to chronic activation of inflammatory signalling pathways.[1] The onset of the inflammatory response is marked by the release of pro-inflammatory cytokines[2] resulting in the infiltration of inflammatory cells, e.g. macrophages, in the tissue.[3]

The exact molecular mechanisms responsible for the activation of inflammatory pathways in obesity are still poorly understood. One mechanism may be related to the finding that fatty acids and fatty acid derivative are able to activate TLRs.[4] TLRs play a key role in the innate immune response and are not only expressed on immune cells, but also by other cell types including cardiomyocytes.[4, 5] Thus far thirteen different TLRs have been discovered, and particularly the role of TLR2 and TLR4 in CVD and atherosclerosis have been studied extensively.[6] It has been observed that the absence of TLR2 and TLR4 has favourable effects on post-infarction healing during cardiac ischemia[7-10], and in atherosclerosis results in a reduced plaque formation.[11-13] Furthermore, there is evidence that TLRs also have adverse effects on the development of acute coronary syndrome[14] and aggravate heart failure.[15]

As HFD is clearly related to the development of coronary heart diseases, deleterious effects of HFD on the heart may be, at least partially, mediated through TLRs, which to our knowledge has not been studied before. We previously demonstrated that HFD feeding impairs cardiac function, preferentially in male mice.[16] In the current study, we show that a HFD intervention in TLR2 and TLR4 deficient mice results in very mild changes in cardiac function, thereby suggesting that TLR2 and TLR4, if anything, play a moderately protective role in HFD-induced cardiac dysfunction.

Materials and methods

Animals and experimental design

We used male B6.129-Tlr2tm1Kir/J (TLR2$^{-/-}$) mice, purchased from The Jackson Laboratory (Indianapolis, USA), TLR4 knock out (TLR4$^{-/-}$) mice, kindly provided by Prof. S. Akira (Department of Biochemistry, Hyogo College of Medicine, Hyogo, Japan) and T. van der Poll (Center for Experimental and Molecular Medicine, Academic Medical Center, Amsterdam, the Netherlands), and their respective wild-type (WT) littermates (all C57Bl/6J background). All mice were housed under standard conditions with a 12-hour light-dark cycle and had free access to food and water.

At the age of 13-15 weeks (TLR2$^{-/-}$ mice and WT littermates) or 7-12 weeks (TLR4$^{-/-}$ mice and WT littermates) mice were assigned to a lard based low-fat diet (LFD) or HFD which provided 45% energy from lipids (D12451, Research Diets Services, Wijk bij Duurstede, the Netherlands). Body weight was measured weekly and after 10 weeks of diet feeding, blood was drawn to measure plasma lipids. Heart function assessment with echocardiography and pressure volume loops (PV-loops) were performed in week 11 and 12, respectively. At the end of the experiment the mice were sacrificed and hearts were isolated for further examination. The protocol was approved by the Animal Ethics Committee from the Leiden University Medical Center and was conform to the Guide for Care and Use of Laboratory Animals (NIH publication No.85-23, Revised 1996).

Plasma lipids

After a 4 hour fast (9.00-13.00 h), blood was collected via tail vein bleeding in potassium EDTA-coated plastic tubes (Sarstedt, Germany). Plasma total cholesterol, triglycerides and phospholipids were determined individually using commercially available kits (kit no. 1489232; 11488872 and 101140, Roche Diagnostics, Mannheim, Germany) in 96-wells plates (Greiner Bio-One), according to the manufacturer's protocols.

Hemodynamic measurements

At week 12, left ventricular (LV) function was assessed by invasive PV-loops as described earlier.[16] Briefly, mice were anesthetized with 4% isoflurane, intubated, ventilated and the jugular vein was cannulated for infusion of hypertonic saline to determine parallel conductance. Via the right carotid artery a 1.2F PV catheter (FTS-1212B-4518, Scisense Inc., London, Ontario, Canada) was placed into the LV. The catheter was connected to a Scisense ADV signal processor (Scisense Inc) to generate high-fidelity pressure and volume signals. Positioning of the catheter was guided by online pressure and volume signals. On-line display and acquisition of the signals (2000 samples/s) was performed with a PowerLab 8/30 data acquisition system and LabChart Pro software (AD Instruments GmbH, Spechbach, Germany). Off-line data analysis was performed with custom-made software (CircLab, P. Steendijk).

Immunohistochemistry

After isolation, hearts were fixed in formalin and cut into five 1-2mm thick slices perpendicular to the long axis of the heart. These slices were flat embedded in paraffin and cross-sectioned (5 μm-thick) throughout the entire heart for immunohistological analysis. To determine the amount of macrophages in the myocardium an F4/80 staining was performed (F4/80; 1:10. The F4/80 monoclonal antibody was a gift from Dr. P.J. Nijweide, (Dept. of Molecular Cell Biology, Leiden University Medical Centre, the Netherlands). Five images were acquired throughout the ventricles of the heart with a 400x magnification. The number of macrophages per image was counted by two observers blinded for the study results. A macrophage was defined as brown/red staining which touched a blue nucleus and the average number of macrophages in the heart was calculated.

Statistical analysis

Significance of differences between the groups was calculated non-parametrically using a Kruskal-Wallis test for independent samples, followed by a Mann-Whitney U-test for independent samples. P-values ≤0.05 were considered statistically significant. SPSS 17.0 for Windows (SPSS, Chicago, IL, USA) was used for statistical analysis. Values are presented as means ± SD.

Results

HFD feeding similarly increases body weight gain in TLR2$^{-/-}$, TLR4$^{-/-}$ and WT mice

To determine the effect of HFD feeding on induction of obesity in TLR2$^{-/-}$ and TLR4$^{-/-}$ mice, body weight was measured weekly. At the start of the experiment, body weight did not significantly differ between groups. After HFD feeding for 12 weeks no differences in body weight between HFD fed TLR2$^{-/-}$ and TLR4$^{-/-}$ mice and corresponding WT mice were observed, although there was a tendency towards a diminished body weight gain for the TLR2$^{-/-}$ group (figure 1). However, 12 weeks of HFD feeding significantly increased body weights in all strains as compared to their LFD controls. LFD feeding in TLR2$^{-/-}$ resulted in a lower body weight gain compared to WT mice, whereas TLR4$^{-/-}$ mice did not differ in body weight gain compared to WT mice (supplemental figure A).

HFD feeding does not lead to differences in plasma lipids between TLR2$^{-/-}$ and TLR4$^{-/-}$ and WT mice

After 10 weeks of HFD feeding, blood was drawn to determine the concentration of total cholesterol, triglycerides and phospholipids in plasma (figure 2). For total cholesterol levels no differences were observed between the TLR2$^{-/-}$ and TLR4$^{-/-}$ mice and WT mice after HFD feeding, whereas HFD feeding did increase total cholesterol levels in all groups as compared to the LFD controls. LFD feeding did not influence cholesterol levels (supplemental figure B).

HFD feeding did not induce differences in triglyceride levels between TLR2$^{-/-}$ and TLR4$^{-/-}$ mice and WT mice. No differences in triglyceride levels were observed between HFD and LFD fed mice for TLR$^{-/-}$ and WT groups. Also, compared to LFD feeding, triglyceride levels were hardly affected. However, triglyceride levels tended to increase in TLR2$^{-/-}$ mice compared to WT mice, whereas TLR4$^{-/-}$ mice did not show an increase in triglyceride levels compared to WT mice. Phospholipids showed no differences between

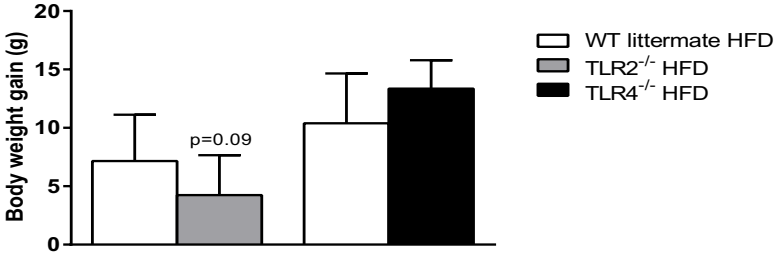

Figure 1 **Effect of TLR deficiency in HFD fed mice on body weight gain.** Male TLR2$^{-/-}$ and TLR4$^{-/-}$ mice and WT littermates were fed a high-fat diet (HFD) for 12 weeks. Body weight was measured at the beginning and end of the dietary intervention. Values represent means ± SD (n=7-8 per group), p=0.09 as compared to WT littermates.

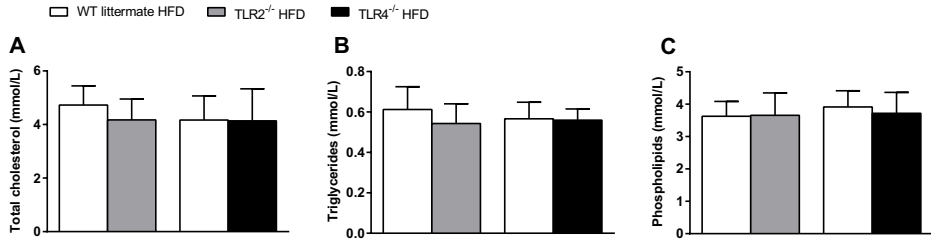

Figure 2 **Effect of TLR deficiency on HFD fed mice on plasma lipids.** Male TLR2$^{-/-}$ and TLR4$^{-/-}$ mice and corresponding WT littermates were fed a high-fat diet (HFD) for 12 weeks. After 10 weeks blood was drawn to determine total cholesterol (A), triglyceride (B) and phospholipid levels (C). Values represent means ± SD (n=5-8 per group)

both TLR$^{-/-}$ and WT mice after HFD. Levels were increase in all groups upon HFD feeding compared to LFD feeding, whereas phospholipid levels after LFD feeding alone did not differ between both TLR$^{-/-}$ and WT mice.

HFD feeding influences heart function modestly in TLR2$^{-/-}$ and TLR4$^{-/-}$ mice

To examine the effect of HFD feeding on cardiac function in TLR$^{-/-}$ mice, PV-loops were performed in all groups and the obtained results are summarized in table 1. Based on the mean values for end-diastolic and end-systolic volumes, average PV-loops of HFD groups were generated and corresponding end-diastolic and end-systolic PV-relations were calculated (figure 3).

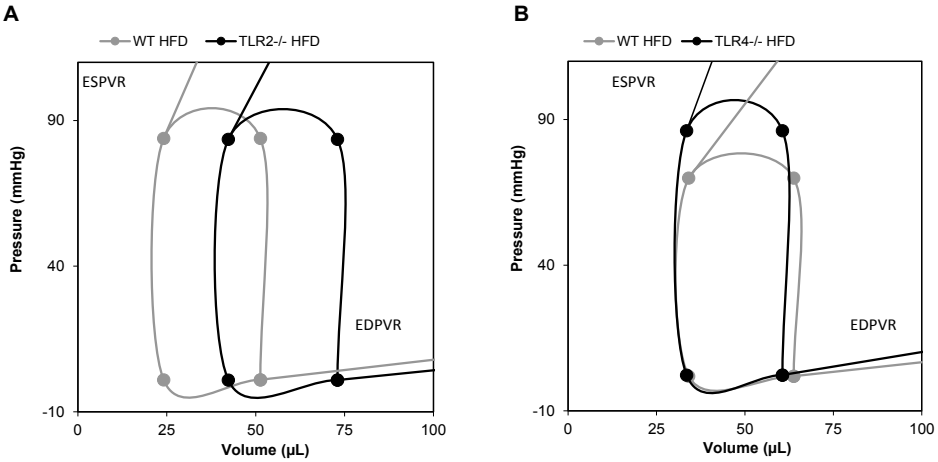

Figure 3 **Effect of TLR deficiency on HFD fed mice on pressure-volume loops and pressure-volume relations.** Male TLR2$^{-/-}$ (A) and TLR4$^{-/-}$ (B) mice and corresponding WT littermates were fed a high-fat diet (HFD). After 12 weeks pressure-volume loops (PV-loops) were recorded in each mouse, and average PV-loops are shown per group (n= 3-8 per group).

After HFD feeding differences were observed between the $TLR^{-/-}$ and WT mice. $TLR2^{-/-}$ mice increased ESV (+76%, p<0.009) and EDV (+42%, p<0.03) compared to their respective littermates. $TLR4^{-/-}$ mice tended to decrease pressure half time (-18%, P<0.06) and tended to increase end-systolic elastance (E_{ES}) (+200%, p<0.07) under HFD conditions compared to their respective littermates.

Both studies showed differences between LFD and HFD fed $TLR^{-/-}$ and WT mice, although not on similar parameters and not in a similar direction. $TLR2^{-/-}$ mice fed a HFD had a tendency towards an increased ESV (+46%, p<0.09) and an EDP (+360%, p<0.06) compared to LFD fed mice. WT mice in this study increased arterial elastance

Table 1 **Effect of TLR deficiency in HFD fed mice cardiac function**

	HFD			HFD		
	WT littermate	**$TLR2^{-/-}$**	**P-value**	**WT littermate**	**$TLR4^{-/-}$**	**P-value**
General						
HR (beats/min)	494 ± 45	514 ± 33	0.49	546 ± 77	601 ± 74	0.14
SV (µL)	27 ± 10	31 ± 8	0.30	30 ± 13	27 ± 16	0.12
CO (mL/min)	13 ± 5	16 ± 4	0.36	17 ± 9	17 ± 10	0.29
SW (mm Hg.µL)	2559 ± 866	2883 ± 803	0.42	2178 ± 1029	2468 ± 1535	0.29
E_A (mm Hg/µL)	3.6 ± 1.3	2.9 ± 0.7	0.22	2.7 ± 1.0	4.1 ± 1.8	0.19
PHT (ms)	5.3 ± 0.8	4.9 ± 0.5	0.77	5.3 ± 1.0	4.3 ± 0.6	**0.06**
Systolic						
ESP (mm Hg)	84 ± 11	84 ± 11	1.00	70 ± 18	86 ± 8	0.37
ESV (µL)	24 ± 4	42 ± 14	**0.009**	34 ± 17	33 ± 9	0.17
EF (%)	52 ± 8	43 ± 9	0.30	48 ± 23	43 ± 13	0.94
dP/dt_{MAX} (mm Hg/ms)	7120 ± 1245	7254 ± 1250	0.91	6060 ± 2499	8583 ± 1738	0.12
$SB\text{-}E_{ES}$ (mm Hg/µL)	2.8 ± 0.4	2.3 ± 0.5	0.09	1.6 ± 0.6	3.3 ± 2.0	**0.07**
Diastolic						
EDP (mm Hg)	1.0 ± 2.5	0.9 ± 2.1	0.64	1.9 ± 1.0	2.3 ± 2.8	0.94
EDV (µL)	51 ± 12	73 ± 18	**0.028**	64 ± 5	61 ± 17	0.12
Tau (ms)	10.6 ± 1.5	9.9 ± 0.8	0.91	10.3 ± 2.3	8.4 ± 1.3	0.14
$-dP/dt_{MIN}$ (mm Hg/ms)	-6096 ± 1493	-6358 ± 904	0.73	-5209 ± 1937	-7911 ± 1499	0.17
$SB\text{-}E_{ED}$ (mm Hg/µL)	0.14 ±0.03	0.12 ± 0.05	0.20	0.13 ± 0.04	0.20 ±0.09	0.12

Mice were fed a high-fat diet (HFD) for 12 weeks and cardiac function was determined. LV volume signals obtained by conductance catheter were calibrated by matching EF and CO with corresponding echocardiographic values obtained by measurements four days earlier. Values represent means ± SD (n= 4-8 per group). HR, heart rate; SV, stroke volume; CO, cardiac output; SW, stroke work; E_A, arterial elastance (afterload); PHT, pressure half time; ESP, end-systolic pressure; ESV, end-systolic volume; EF, ejection fraction; dP/dt_{MAX}, maximal rate of pressure increase; $SB\text{-}E_{ES}$, end-systolic elastance; EDP, end-diastolic pressure; EDV, end-diastolic volume; Tau, relaxation time constant; $-dP/dt_{MIN}$, maximal rate op pressure decline; $SB\text{-}E_{ED}$, end-diastolic elastance (diastolic stiffness).

(E_A) (+55%, p=0.03) and E_{ES} (+44%, p=0.02) and tended to increase the ESP (+15%, p=0.09) on a HFD compared to WT mice on a LFD. TLR4$^{-/-}$ mice fed a HFD showed a tendency towards a decreased pressure half time (-12%, p=0.06) and an increased end-diastolic elastance (E_{ED}) (+62%, p=0.07) compared to TLR4$^{-/-}$ mice on a LFD. WT mice in this study on a HFD showed a tendency towards a decreased dP/dt_{MAX} (-32%, p=0.08) and a decreased SB-E_{ES} (-50%, P=0.07) compared with LFD feeding in WT mice.

In LFD conditions, differences in cardiac function were observed between the TLR$^{-/-}$ and WT mice (supplemental table 1 and supplemental figure C). Compared with their respective LFD WT littermates, TLR2$^{-/-}$ mice showed an increase in E_{ES} (+54%, P<0.02), whereas TLR4$^{-/-}$ mice on a LFD showed an increased stroke volume (+69%, P<0.02) and EDV (+32%, P=0.05) and a decreased heart rate (-13%, P<0.02), dP/dt_{MAX} (-19%, P=0.05), E_A (-41%, P=0.05), E_{ES} (-38%, P=0.05) and E_{ED} (-46%, P<0.03).

HFD feeding does not increase cardiac macrophage numbers in TLR2$^{-/-}$ TLR4$^{-/-}$ and WT mice

To determine if macrophages infiltrated more in cardiac tissue by HFD feeding, and their possible influence on cardiac dysfunction, the number of macrophages in the ventricles was counted. Images of representative pictures are given in figure 4. There were no differences in the average number of macrophages per image in HFD fed TLR2$^{-/-}$ mice compared to WT (1.2±1.9 vs. 2.9±1.2 macrophages per image). Likewise, no difference was found between HFD TLR4$^{-/-}$ and WT mice (11.4±16.4 vs. 14.1±13.8 macrophages per image). HFD feeding itself did not result in an increased number of macrophages neither in both TLR$^{-/-}$ groups nor WT groups as compared to the LFD control groups. Furthermore, no difference was observed for the amount of macrophages in all LFD fed groups (supplemental figure D).

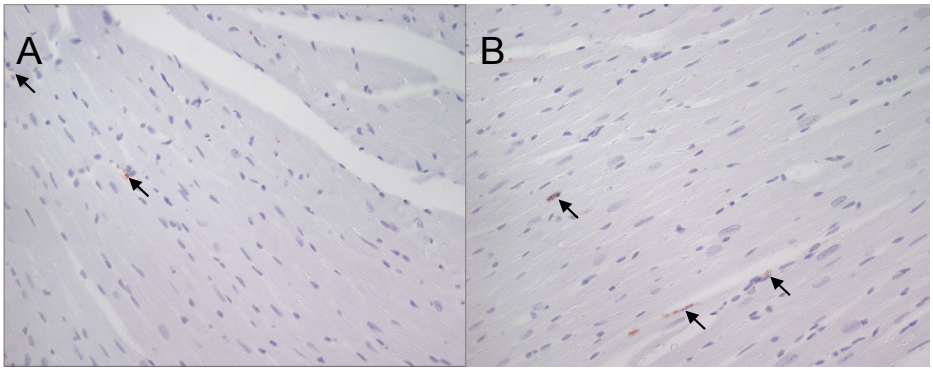

Figure 4 **Effect of TLR deficiency in HFD fed mice on cardiac macrophage infiltration.** Representative images of macrophage staining by F4/80 in cardiac tissue for of high-fat diet (HFD) fed WT mice (A) and TLR2$^{-/-}$ mice (B). The shown example was from the TLR2$^{-/-}$ experiment, no between group differences were observed. Magnification 400x.

Discussion

Since the discovery that HFD derived ligands activate TLR2- and TLR4-dependent pathways and play a role in HFD induced obesity, insulin resistance[4] and atherosclerosis[13], studies have been performed to further investigate the underlying mechanisms. We previously demonstrated that HFD feeding impairs cardiac function specifically in male and not female mice. Therefore we set out to determine the role of TLR2 and TLR4 signaling in HFD-induced cardiac function. Here, we show that TLR2 or TLR4 deficiency does not induce major differences in heart function under HFD conditions. HFD intervention for 12 weeks results in subtle differences in cardiac function in TLR2$^{-/-}$ and TLR4$^{-/-}$ mice compared to HFD fed WT littermates, even though body weight and some plasma lipid parameters are increased due to HFD feeding.

The modestly induced cardiac dysfunction between TLR deficient mice and WT littermates after HFD intervention is independent of the HFD, as high-fat feeding did induce several other previously described metabolic changes. First, HFD feeding significantly induced body weight gain in all groups. Second, as expected, HFD feeding increased total cholesterol levels in all HFD fed groups. Plasma phospholipids levels also tended to be increased upon high-fat feeding. Interestingly, possibly due to the genetic background, the mice displayed triglyceride levels just above detection level. Therefore, small variations in triglyceride levels may result in larger and thus significant differences. Third, contrary to expectations, we observed no difference in macrophages between the different groups. The HFD we used, without supplemented cholesterol, might be a too mild inflammatory trigger unable to stimulate macrophage attraction to the myocardium. Overall, these data show that HFD feeding resulted in the expected phenotypic effects, even though cardiac dysfunction was only mildly induced.

Despite evidence that mice lacking TLRs have a lower incidence of atherosclerosis and other cardiovascular pathology, in this study cardiac function in the TLR2$^{-/-}$ and TLR4$^{-/-}$ mice was slightly impaired when compared to their corresponding HFD fed WT littermates.

One of the contributing factors to the activation of TLRs, leading to the onset of inflammatory pathways, are fatty acids derived from the diet. Lard based HFD is rich in mainly C18:1 (43.3%), C16:0 (29.2%) and C18:0 (15.0%). *In vitro* studies show that in particular C12:0 and C16:0; and C14:0 and C18:0; are able to activate TLR2 and TLR4, respectively.[4, 17, 18] Therefore we assume that this particular lard diet is able to stimulate those specific TLRs, and thus does not clarify the lack of the TLR effect.

A possible explanation for the mild effects of the HFD in TLR deficient mice on cardiac function might be that we have chosen for male mice in this experiment. A sexual dimorphism has been reported for TLR deficient mice, showing that TLR2$^{-/-}$ and TLR4$^{-/-}$ female mice fed a HFD are more evidently protected against metabolic disturbances compared to males, who showed no difference in insulin response between WT and TLR deficient mice.[4, 19] In addition, as more often is seen with receptors belonging to the innate immune system, it is possible that the absence of one TLR causes compensatory up regulation of other TLRs, resulting in a similar inflammatory status which thus not lead to cardiac dysfunction.

Contradictory to previous findings[16], in the current study HFD-induced cardiac dysfunction in WT mice did not reach statistical significance. The fact that these WT mice have a less pronounced cardiac impairment could explain why only subtle differences were found in cardiac function between $TLR^{-/-}$ and WT mice. We cannot explain why the WT mice react differently to the HFD feeding compared to an earlier study, however it might be that small variations in study setup, e.g. the average age of the mice or environmental factors in the animal facilities, are causing this effect. Clearly, more research is needed to fully determine the exact role of TLR2 and TLR4 signaling in HFD-induced cardiac function.

To summarize, in this study we show that HFD feeding in $TLR2^{-/-}$ mice and $TLR4^{-/-}$ mice, compared to WT mice, neither results in differences in body weight nor in plasma lipids. Cardiac dysfunction is observed HFD fed $TLR2^{-/-}$ mice for the EDV parameter, whereas HFD fed $TLR4^{-/-}$ mice showed a tendency towards a decreased pressure half time and an increased SB-E_{ES}, leading to the conclusion that TLR2 and TLR4, if anything play a moderately protective role in HFD-induced cardiac dysfunction.

Acknowledgements

We thank Prof. S. Akira (Department of Biochemistry, Hyogo College of Medicine, Hyogo, Japan) and Dr. T. van der Poll (Center for Experimental and Molecular Medicine, Academic Medical Center, Amsterdam, the Netherlands), who kindly provided the TLR4 deficient mice. We thank Dr. P.J. Nijweide (Dept. of Molecular Cell Biology, Leiden University Medical Centre, the Netherlands) for the F4/80 antibody. Furthermore, we thank Lianne van der Wee-Pals for her excellent technical assistance.

This research was performed within the framework of CTMM, the Center for Translational Molecular Medicine (www.ctmm.nl), project PREDICCt (grant 01C-104), and supported by the Netherlands Heart Foundation, Dutch Diabetes Research Foundation and Dutch Kidney Foundation and Netherlands Consortium for Systems Biology. PCNR is an Established Investigator of the Netherlands Heart Foundation (2009T038).

References

1 Kennedy A, Martinez K, Chuang CC, LaPoint K, McIntosh M. Saturated fatty acid-mediated inflammation and insulin resistance in adipose tissue: mechanisms of action and implications. *J Nutr* 2009 January;139(1):1-4.

2 Visser M, Bouter LM, McQuillan GM, Wener MH, Harris TB. Elevated C-reactive protein levels in overweight and obese adults. *JAMA* 1999 December 8;282(22):2131-5.

3 Weisberg SP, McCann D, Desai M, Rosenbaum M, Leibel RL, Ferrante AW, Jr. Obesity is associated with macrophage accumulation in adipose tissue. *J Clin Invest* 2003 December;112(12):1796-808.

4 Shi H, Kokoeva MV, Inouye K, Tzameli I, Yin H, Flier JS. TLR4 links innate immunity and fatty acid-induced insulin resistance. *J Clin Invest* 2006 November;116(11):3015-25.

5 Frantz S, Kobzik L, Kim YD et al. Toll4 (TLR4) expression in cardiac myocytes in normal and failing myocardium. *J Clin Invest* 1999 August;104(3):271-80.

6 Ionita MG, Arslan F, de Kleijn DP, Pasterkamp G. Endogenous inflammatory molecules engage Toll-like receptors in cardiovascular disease. *J Innate Immun* 2010;2(4):307-15.

7 Chong AJ, Shimamoto A, Hampton CR et al. Toll-like receptor 4 mediates ischemia/reperfusion injury of the heart. *J Thorac Cardiovasc Surg* 2004 August;128(2):170-9.

8 Oyama J, Blais C, Jr., Liu X et al. Reduced myocardial ischemia-reperfusion injury in toll-like receptor 4-deficient mice. *Circulation* 2004 February 17;109(6):784-9.

9 Shimamoto A, Chong AJ, Yada M et al. Inhibition of Toll-like receptor 4 with eritoran attenuates myocardial ischemia-reperfusion injury. *Circulation* 2006 July 4;114(1 Suppl):I270-I274.

10 Shishido T, Nozaki N, Yamaguchi S et al. Toll-like receptor-2 modulates ventricular remodeling after myocardial infarction. *Circulation* 2003 December 9;108(23):2905-10.

11 Hollestelle SC, De Vries MR, van Keulen JK et al. Toll-like receptor 4 is involved in outward arterial remodeling. *Circulation* 2004 January 27;109(3):393-8.

12 Michelsen KS, Wong MH, Shah PK et al. Lack of Toll-like receptor 4 or myeloid differentiation factor 88 reduces atherosclerosis and alters plaque phenotype in mice deficient in apolipoprotein E. *Proc Natl Acad Sci U S A* 2004 July 20;101(29):10679-84.

13 Mullick AE, Tobias PS, Curtiss LK. Modulation of atherosclerosis in mice by Toll-like receptor 2. *J Clin Invest* 2005 November;115(11):3149-56.

14 Mann DL. The emerging role of innate immunity in the heart and vascular system: for whom the cell tolls. *Circ Res* 2011 April 29;108(9):1133-45.

15 Frantz S, Ertl G, Bauersachs J. Mechanisms of disease: Toll-like receptors in cardiovascular disease. *Nat Clin Pract Cardiovasc Med* 2007 August;4(8):444-54.

16 Louwe MC, van der Hoorn JW, van den Berg SA et al. Gender-dependent effects of high-fat lard diet on cardiac function in C57Bl/6J mice. *Appl Physiol Nutr Metab* 2012 April;37(2):214-24.

17 Lee JY, Zhao L, Youn HS et al. Saturated fatty acid activates but polyunsaturated fatty acid inhibits Toll-like receptor 2 dimerized with Toll-like receptor 6 or 1. *J Biol Chem* 2004 April 23;279(17):16971-9.

18 Senn JJ. Toll-like receptor-2 is essential for the development of palmitate-induced insulin resistance in myotubes. *J Biol Chem* 2006 September 15;281(37):26865-75.

19 Ehses JA, Meier DT, Wueest S et al. Toll-like receptor 2-deficient mice are protected from insulin resistance and beta cell dysfunction induced by a high-fat diet. *Diabetologia* 2010 August;53(8):1795-806.

Supplemental data

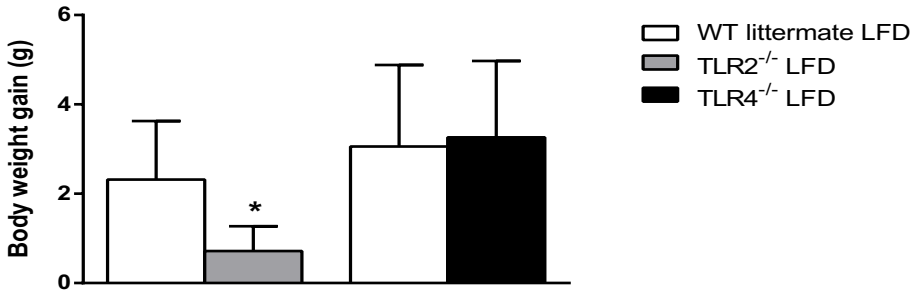

Supplemental figure A **Effect of LFD feeding on body weight gain.** Male TLR2$^{-/-}$ and TLR4$^{-/-}$ mice and WT littermates were fed a low-fat diet (LFD) for 12 weeks. Body weight was measured at the beginning and end of the dietary intervention. Values represent means ± SD (n=6-8 per group), *p<0.05 as compared to WT littermates.

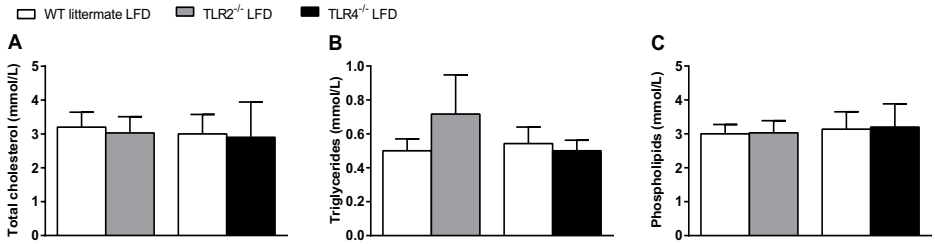

Supplemental figure B **Effect of LFD feeding on plasma lipids.** Male TLR2$^{-/-}$ and TLR4$^{-/-}$ mice and corresponding WT littermates were fed a low fat diet (LFD) for 12 weeks. After 10 weeks blood was drawn to determine total cholesterol (A), triglyceride (B) and phospholipid (C) levels. Values represent means ± SD (n=5-6 per group).

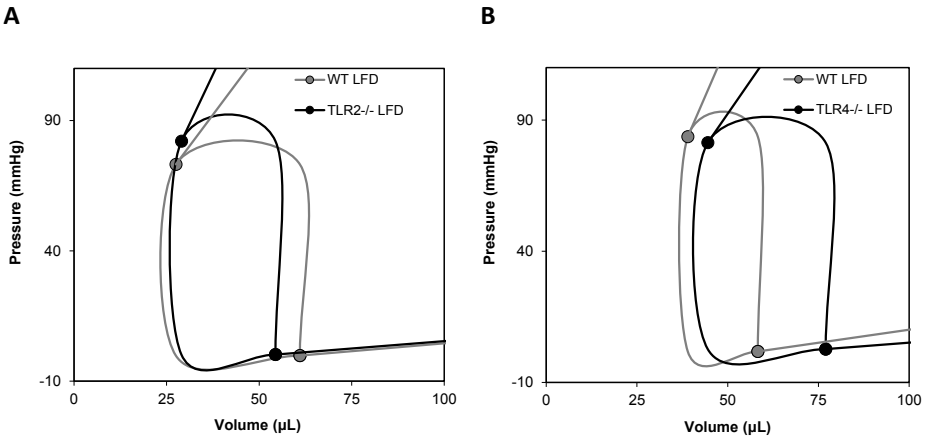

Supplemental figure C **Effect of LFD feeding on pressure-volume loops and pressure-volume relations.** Male TLR2$^{-/-}$ (A) and TLR4$^{-/-}$ (B) mice and corresponding WT littermates were fed a low-fat diet (LFD). After 12 weeks pressure-volume loops (PV-loops)were recorded in each mouse, and average PV-loops are shown per group (n= 4-5 per group).

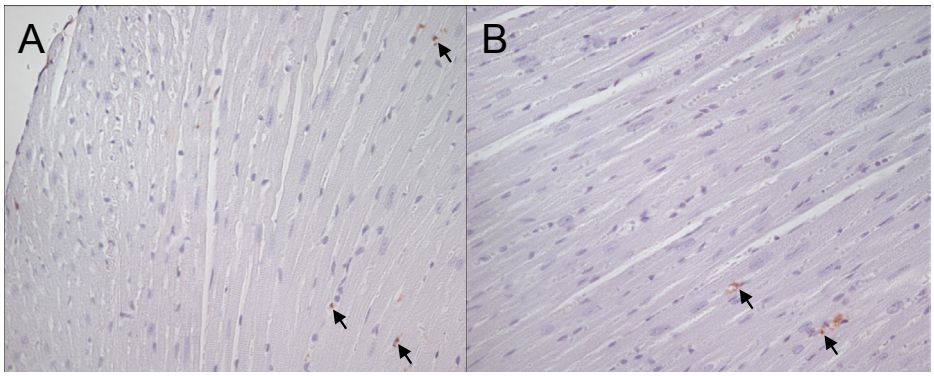

Supplemental figure D **Effect of LFD feeding on cardiac macrophage infiltration.** Representative images of macrophages stained cardiac tissue for A) low-fat diet (LFD) WT littermate group and B) LFD TLR$^{-/-}$ group. The shown example was from the TLR2$^{-/-}$ experiment, no between group differences was observed. Magnification 400x.

Supplemental Table A **Effect of diet intervention in TLR2$^{-/-}$, TLR4$^{-/-}$ and littermates on cardiac function**

	LFD			LFD		
	WT littermate	TLR2$^{-/-}$	P-value	WT littermate	TLR4$^{-/-}$	P-value
General						
HR (beats/min)	499 ± 59	526 ± 51	0.46	640 ± 18	558 ± 46	**0.014**
SV (µL)	33 ± 8	25 ± 14	0.33	19 ± 6	33 ± 12	**0.014**
CO (mL/min)	17 ± 5	13 ± 7	0.33	12 ± 4	18 ± 8	0.22
SW (mm Hg.µL)	2331 ± 612	2192 ± 1372	0.62	2105 ± 564	2683 ± 842	0.62
E_A (mm Hg/µL)	2.3 ± 0.4	4.3 ± 2.2	0.07	4.8 ± 1.5	2.8 ± 0.9	**0.05**
PHT (ms)	5.1 ± 1.21	5.1 ± 0.6	0.62	4.3 ± 0.6	4.9 ± 0.6	0.14
Systolic						
ESP (mm Hg)	73 ± 12	82 ± 16	0.33	84 ± 6	81 ± 13	0.62
ESV (µL)	28 ± 11	29 ± 8	0.81	39 ± 13	45 ± 12	0.46
EF (%)	56 ± 10	44 ± 10	0.09	35 ± 15	43 ± 10	0.33
dP/dt_{MAX} (mm Hg/ms)	6248 ± 1938	6948 ± 1997	0.62	8870 ± 1254	7224 ± 1160	**0.05**
SB-E_{ES} (mm Hg/µL)	1.9 ± 0.3	3.0 ± 0.5	**0.019**	3.2 ± 0.9	2.0 ± 0.6	**0.05**
Diastolic						
EDP (mm Hg)	-0.2 ± 1.9	0.2 ± 2.1	0.81	1.8 ± 1.9	2.7 ± 4.2	1.00
EDV (µL)	61 ± 14	54 ± 20	0.62	58 ± 10	77 ± 16	**0.05**
Tau (ms)	10.5 ± 2.1	10.0 ± 1.3	1.00	8.3 ± 1.4	9.4 ± 1.2	0.14
$-dP/dt_{MIN}$ (mm Hg/ms)	-5393 ± 1446	-6249 ± 1581	0.14	-7808 ± 1369	-6592 ± 995	0.22
SB-E_{ED} (mm Hg/µL)	0.12 ± 0.03	0.11 ± 0.03	0.81	0.20 ± 0.11	0.11 ± 0.02	**0.027**

Mice were fed a low-fat diet (LFD) for 12 weeks and cardiac function was determined. LV volume signals obtained by conductance catheter were calibrated by matching EF and CO with corresponding echocardiographic values obtained by measurements four days earlier. Values represent means ± SD (n= 4-5 per group). HR, heart rate; SV, stroke volume; CO, cardiac output; SW, stroke work; E_A, arterial elastance (afterload); PHT, pressure half time; ESP, end-systolic pressure; ESV, end-systolic volume; EF, ejection fraction; dP/dt_{MAX}, maximal rate of pressure increase; SB-E_{ES}, end-systolic elastance; EDP, end-diastolic pressure; EDV, end-diastolic volume; Tau, relaxation time constant; $-dP/dt_{MIN}$, maximal rate op pressure decline; SB-E_{ED}, end-diastolic elastance.

CHAPTER 7

Niacin reduces atherosclerosis development in APOE*3Leiden.CETP mice mainly by reducing nonHDL-cholesterol

Accepted for publication in PLOS ONE

Mieke C. Louwe[*1,4], Susan Kühnast*[*2,4,5], Mattijs M. Heemskerk[3,4], Elsbet J. Pieterman[5], Jan B. van Klinken[3,4], Sjoerd A.A. van den Berg[3,4], Johannes W.A. Smit[1], Louis M. Havekes[1,4,5], Patrick C.N. Rensen[1,4], José W.A. van der Hoorn[2,4,5], Hans M.G. Princen†[5] and J. Wouter Jukema†[2,4] *These authors contributed equally to the manuscript, †These authors share equal responsibility for the manuscript.*

Dept. of [1]Endocrinology and Metabolic Diseases, [2]Cardiology, [3]Human Genetics and [4]Einthoven Laboratory for Experimental Vascular Medicine, Leiden University Medical Center, Leiden, the Netherlands
[5]TNO - Metabolic Health Research, Leiden, the Netherlands

Niacin reduces atherosclerosis development in APOE*3Leiden.CETP mice mainly by reducing nonHDL-cholesterol

Abstract

Niacin potently lowers triglycerides, mildly decreases LDL-cholesterol, and largely increases HDL-cholesterol. Despite evidence for an atheroprotective effect of niacin from previous small clinical studies, the large outcome trials, AIM-HIGH and HPS2-THRIVE did not reveal additional beneficial effects of niacin (alone or in combination with laropiprant) on top of statin treatment. We aimed to address this apparent discrepancy by investigating the effects of niacin without and with simvastatin on atherosclerosis development and determine the underlying mechanisms, in APOE*3Leiden.CETP mice, a model for familial dysbetalipoproteinemia (FD).

Mice were fed a western-type diet containing cholesterol without or with niacin (120 mg/kg/day), simvastatin (36 mg/kg/day) or their combination for 18 weeks. Similarly as in FD patients, niacin reduced total cholesterol by -39% and triglycerides by -50%, (both $p<0.001$). Simvastatin and the combination reduced total cholesterol (-30%; -55%, $p<0.001$) where the combination revealed a greater reduction compared to simvastatin (-36%, $p<0.001$). Niacin decreased total cholesterol and triglycerides primarily by increasing VLDL clearance. Niacin increased HDL-cholesterol (+28%, $p<0.01$) and mildly increased reverse cholesterol transport. All treatments reduced monocyte adhesion to the endothelium (-46%; -47%, $p<0.01$; -53%, $p<0.001$), atherosclerotic lesion area (-78%; -49%, $p<0.01$; -87%, $p<0.001$) and severity. Compared to simvastatin, the combination increased plaque stability index [(SMC+collagen)/ macrophages] (3-fold, $p<0.01$). Niacin and the combination reduced T-cells in the aortic root (-71%, $p<0.01$; -81%, $p<0.001$). Lesion area was strongly predicted by nonHDL-cholesterol ($R^2=0.69$, $p<0.001$) and to a much lesser extent by HDL-cholesterol ($R^2=0.20$, $p<0.001$).

Niacin decreases atherosclerosis development mainly by reducing nonHDL-cholesterol with modest HDL-cholesterol-raising and additional anti-inflammatory effects. The additive effect of niacin on top of simvastatin is mostly dependent on its nonHDL-cholesterol-lowering capacities. These data suggest that clinical beneficial effects of niacin are largely dependent on its ability to lower LDL-cholesterol on top of concomitant lipid-lowering therapy.

Introduction

The beneficial effects of niacin, also known as nicotinic acid or vitamin B3, on plasma lipids and lipoproteins were first described in the 1950s.[1] According to a meta-analysis of 30 randomized controlled trials, niacin potently reduced triglycerides (TG) by ~15-30% and increased HDL-cholesterol (HDL-C) by ~10-25%, while mildly reducing plasma total cholesterol (TC) by ~5-15% and LDL-cholesterol (LDL-C) by ~5-20%, suggesting an atheroprotective effect.[2] Whereas previous small clinical studies supported this notion[3-6], the recent large outcome trials AIM-HIGH and HPS2-THRIVE failed to reveal additional beneficial effects of niacin on top of statin treatment.[7, 8]

In patients with atherosclerotic disease or those at risk for atherosclerotic disease due to dyslipidemia, the primary goal of lipid-modifying therapy is the lowering of LDL-C.[9] To this end, statins are currently the standard treatment for cardiovascular disease (CVD) resulting in a 25-45% risk reduction for cardiovascular events.[10] However, a substantial residual risk for adverse cardiovascular outcomes remains with statin therapy.[3, 11] Moreover, despite maximally tolerated statin treatment, some patients cannot reach LDL-C goals. This high risk population together with statin intolerant patients verify the need for another LDL-C-lowering agent to (further) reduce LDL-C levels.[12] Treatment of low HDL-C is currently considered a secondary lipid target in the reduction of cardiovascular risk[3], since low HDL-C is an independent risk factor for CVD.[2, 13] Considering the current treatment options, the question remains whether to further reduce LDL-C or to increase HDL-C in addition to LDL-C-lowering.[12] Therefore, due to both its nonHDL-C-lowering and HDL-C-raising properties, niacin was considered an attractive candidate for further cardiovascular risk reduction in addition to statin therapy.

Indeed, an initial small clinical study suggested that the addition of niacin to statin treatment may cause potentially clinical significant reductions in relative risk of cardiovascular events.[6] Recently a number of relatively small secondary prevention studies (ARBITER-2 [4], ARBITER-3 [5] and ARBITER-6-HALTS [3]) have shown reduced progression and even regression of atherosclerosis with combination treatment of niacin and statins compared to statins alone, as measured by carotid artery intima media thickness as a surrogate for clinical endpoints. Magnetic resonance imaging results from another study confirmed the reduction in carotid atherosclerosis with niacin in statin-treated patients.[14] These clinical data were corroborated by recent observations that niacin reduces atherosclerosis development, independent of lipid-lowering or HDL-C-elevation, in hyperlipidemic LDL receptor knockout mice on a high-fat diet containing 1.5% cholesterol.[15] Despite these promising data, the large outcome trial, AIM-HIGH, addressing the effect of niacin on top of aggressive LDL-lowering treatment, has recently been prematurely terminated due to futility.[8] In accordance, the much larger HPS2-THRIVE trial failed to reveal additional risk reduction of cardiovascular events with extended-release (ER)-niacin/laropiprant in combination with statin treatment as compared to statin mono-treatment.[7] ER-niacin[2] and ER-niacin/laropiprant combination treatment[16] are more tolerable formulations that have been developed due to a reluctance to use niacin for clinical treatment as a result of extreme flushing as a side effect.[17]

In the present study, we aimed to address the seeming discrepancy between the beneficial effects of niacin in initial clinical trials[3-6, 14], as well as in LDL receptor knockout mice, a model irresponsive to the lipid-modulating effects of niacin[15], and the lack of effect of niacin on top of statin treatment on reduction of cardiovascular events in the AIM-HIGH [8] and HPS2-THRIVE trials.[7] Therefore, we evaluated the effects of niacin without and with simvastatin on atherosclerosis development and investigated the underlying mechanisms and contributing factors in APOE*3Leiden.CETP mice. This is a well-established mouse model for familial dysbetalipoproteinemia (FD) with human-like lipoprotein metabolism and atherosclerosis development. These mice respond to the lipid-lowering effects of both niacin[18] and statins, e.g. atorvastatin[19], as well as the HDL-C-raising effect of niacin[18].

Materials and methods

Animals, diets and experimental design

Female APOE*3Leiden.CETP transgenic mice[20], expressing human cholesteryl ester transfer protein (CETP) under control of its natural flanking regions, were housed under standard conditions with a 12 h light-dark cycle and had free access to food and water during the experiment unless indicated otherwise. Body weight (BW) and food intake were monitored during the entire study. To increase plasma cholesterol levels up to ~12 mmol/L, 8-12 week-old mice were fed a semi-synthetic cholesterol-rich diet, containing 15% (w/w) cacao butter and 0.1% cholesterol (Western-type diet; Hope Farms, Woerden, the Netherlands) for 3 weeks. After matching based on age, BW, TC, TG and HDL-C mice (n=15 per group) received a control western-type diet (WTD) without or with 0.1% (w/w) niacin (120 mg/kg/day), 0.03% (w/w) simvastatin (36 mg/kg/day) or their combination for 18 weeks. During the treatment period, the effects of treatment on plasma lipids, lipoprotein profiles, CETP activity and CETP mass were assessed at the indicated time points.

The dose of simvastatin targeted a 30-35% reduction in TC and that of niacin a 20-30% increase in HDL-C. While we achieved these targets, it should be noted that the dose of simvastatin was 3 times higher than the maximum dose used in the clinic taking into account a 10 times faster metabolism in mice. For niacin the dose was comparable to that in patients, about 1 g/day. At the end of the experiment all animals were sacrificed by CO_2 inhalation. Liver and white adipose tissue (WAT) were isolated to assess CETP expression (n=6-8 per group) and hearts were isolated to assess atherosclerosis development (n=15 per group). Separate additional experiments were performed to evaluate the effects of niacin on VLDL production and clearance, as well as reverse cholesterol transport (RCT). Animal experiments were approved by the Institutional Animal Care and Use Committee of The Netherlands Organization for Applied Research (TNO).

Plasma lipids and lipoprotein profiles

After a 4 h fast, blood was collected via tail vein bleeding and plasma was isolated. Plasma TC, HDL-C after precipitation of apoB-containing lipoproteins using $MnCl_2$ [21] and TG were determined individually using enzymatic kits 1489437 and 1488872 (both from Roche diagnostics), according to the manufacturer's protocols. After 4 and 18 weeks of treatment, pooled lipoprotein profiles for TC were measured by fast protein liquid chromatography (FPLC).[20]

VLDL production and clearance experiments

APOE*3Leiden.CETP mice (11-14 weeks of age) were fed a WTD containing 0.1% cholesterol for 3 weeks. Upon subsequent matching according to plasma TC and TG levels, mice received the cholesterol-containing WTD without or with 0.1% (w/w) niacin for an additional 3 weeks[18] and VLDL production and clearance were determined as described.[22]

Plasma was obtained via tail vein bleeding in heparin microvettes for randomization (Sarstedt, Germany) and in chilled paraoxon-coated capillary tubes to prevent *ex vivo* TG hydrolysis for VLDL production and clearance, and assayed for TG and TC using commercially available kits 1488872 and 236691 (Roche Molecular Biochemicals, Indianapolis, IN, USA), respectively.

For the VLDL production experiment, 6 control and 6 niacin-treated mice were fasted for 4 h. During the experiment, mice were sedated with 6.25 mg/kg acepromazine (Alfasan), 6.25 mg/kg midazolam (Roche) and 0.31 mg/kg fentanyl (Janssen-Cilag). At t=0 min, blood was taken via tail bleeding and mice were injected intravenously with 100 µL PBS containing 100 µCi Trans^{35}S label to measure de novo total apoB synthesis. After 30 min, the mice received 500 mg of tyloxapol (Triton WR-1339, Sigma-Aldrich) per kg BW as a 10% (w/w) solution in sterile saline, to prevent systemic lipolysis of newly secreted hepatic VLDL-TG. Additional blood samples were taken 15, 30, 60, and 90 min after tyloxapol injection and used for determination of plasma TG concentration. After 120 min, the mice were sacrificed and blood was collected by orbital puncture for isolation of VLDL by density gradient ultracentrifugation. Incorporation of ^{35}S-label was measured in the VLDL fraction as marker of *de novo* apoB synthesis.

For the VLDL clearance experiment, glycerol tri[^{3}H]oleate (triolein, TO)- and [1α,2α(n)-^{14}C] cholesteryl oleate (CO)-double labeled VLDL-like emulsion particles (80 nm) were used.[23] In short, radiolabeled emulsions were obtained by adding 100 µCi of [^{3}H]TO and 10 µCi of [^{14}C]CO to 100 mg of emulsion lipids before sonication (isotopes obtained from GE Healthcare, Little Chalfont, UK). APOE*3Leiden.CETP mice (5 control and 5 niacin-treated mice) were fasted for 4 h, sedated as described above, and injected intravenously with the radiolabeled emulsion particles (1.0 mg TG in 200 µL PBS). Blood was taken from the tail vein to determine the content of [^{3}H]TO and [^{14}C]CO in serum at 2, 5, 10 and 15 min after emulsion injection. Fifteen min after injection, plasma was collected by orbital puncture and mice were sacrificed by cervical dislocation. Organs were harvested and saponified to determine uptake of radioactivity derived from [^{3}H]TO and [^{14}C]CO by various organs.[22]

Endogenous CETP activity, CETP mass and CETP mRNA expression analysis

Plasma endogenous CETP activity was determined by a fluorescent method using donor liposomes enriched with nitrobenzoxadiazole-labeled cholesteryl esters (RB-CETP, Roar Biomedical, New York, NY) as described.[19] CETP activity was calculated as nmol cholesteryl ester transfer/mL plasma/h. Plasma CETP mass was determined by using the DAIICHI CETP ELISA kit according to manufacturer's instructions (Daiichi, Tokyo, Japan).[18] Total RNA was extracted from liver and white adipose tissue (WAT) using an RNA isolation kit according to manufacturer's specifications (Macherey-Nagel, Düren, Germany). Total RNA concentrations were measured with Nanodrop. One µg of RNA was reversed-transcribed to cDNA with iScriptcDNA Synthesis kit (Bio-Rad) and purified with Nucleospin Extract II kit (Macherey-Nagel, Düren, Germany). Real-time PCR (RT-PCR) was carried out on an iQ5 PCR detection system (Bio-Rad) using Sensimix SYBR Green RT-PCR mix (Quantace, London, UK). Hypoxanthine-guanine phosporibosyltransferase (HPRT) and acidic ribosomal phosphoprotein PO (36B4) were used as the standard housekeeping genes

and expression levels were normalized to these housekeeping genes. Primer sequences are listed in supplemental table 1.

Histological assessment of atherosclerosis

After isolation, hearts were fixed in formalin, embedded in paraffin and cross-sectioned (5 μm) throughout the aortic root area. For each mouse, four sections at intervals of 50 μm were used for quantitative and qualitative assessment of the atherosclerotic lesions after staining with hematoxylin-phloxin-saffron. For determination of severity of atherosclerosis, the lesions were classified into five categories: I) early fatty streak, II) regular fatty streak, III) mild plaque, IV) moderate plaque, and V) severe plaque according to the American Heart Association classification.[19, 24] Lesion severity as a percentage of the number of lesions was calculated. To this end, type I-III lesions were classified as mild lesions and type IV-V lesions were classified as severe lesions. Total lesion area and number of lesions per cross section, as well as the percentage undiseased segments, were calculated. In each segment used for lesion quantification, the number of monocytes adhering to the endothelium and the numbers of T-cells in the total aortic root area were counted after immunostaining with AIA 31240 antibody (1:1000; Accurate Chemical and Scientific, New York, New York, USA) and CD3 (1:500; AbD Serotec, Oxford, UK), respectively. Macrophage content of the lesions was measured after immunostaining with Mac-3 (1:50; BD Pharmingen, the Netherlands). In addition, sirius red staining was used to quantify the collagen content in the plaque [25] and the antibody alpha actin (1:800; DAKO, Glostrup, Denmark) was used to quantify the smooth muscle cell (SMC) content.[26] Stained areas were measured using Cell^D imaging software (Olympus Soft Imaging Solutions, Tokyo, Japan).

Reverse cholesterol transport experiment

16 recipient APOE*3Leiden.CETP mice (10-12 weeks of age) were fed a WTD containing 0.1% cholesterol for a run-in period of 3 weeks after which they were subdivided into 2 groups according to age, BW, TC, TG and HDL-C. After matching, mice (n=8 per group) received a control cholesterol-containing WTD without or with 0.1% (w/w) niacin (120 mg/kg/day) for 3 weeks.

6 donor APOE*3Leiden.CETP mice (10-12 weeks of age) fed a WTD containing 0.1% cholesterol for 3 weeks were injected intraperitoneally with 1 mL solution of 3% thioglycollate to induce an inflammatory response. Three days after the injection, mice were injected intraperitoneally with approximately 300 μCi [^{3}H]-cholesterol together with 100 μg/mL acetylated LDL. Mice were sacrificed 1 h later by CO_2 inhalation. [^{3}H]-cholesterol-labeled macrophages were collected from the 6 donor mice by peritoneal lavage. These macrophages were washed twice with cold PBS and injected intraperitoneally into the 16 recipient APOE*3Leiden.CETP mice. Each recipient mouse received 2.8 x 10^6 [^{3}H]-cholesterol-labeled macrophages containing 7.8 x 10^6 dpm [^{3}H]-cholesterol. Mice were individually caged for 48 h in order to collect feces and sacrificed by CO_2 inhalation. 3H-activity was determined in the plasma, liver and feces. The in vivo RCT experiment was based on methods previously described.[27, 28]

Statistical analyses

Significance of differences between the groups was calculated non-parametrically using a Kruskal-Wallis test followed by a Mann-Whitney U-test for independent samples. We performed a univariate analysis of variance (ANOVA) to investigate the role of TC, nonHDL-C and HDL-C exposure as contributing factors in lesion development. A two-way analysis of covariance

(ANCOVA) was performed to test for group differences in lesion area, monocyte adhesion, T-cell abundance and macrophage area after correcting for HDL-C and nonHDL-C exposure. SPSS 17.0 for Windows (SPSS, Chicago, USA) was used for statistical analysis. All groups were compared to the control group and the combination group was also compared to the simvastatin group. Values are presented as means ± SD. P-values <0.05 were considered statistically significant. In the figures, the symbol * is used to compare to the control group, and # to compare to the simvastatin group.

Results

Niacin, simvastatin and their combination reduce plasma total cholesterol and triglycerides and niacin increases HDL-cholesterol in APOE*3Leiden.CETP mice

To verify the lipid-lowering effect of niacin alone and in combination with simvastatin, we measured plasma TC (figure 1A), TG (figure 1B) and HDL-C (figure 1C) levels during the study. The western-type diet resulted in an average TC of 13.4 ± 1.7 mmol/L, TG of 4.3 ± 1.4 mmol/L and HDL-C of 0.65 ± 0.13 mmol/L (control group). TC and TG levels were reduced by niacin (-39%, p<0.001; -50%, p<0.001), simvastatin (-30%, p<0.001; -19%, NS) and the combination (-55%, p<0.001; -52%, p<0.001). The combination reduced TC to a greater extent than simvastatin alone (-36%, p<0.001). Niacin increased HDL-C by +28% (p<0.01) as compared to the control, whereas the combination increased HDL-C by +14% (p<0.05) as compared to simvastatin mono-treatment. Niacin alone resulted in higher HDL-C than the combination (p<0.001). The reductions in plasma TC induced by niacin, simvastatin and the combination were confined to apoB-containing lipoproteins as measured after lipoprotein separation by FPLC (figure 1D).

Niacin reduces apoB-containing lipoprotein cholesterol by modestly increasing VLDL clearance without affecting VLDL production

To determine by which mechanism the level of apoB-containing lipoprotein cholesterol is decreased, first the VLDL-TG production was assessed after injection of Tran^{35}S label and tyloxapol. VLDL-TG production did not differ between controls and niacin-treated mice (figure 2A; control 6.1 ± 0.7 μmol/mL/h versus niacin 6.2 ± 0.8 μmol/mL/h; p=0.94). In addition, the apoB production rate, as measured by incorporation of ^{35}S-activity in the VLDL fraction (figure 2B; control 2.9 ± 0.5 μmol/mL/h versus niacin 2.9 ± 0.4 μmol/mL/h; p=0.94) and VLDL-apoB lipidation (control 1.3 ± 0.4 nmol/100 dpm versus niacin 1.4 ± 0.3 nmol/100 dpm; p=0.69) did not differ between groups.

We then examined the clearance and uptake of [^{3}H]TO and [^{14}C]CO-labeled VLDL-like emulsion particles. Despite lack of statistical power, due to unexpected loss of mice, there was a trend towards a faster plasma clearance rate of [^{3}H]TO (figure 2C control $t_{1/2}$ = 6.4 ± 2.2 min versus niacin $t_{1/2}$ = 4.9 ± 0.9 min; p=0.19) and a significantly faster

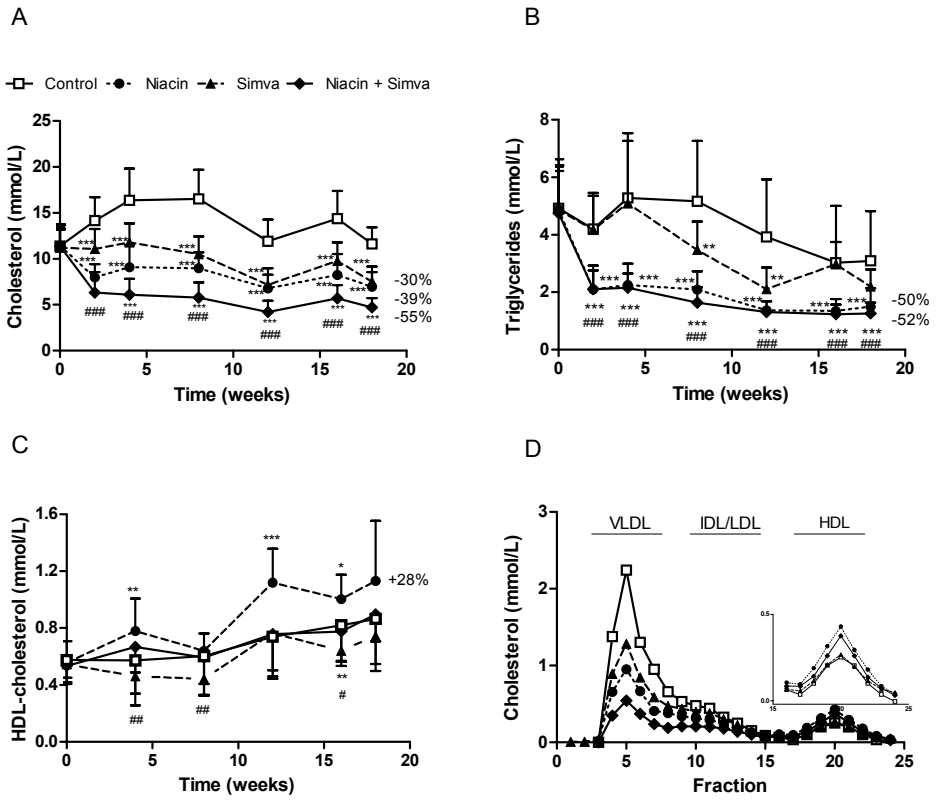

Figure 1 **Effect of niacin, simvastatin and their combination on plasma lipid levels.** Plasma total cholesterol (A), triglycerides (B) and HDL-cholesterol levels were measured at various time points throughout the study. The average HDL-cholesterol levels were calculated for all the treatment groups (C). Lipoproteins were separated by FPLC and cholesterol was measured in the fractions after 18 weeks of treatment (D). (Simva, simvastatin; values are means ± SD; n=15 per group; **p<0.01 and ***p<0.001 as compared to control; #p<0.05 and ###p<0.001 as compared to niacin + simvastatin).

initial [^{3}H]TO clearance in the first 5 min after niacin treatment (p<0.05). Tissue-specific ^{3}H-accumulation did not differ between groups, although there was a tendency (p=0.07) for a higher ^{3}H-accumulation in the spleen from the niacin-treated mice (figure 2D). This was accompanied by a non-significant increase in the plasma clearance rate of [^{14}C] CO (control $t_{1/2}$ = 11.6 ± 5.5 min versus niacin $t_{1/2}$ = 7.1 ± 1.7 min; p=0.12) with no differences in ^{14}C-accumulation in the various organs between groups (data not shown).

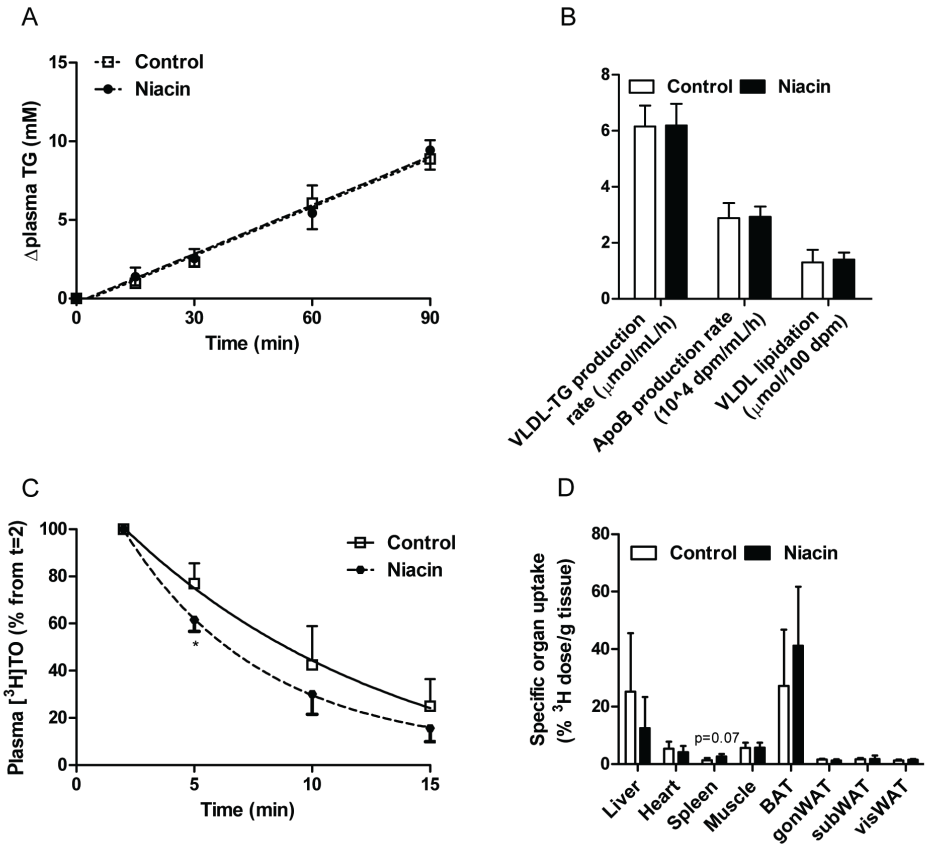

Figure 2 **Effect of niacin on VLDL production and clearance.** To determine VLDL production, mice were injected with Trans^{35}S label and tyloxapol and the accumulation of TG in plasma (A) and the production rate of VLDL-TG and apoB, as well as VLDL lipidation, defined as the ratio of VLDL-TG/apoB, were determined (B). To determine VLDL clearance, mice were injected with glycerol tri[^{3}H]oleate- and [^{14}C]cholesteryl oleate-labeled VLDL-like emulsion particles. Plasma ^{3}H-activity was determined as percentage of the initial dose (C), and uptake of ^{3}H-activity by various organs was determined as percentage of the injected dose per gram wet tissue (D). (BAT, brown adipose tissue; gonWAT, gonadal white adipose tissue; subWAT, subcutaneous white adipose tissue; visWAT, visceral white adipose tissue; values are means ± SD; n=6 per group for VLDL production and n=3-5 per group for VLDL clearance; *p<0.05 as compared to control).

Niacin, simvastatin and their combination reduce plasma CETP activity, CETP mass and niacin alone and together with simvastatin reduces hepatic CETP gene expression

In a previous study we showed that niacin increased HDL-C by decreasing hepatic CETP expression and plasma CETP concentration.[18] To verify this, we measured plasma CETP activity and mass and hepatic CETP mRNA expression after 4 and/or 18 weeks of treatment (table 1). Niacin, which most prominently increased HDL-C, reduced the average plasma CETP activity by -21% (p<0.01) and mass by -22% (p<0.01). Simvastatin

Table 1 **The effect of niacin, simvastatin and their combination on plasma CETP activity after 4 and 18 weeks of treatment, as well as plasma CETP mass and hepatic CETP expression after 18 weeks of treatment.**

	Average plasma CETP activity (nmol/mL/h)	Plasma CETP mass (µg/mL)	Hepatic CETP expression (% of control)
Control	64.3 ± 11.4	21.3 ± 3.4	100 ± 30
Niacin	50.6 ± 6.6 **	16.6 ± 3.5 **	76 ± 23 p=0.072
Simva	48.1 ± 8.4 *** p=0.081	13.4 ± 3.5 *** p=0.050	76 ± 25
Niacin + Simva	42.6 ± 8.9 ***	11.0 ± 2.2 ***	58 ± 33 p=0.059

CETP, cholesteryl ester transfer protein; Simva, simvastatin. Values are means ± SD (n=15 per group for plasma CETP activity and mass and n=6-8 per group for hepatic CETP expression). **p<0.01 and ***p<0.001 as compared to control

reduced CETP activity and mass by -25% and -37%, respectively (both p<0.001) without affecting HDL-C levels. The combination reduced CETP activity (-34%; p<0.001) and mass (-48%; p<0.001) to an even higher extent. Previously, we demonstrated that this reduction was due to reduced CETP mRNA expression in the liver. In line with these results, we found that niacin alone and in combination with simvastatin tended to reduce hepatic CETP expression to -76% (p=0.072) and -58% (p=0.059), respectively. Besides the liver, WAT is considered as a major source of CETP and since WAT is a target of niacin[29], we also determined the effect of all treatments on CETP mRNA expression in WAT. Niacin did not decrease CETP expression in WAT (data not shown), which is consistent with a recent study in CETP transgenic mice.[30] For the control group, a 125 times lower relative CETP expression was measured in WAT compared to the liver (data not shown). A mild correlation was found between hepatic CETP expression and plasma CETP mass (R^2=0.25, p=0.006), whereas CETP expression in WAT did not correlate with plasma CETP mass (R^2=0.02, p=0.45) (data not shown). Taken together, we concluded that the liver is the major determinant for circulating CETP levels in this model, which were affected by all the treatments.

Niacin alone and in combination with simvastatin reduces atherosclerosis development to a greater extent than simvastatin treatment alone

After 18 weeks of treatment, we measured the effect of niacin, with and without simvastatin on atherosclerosis development in the aortic root. Figure 3 illustrates representative images of atherosclerotic lesions for each group. We determined the number of lesions per cross section (figure 4A), the lesion severity as a percentage of all lesions (figure 4B), the percentage undiseased segments (figure 4C) and the total lesion area per cross section (figure 4D). To determine lesion severity as a percentage of all lesions, type I-III lesions were classified as mild lesions and type IV-V lesions were classified as severe lesions.

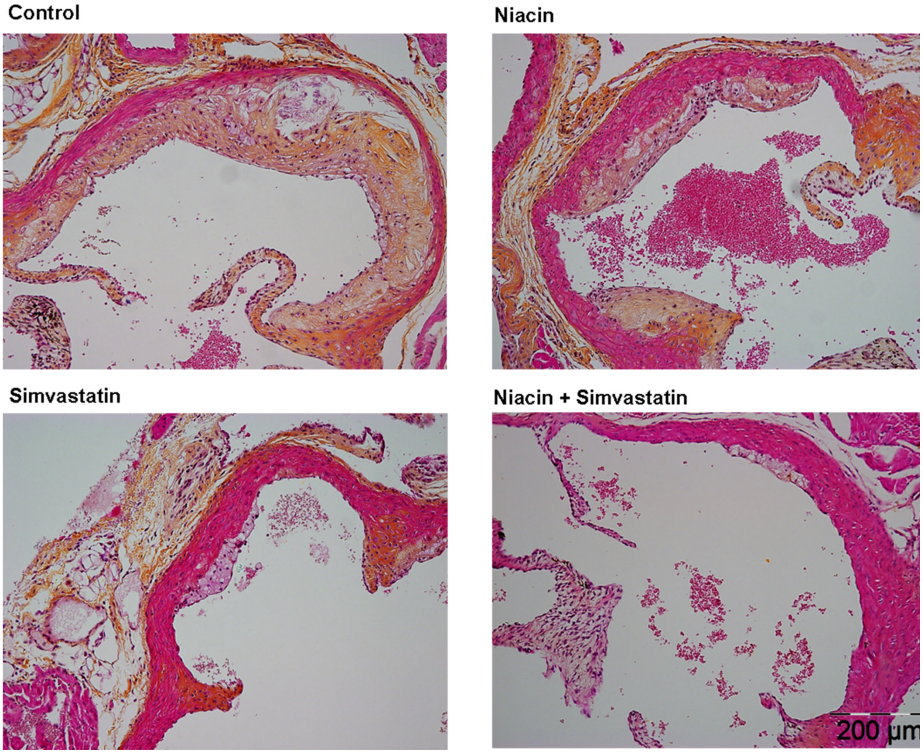

Figure 3 **Effect of niacin, simvastatin and their combination on plaque morphology.** Representative images of hematoxylin-phloxine-saffron-stained atherosclerotic lesions in a cross section of the aortic root area for the control group (A), niacin group (B), simvastatin group (C) and the combination group (D) after 18 weeks of treatment.

In the control group, a fair amount of atherosclerosis developed with 3.5 ± 0.9 lesions per cross section, of which 62 ± 16% were severe and only 17 ± 16% undiseased segments. The total lesion area was 144 ± 63 x10^3 µm^2 per cross section. When compared to the control, niacin reduced the number of lesions (-23%; p=0.056), attenuated lesion severity (p<0.001) and increased the percentage undiseased segments (+141%, p<0.001). Furthermore, niacin strongly decreased the total lesion area by -78% (p<0.001). Simvastatin alone was less effective as it only reduced lesion severity (p<0.01) and total lesion area (-49%, p<0.01). The combination had potent inhibiting effects on lesion development, as evidenced by reductions in lesion number (-48%, p<0.001), severity (p<0.001) and area (-87%, p<0.001), and by an increase in the percentage of undiseased segments (+210%, p<0.001). Furthermore, the percentage undiseased segments, as well as the reduction in the lesion number and area was greater after the combination compared to simvastatin alone (-44%; +110%; -74%, all p<0.01). These results showed that niacin mono-treatment was very potent in inhibiting atherosclerotic lesion development in APOE*3Leiden.CETP mice and that niacin added to the atherosclerosis-reducing effects of simvastatin.

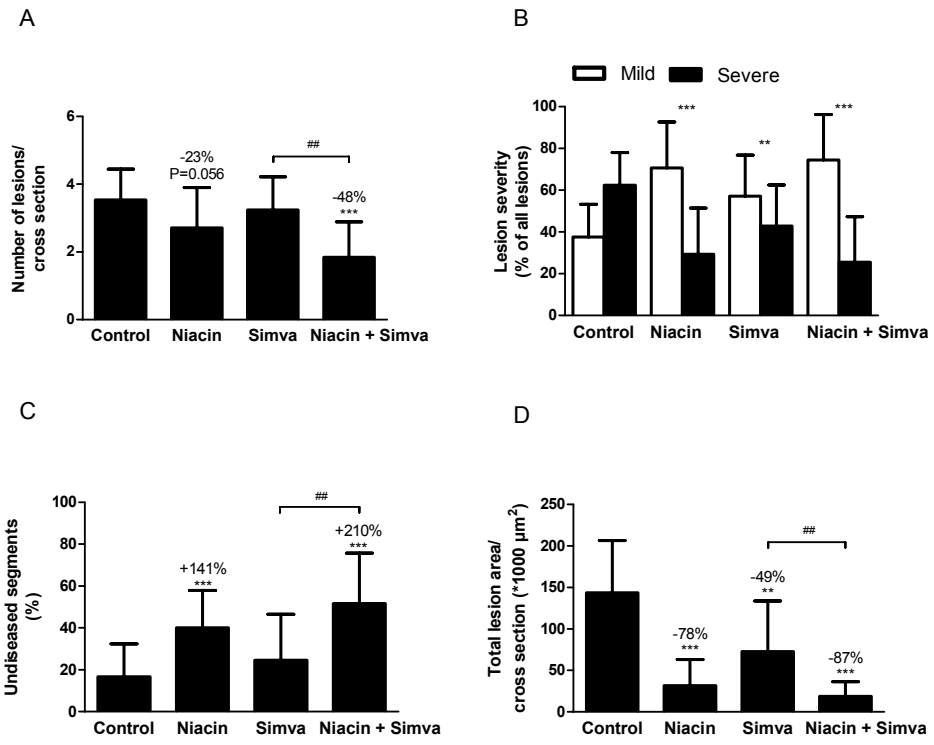

Figure 4 **Effect of niacin, simvastatin and their combination on atherosclerosis development in aortic root area.** After 18 weeks of treatment, number of lesions (A), lesion severity (B), percentage undiseased segments (C) and total lesion area (D) were determined per cross section. Lesion severity was classified as mild (type I-III) and severe (type IV-V) lesions. (Simva, simvastatin; values are means ± SD; n=15 per group; **p<0.01 and ***p<0.001 as compared to control; ##p<0.01 as compared to niacin + simvastatin).

Niacin improves lesion stability index and decreases functional markers of vascular inflammation

After investigation of lesion morphology, we analyzed the treatment effects on plaque composition. For all lesions, the macrophage area as destabilization factor (figure 5A), as well as SMC (figure 5B) and collagen area (data not shown) as stabilization factors were calculated per cross section. The macrophage, SMC and collagen area per cross section in the control group were 24.3 ± 8.6 x10^3 µm^2, 4.6 ± 2.3 x10^3 µm^2 and 64.2 ± 37.0 x10^3 µm^2, respectively. All treatments reduced the macrophage (-73%, -52% and -90%; all p<0.001) and the SMC area (-66%, p<0.01; -50%, p<0.01; -79%, p<0.001). As a measure of the lesion stability index, the ratio of collagen and SMC area (i.e. stabilization factors) to macrophage area (i.e. destabilization factor) was determined for all lesions (data not shown). The lesion stability ratio for the control group was 2.7 ± 1.4. Combination treatment tended to increase this ratio by +201% (p=0.085).

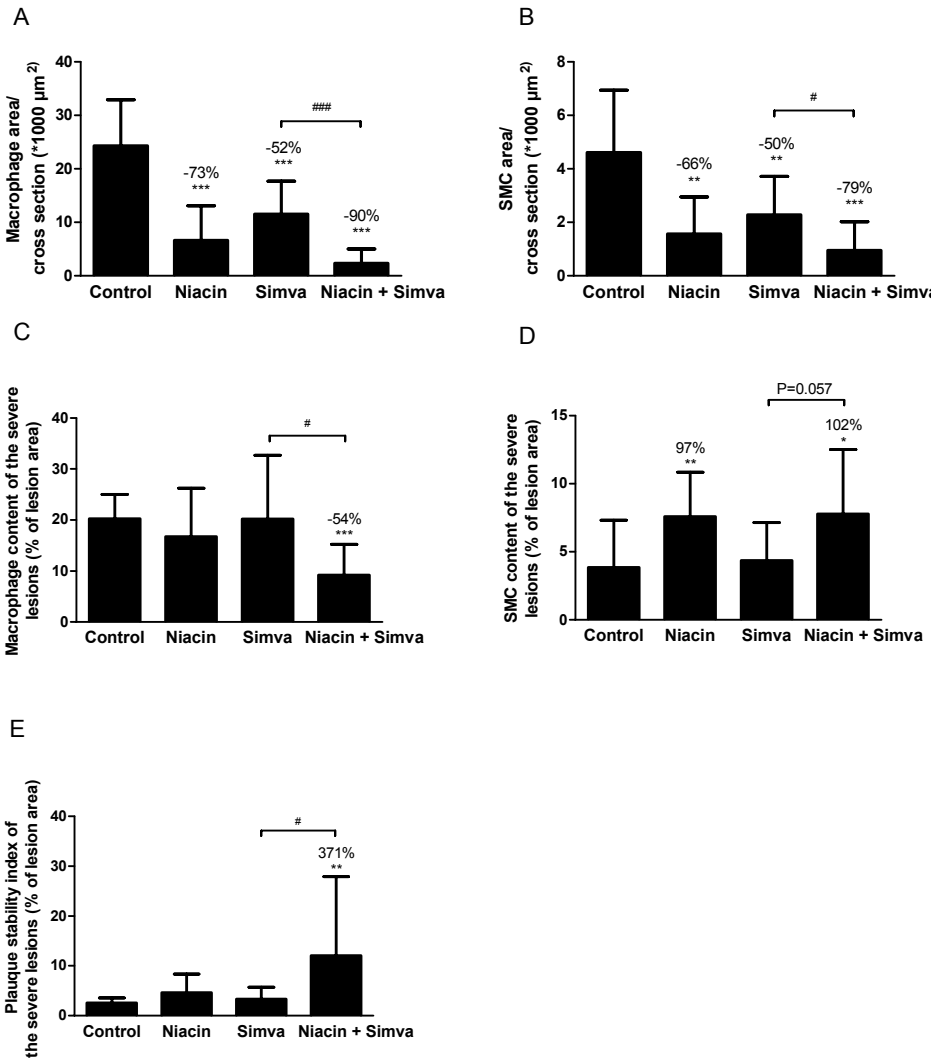

Figure 5 **Effect of niacin, simvastatin and their combination on lesion composition.** Macrophage area (A) and SMC area (B) were determined for all lesions and calculated per cross section. To correct for lesion size, macrophage content (C), SMC content (D), as well as plaque stability index (ratio of collagen and SMC content to macrophage content) (E) were also calculated as a percentage of lesion area, specifically in severe lesions (type IV-V). (Simva, simvastatin; SMC, smooth muscle cells; values are means ± SD; n=15 per group; *p<0.05, **p<0.01 and ***p<0.001 as compared to control; #p<0.05, and ###p<0.001 as compared to niacin + simvastatin).

After finding indications for more stable lesions, we specifically focused on the composition of the more severe lesions, which are considered to be the most vulnerable lesions. Additionally, we corrected for the lesion area. Thus, we measured the macrophage (figure 5C), SMC (figure 5D) and collagen content (data not shown) as a percentage of

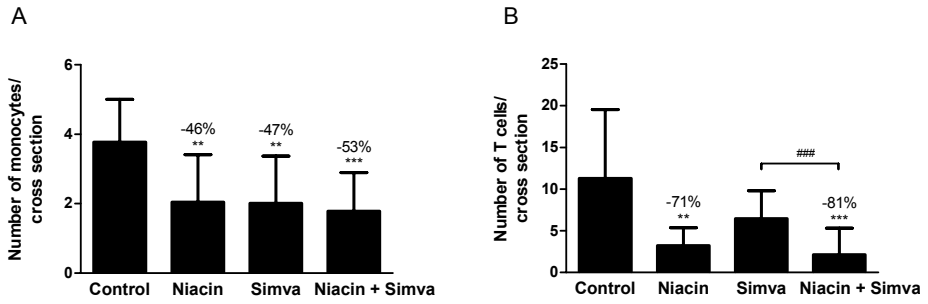

Figure 6 **Effect of niacin, simvastatin and their combination on monocyte adhesion and T-cell number.** The number of monocytes adhering to the endothelium (A) and the number of T-cells in the aortic root area (B) were determined per cross section. (Simva, simvastatin; values are means ± SD; n=15 per group; **p<0.01; ***p<0.001 as compared to control; ###p<0.001 as compared to niacin + simvastatin).

lesion area. The severe lesions in the control group consisted of 20% macrophages, 4% SMC and 45% collagen (latter data not shown). Niacin alone and in combination with simvastatin reduced the relative macrophage content by -18% (NS) and -54% (p<0.001), respectively and increased the relative SMC content by +97% (p<0.01) and +102% (p<0.05), respectively. The combination was superior to simvastatin mono-treatment in stabilizing the plaque as seen by a reduction in macrophage content (-54%; p<0.05) and an increase in SMC content (+79%; p=0.057). There were no significant differences in collagen content between groups (data not shown). The lesion stability index was also calculated for the severe lesions based on the relative area (figure 5E). Combination treatment increased this ratio by +371% (p<0.01) compared to the control (2.6 ± 1.0) and to a greater extent compared to simvastatin (p<0.05) alone.

As functional markers of vessel wall inflammation, the number of monocytes adhering to the activated endothelium (figure 6A) and T-cells in the aortic root area (figure 6B) were counted and calculated per cross section. In the control group, 3.8 ± 1.2 adhering monocytes and 11.3 ± 8.3 T-cells were present. A marked reduction of adhering monocytes of more than -45% (p<0.01; p<0.01 and p<0.001, respectively) was found in all treatment groups, where T-cells abundance was reduced by niacin alone (-71%, p<0.01) and in combination with simvastatin (-81%, p<0.001).

Niacin reduces atherosclerosis progression primarily by reducing nonHDL-cholesterol

In addition to inflammation, plasma cholesterol is certainly a strong determinant for atherosclerosis progression. We evaluated whether the anti-atherogenic effect of niacin and simvastatin could be explained by the reduction in plasma TC (figure 7). Since atherosclerotic lesion area showed a quadratic dependence on plasma TC exposure, lesion area was transformed using a square root transformation. Lesion area was strongly predicted by plasma TC exposure (R^2=0.70, p<0.001; figure 7A), and nonHDL-C

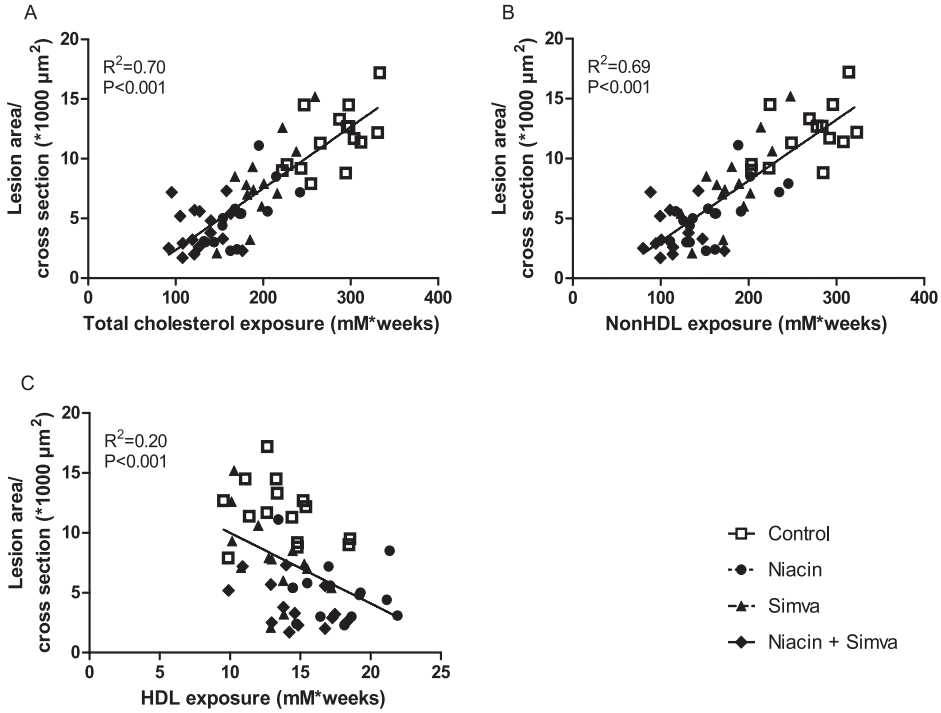

Figure 7 **Correlation between plasma cholesterol exposure and lesion area.** The square root of the lesion area was plotted against total cholesterol exposure (A), nonHDL-cholesterol exposure (B) and HDL-cholesterol exposure (C). Linear regression analyses were performed. (Simva, simvastatin; n=15 per group).

exposure (R^2=0.69, p<0.001; figure 7B) and to a much lesser extent by HDL-C exposure (R^2=0.20, p<0.001; figure 7C). Together, nonHDL-C and HDL-C exposure accounted for 71% of the variability in lesion area and predicted the lesion area independently of each other (p<0.001 and p<0.05, respectively). Importantly, the effects of niacin and simvastatin on lesion area were lost after correcting for both HDL-C and nonHDL-C exposure (p=0.16; p=0.61, respectively). Furthermore, no effect of niacin and simvastatin on monocyte adhesion was found after correcting for nonHDL-C exposure (p=0.50; p=0.20, respectively). However, niacin decreased the square-root transformed macrophage area and T-cell abundance even after correcting for nonHDL-C exposure (both p<0.01), whereas simvastatin did not (p=0.12; p=0.26, respectively).

Collectively, these data are compatible with a mechanism that niacin and simvastatin mainly decrease atherosclerotic lesion development via a reduction of nonHDL-C with an additional effect of HDL-C-elevation for niacin, while a direct effect on lesion macrophages and T-cell abundance may contribute to the anti-atherogenic effect of niacin, but not simvastatin.

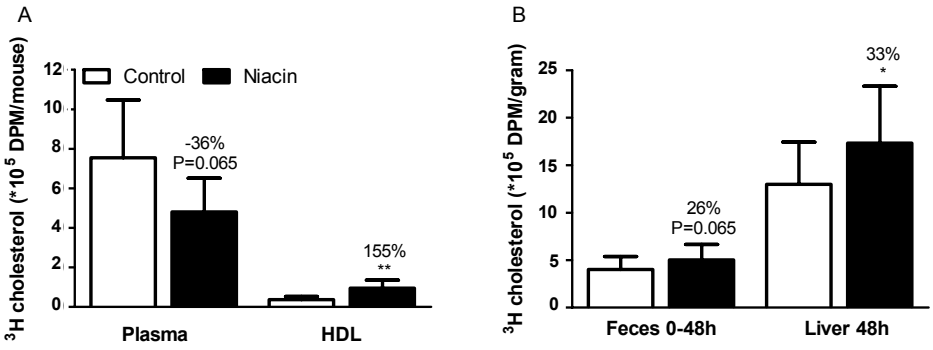

Figure 8 **Effect of niacin on reverse cholesterol transport.** [^{3}H]-cholesterol-labeled macrophages were injected in control and niacin-treated mice and ^{3}H activity was determined in plasma and HDL (A) and the liver 48 h after injection, as well as in feces collection between 0-48 h after injection (B). (Values are means ± SD; n=8 per group; *p<0.05 and ** p<0.01 as compared to control).

Niacin mildly increases reverse cholesterol transport

To investigate the possible mechanism by which the HDL-C-raising effect of niacin may contribute to its anti-atherogenic effect, we performed an *in vivo* RCT experiment. After 3 weeks of treatment, mice were injected with [^{3}H]-cholesterol-labeled macrophages. Forty eight hours after injection, plasma total ^{3}H-activity tended to be decreased (-36%, P=0.065), whereas ^{3}H-activity in the HDL fraction was increased after niacin treatment (+155%, p<0.01; figure 8A). In addition, niacin increased ^{3}H-activity in the liver (+33%; p<0.05) and tended to increase fecal ^{3}H-activity (+26%; p=0.065; figure 8B).

Discussion

In this study, we aimed to address the discrepancy between the beneficial effects of niacin in initial clinical trials[3-6, 14] and the lack of effect of niacin on top of statin treatment on reduction of cardiovascular events in the AIM-HIGH[8] and HPS2-THRIVE[7] trials by investigating the effects of niacin without and with simvastatin on atherosclerosis development and determine the underlying mechanisms in APOE*3Leiden.CETP mice, a mouse model for FD. We demonstrated that niacin decreased atherosclerosis development mainly by reducing nonHDL-C with a modest HDL-C-raising and anti-inflammatory effect and that the additive effect of niacin on top of simvastatin was mostly dependent on its nonHDL-C-lowering capacities.

First, we showed that niacin and simvastatin both reduced plasma lipid levels. Niacin reduced (V)LDL-C and (V)LDL-TG and increased HDL-C, whereas simvastatin mainly reduced (V)LDL-C. Combination treatment of niacin and simvastatin reduced nonHDL-C more effectively as compared to simvastatin alone. In our study,

the reduction in plasma TC after niacin treatment alone and in combination with simvastatin was greater compared to recent clinical trials. The APOE*3Leiden mouse was initially developed as an animal model for FD or type III hyperlipoproteinemia, which is characterized by elevated levels of cholesterol and an increased ratio of cholesterol to TG in the VLDL and intermediate density lipoprotein (IDL) fractions, resulting in the appearance of β-VLDL particles.[31, 32] Similarly as in FD patients, in APOE*3Leiden and APOE*3Leiden.CETP mice as a model for mixed dyslipoproteinemia, a major part of plasma cholesterol is contained in the VLDL and VLDL-remnant particles, leading to formation of β-VLDL particles, which further increases after cholesterol feeding. Whereas niacin reduces plasma TC by ~5-15%, LDL-C by ~5-20% and TG by ~15-30% in patients with hyperlipidemia[2], in two small studies in FD patients, niacin decreased TC by 23-50% and TG by 43-62% [33, 34] with -56% reduction of VLDL-C and 48% reduction of VLDL-TG.[34] Thus, the extent of lipid-lowering observed with niacin in APOE*3Leiden. CETP mice is comparable to that of FD patients.

Since plasma VLDL-TG and apoB levels are determined by the balance between VLDL production and clearance, we evaluated their individual contribution. VLDL production was not affected in niacin-treated mice, neither was apoB production or lipidation of the VLDL particle. However, a modest effect of niacin on VLDL clearance was observed. The mechanism behind the lipid-lowering effect of niacin has been generally ascribed to a reduced hepatic VLDL production, as a result of decreased free fatty acid (FFA) flux from WAT after inhibition of hormone sensitive lipase. However, an initially decreased FFA flux is followed by a rebound effect with increased release of FFA.[1, 35] In humans, contradicting data describe that niacin decreased VLDL production without affecting VLDL clearance[36-38] and on the other hand that niacin enhanced clearance of apoB without affecting production.[39] The latter study is in line with our results, which implicate VLDL clearance rather than VLDL production as the possible mechanism by which niacin reduces apoB.

The niacin-induced increase in HDL-C in the present study may be attributed to a decrease in hepatic and plasma CETP leading to an inhibition of HDL delipidation as previously described.[18] As similar effects on CETP levels and activity were observed after simvastatin treatment, without affecting HDL, different mechanisms are likely involved in either treatment. Interestingly, a decreased macrophage content accompanying decreased hepatic cholesterol accumulation as a result of niacin's lipid-lowering effect was recently proposed as a mechanism by which niacin decreases hepatic CETP expression.[30]

An important observation from our studies is that niacin decreases atherosclerosis progression and adds to the anti-atherogenic effect of simvastatin, in particular regarding its enhancing effect on plaque stability. Niacin decreased lesion number, severity and area, and increased the percentage undiseased segments. Moreover, niacin improved lesion composition by reducing the macrophage content and increasing the SMC content. Importantly, the combination treatment increased the plaque stability index, defined as the ratio of SMC and collagen over macrophage area, as compared to either niacin or simvastatin alone.

It is interesting to speculate on the mechanism(s) underlying the anti-atherogenic effect of niacin. In the APOE*3Leiden.CETP mouse model, statistical analyses revealed that the effects of niacin and simvastatin were largely explained by their reduction in nonHDL-C, as evidenced by a strong correlation between plasma nonHDL-C and lesion area. The fact that the combination treatment reduced nonHDL-C beyond the level reached by simvastatin alone can thus largely explain why niacin added to the anti-atherosclerotic effect of simvastatin. Though, HDL-C also appeared to predict lesion area independent of nonHDL-C, albeit that the predictive value of HDL-C was much smaller than that of nonHDL-C. The HDL-C-raising effect of niacin, may, therefore, have contributed to some extent to the anti-atherosclerotic activity of niacin.

To explore the contribution of the niacin-induced increase in HDL-C to the reduction of atherosclerosis, we investigated the functionality of HDL by performing an RCT experiment. From this experiment, we conclude that the effect of niacin on RCT may partially contribute to, but is not the driving force behind its anti-atherogenic effects. This is in accordance with our statistical correlations, which showed nonHDL-C to be a much stronger contributor to atherogenesis. Although HDL-C contributed to some extent, we observed that niacin's attenuating effect on atherosclerosis development in APOE*3Leiden.CETP mice, fed a Western-type diet with 0.1% cholesterol, is largely explained by its lipid-lowering effect. At first sight, this seems to contradict a recent report showing that niacin reduced atherosclerosis development in LDL receptor-deficient mice under conditions that left plasma cholesterol levels unaffected.[15] In that mouse model, the atheroprotective effects of niacin were mainly explained by impaired homing macrophage recruitment to atherosclerotic plaques and by promoting cholesterol efflux from macrophages by upregulation of ABCG1. However, it should be noted that those mice were fed a high-fat diet containing as much as 1.5% cholesterol. A previous study from our laboratory showed that dietary cholesterol induced dose-dependent marked inflammation in mice[40], where the liver switches to an inflammatory, pro-atherosclerotic state as reflected by a strong increase in serum amyloid A levels at dietary cholesterol levels exceeding 0.5%. Previously, Lukasova *et al.*[15] evaluated the anti-atherogenic effect of niacin under highly inflammatory conditions, at which the anti-inflammatory properties of niacin may become dominant and may not necessarily reflect the mode of action for niacin under mild cholesterol intake as used in the present study.

It should be noted that we also obtained evidence that niacin exerted anti-inflammatory effects in our mouse model under milder dietary conditions. Firstly, niacin reduced monocyte adhesion and macrophage area of the atherosclerotic lesions. In fact, niacin reduced macrophage area independent of nonHDL-C, whereas simvastatin did not. These data not only corroborate the findings in LDL receptor-deficient mice [15], but also the recent observations that niacin reduced collar-inflicted vascular inflammation and inhibited intima-media neutrophil recruitment in New Zealand White rabbits independent of changes in plasma lipids.[41] Secondly, we observed that niacin, but not simvastatin, strongly reduced the number of T-cells in the aortic root area, which are involved in the progression of atherosclerosis.[42] The reduction was independent of nonHDL-C exposure, suggesting the anti-inflammatory effect observed was brought about by niacin, instead of HDL derived. This is in accordance with a study where niacin inhibited monocyte chemotactic protein 1 (MCP-1), RANTES and fractalkine in

adipocytes. These chemokines contribute to the recruitment of T-cells and macrophages. WAT is known to express the GPR109A receptor and has the ability to contribute to both systemic and local (perivascular) inflammation associated with atherosclerosis.[29, 43]

Although initial clinical studies showed that niacin reduced atherosclerosis development in combination with statins[3-5] and reduced the relative risk of cardiovascular events[6], results from the large outcome trials AIM-HIGH and HPS2-THRIVE did not confirm earlier findings.[8, 44, 45] In order to test the HDL hypothesis, the AIM-HIGH investigators minimized the differences in LDL levels between the groups. Patients enrolled in the trial were subjected to aggressive LDL-C-lowering treatment, aimed at LDL-C of 40-80 mg/dL (1.03-2.07 mmol/L), reaching mean baseline LDL-C of 71 mg/dL (1.84 mmol/L) and HDL-C of 35 mg/dl (0.91 mmol/L).[46] A modest increase in HDL-C was observed in the placebo group, resulting in a 4-5 mg/dl (0.10-0.13 mmol/L) difference in HDL-C between groups. This, together with the aggressive LDL-C-lowering may have given rise to insufficient power to detect a reduction in events.[45] Unexpectedly, the much larger outcome trial HPS2-THRIVE failed to reveal further cardiovascular risk reduction when adding ER-niacin/laropiprant to vigorous statin treatment, plus if required ezetimibe, as compared to statin/(ezetimibe) mono-treatment.[7] Furthermore, there was a significant increase in non-fatal serious adverse events and drop-out rate in the ER-niacin/laropiprant-treated patients. The lack of inclusion criteria for HDL-C resulted in a baseline HDL-C of >40 mg/dl (1.14 mmol/L) with a low baseline LDL-C level of <70 mg/dl (1.64 mmol/L). Patient stratification revealed that baseline HDL-C levels did not predict efficacy of niacin and that indeed only in patients with high LDL-C niacin reduced major cardiovascular events.

In conclusion, our results show that niacin decreases atherosclerosis development mainly by reducing nonHDL-C with modest HDL-C-raising and additional anti-inflammatory effects. The additive effect of niacin on top of simvastatin is mostly dependent on its nonHDL-C-lowering capacities. These data suggest that clinically beneficial effects of niacin are largely dependent on its ability to lower LDL-C on top of concomitant lipid-lowering therapy and may explain the failure of niacin in the clinical outcome trials.

Acknowledgement

We thank Erik Offerman, Ria van den Hoogen, Annemarie Maas, Simone van der Drift-Droog, Karin Toet, Wim van Duyvenvoorde and Amanda Pronk for their excellent technical assistance.

References

1 Carlson LA. Nicotinic acid: the broad-spectrum lipid drug. A 50th anniversary review. *J Intern Med* 2005 August;258(2):94-114.

2 Birjmohun RS, Hutten BA, Kastelein JJ, Stroes ES. Efficacy and safety of high-density lipoprotein cholesterol-increasing compounds: a meta-analysis of randomized controlled trials. *J Am Coll Cardiol* 2005 January 18;45(2):185-97.

3 Taylor AJ, Villines TC, Stanek EJ et al. Extended-release niacin or ezetimibe and carotid intima-media thickness. *N Engl J Med* 2009 November 26;361(22):2113-22.

4 Taylor AJ, Sullenberger LE, Lee HJ, Lee JK, Grace KA. Arterial Biology for the Investigation of the Treatment Effects of Reducing Cholesterol (ARBITER) 2: a double-blind, placebo-controlled study of extended-release niacin on atherosclerosis progression in secondary prevention patients treated with statins. *Circulation* 2004 December 7;110(23):3512-7.

5 Taylor AJ, Lee HJ, Sullenberger LE. The effect of 24 months of combination statin and extended-release niacin on carotid intima-media thickness: ARBITER 3. *Curr Med Res Opin* 2006 November;22(11):2243-50.

6 Brown BG, Zhao XQ, Chait A et al. Simvastatin and niacin, antioxidant vitamins, or the combination for the prevention of coronary disease. *N Engl J Med* 2001 November 29;345(22):1583-92.

7) HPS2-THRIVE randomized placebo-controlled trial in 25 673 high-risk patients of ER niacin/laropiprant: trial design, pre-specified muscle and liver outcomes, and reasons for stopping study treatment. *Eur Heart J* 2013 February 26.

8 Sharma M. Combination therapy for dyslipidemia. *Curr Opin Cardiol* 2011 September;26(5):420-3.

9 Sanford M, Curran MP. Niacin extended-release/simvastatin. *Drugs* 2008;68(16):2373-86.

10 Blumenthal RS, Michos ED. The HALTS trial--halting atherosclerosis or halted too early? *N Engl J Med* 2009 November 26;361(22):2178-80.

11) Cannon CP, Braunwald E, McCabe CH et al. Intensive versus moderate lipid lowering with statins after acute coronary syndromes. *N Engl J Med* 2004 April 8;350(15):1495-504.

12 Michos ED, Sibley CT, Baer JT, Blaha MJ, Blumenthal RS. Niacin and statin combination therapy for atherosclerosis regression and prevention of cardiovascular disease events: reconciling the AIM-HIGH (Atherothrombosis Intervention in Metabolic Syndrome With Low HDL/High Triglycerides: Impact on Global Health Outcomes) trial with previous surrogate endpoint trials. *J Am Coll Cardiol* 2012 June 5;59(23):2058-64.

13 Bruckert E, Labreuche J, Amarenco P. Meta-analysis of the effect of nicotinic acid alone or in combination on cardiovascular events and atherosclerosis. *Atherosclerosis* 2010 June;210(2):353-61.

14 Lee JM, Robson MD, Yu LM et al. Effects of high-dose modified-release nicotinic acid on atherosclerosis and vascular function: a randomized, placebo-controlled, magnetic resonance imaging study. *J Am Coll Cardiol* 2009 November 3;54(19):1787-94.

15 Lukasova M, Malaval C, Gille A, Kero J, Offermanns S. Nicotinic acid inhibits progression of atherosclerosis in mice through its receptor GPR109A expressed by immune cells. *J Clin Invest* 2011 March;121(3):1163-73.

16 McKenney J, Bays H, Koren M et al. Safety of extended-release niacin/laropiprant in patients with dyslipidemia. *J Clin Lipidol* 2010 March;4(2):105-12.

17 Meyers CD, Kamanna VS, Kashyap ML. Niacin therapy in atherosclerosis. *Curr Opin Lipidol* 2004 December;15(6):659-65.

18 van der Hoorn JW, de HW, Berbee JF et al. Niacin increases HDL by reducing hepatic expression and plasma levels of cholesteryl ester transfer protein in APOE*3Leiden.CETP mice. *Arterioscler Thromb Vasc Biol* 2008 November;28(11):2016-22.

19 de Haan W, de Vries-van der Weij, van der Hoorn JW et al. Torcetrapib does not reduce atherosclerosis beyond atorvastatin and induces more proinflammatory lesions than atorvastatin. *Circulation* 2008 May 13;117(19):2515-22.

20 Westerterp M, van der Hoogt CC, de Haan W et al. Cholesteryl ester transfer protein decreases high-density lipoprotein and severely aggravates atherosclerosis in APOE*3-Leiden mice. *Arterioscler Thromb Vasc Biol* 2006 November;26(11):2552-9.

21 van der Hoorn JW, Jukema JW, Havekes LM et al. The dual PPARalpha/gamma agonist tesaglitazar blocks progression of pre-existing atherosclerosis in APOE*3Leiden.CETP transgenic mice. *Br J Pharmacol* 2009 April;156(7):1067-75.

22 Bijland S, Pieterman EJ, Maas AC et al. Fenofibrate increases very low density lipoprotein triglyceride production despite reducing plasma triglyceride levels in APOE*3-Leiden.CETP mice. *J Biol Chem* 2010 August 13;285(33):25168-75.

23 Rensen PC, Herijgers N, Netscher MH, Meskers SC, van Eck M, van Berkel TJ. Particle size determines the specificity of apolipoprotein E-containing triglyceride-rich emulsions for the LDL receptor versus hepatic remnant receptor in vivo. *J Lipid Res* 1997 June;38(6):1070-84.

24 Stary HC, Chandler AB, Dinsmore RE et al. A definition of advanced types of atherosclerotic lesions and a histological classification of atherosclerosis. A report from the Committee on Vascular Lesions of the Council on Arteriosclerosis, American Heart Association. *Arterioscler Thromb Vasc Biol* 1995 September;15(9):1512-31.

25 Delsing DJ, Offerman EH, van Duyvenvoorde W et al. Acyl-CoA:cholesterol acyltransferase inhibitor avasimibe reduces atherosclerosis in addition to its cholesterol-lowering effect in ApoE*3-Leiden mice. *Circulation* 2001 April 3;103(13):1778-86.

26 van der Hoorn JW, Kleemann R, Havekes LM, Kooistra T, Princen HM, Jukema JW. Olmesartan and pravastatin additively reduce development of atherosclerosis in APOE*3Leiden transgenic mice. *J Hypertens* 2007 December;25(12):2454-62.

27 Naik SU, Wang X, Da Silva JS et al. Pharmacological activation of liver X receptors promotes reverse cholesterol transport in vivo. *Circulation* 2006 January 3;113(1):90-7.

28 Niesor EJ, Magg C, Ogawa N et al. Modulating cholesteryl ester transfer protein activity maintains efficient pre-beta-HDL formation and increases reverse cholesterol transport. *J Lipid Res* 2010 December;51(12):3443-54.

29 Tunaru S, Kero J, Schaub A et al. PUMA-G and HM74 are receptors for nicotinic acid and mediate its anti-lipolytic effect. *Nat Med* 2003 March;9(3):352-5.

30 Li Z, Wang Y, van der Sluis RJ et al. Niacin reduces plasma CETP levels by diminishing liver macrophage content in CETP transgenic mice. *Biochem Pharmacol* 2012 September 15;84(6):821-9.

31 de Knijff P, van den Maagdenberg AM, Stalenhoef AF et al. Familial dysbetalipoproteinemia associated with apolipoprotein E3-Leiden in an extended multigeneration pedigree. *J Clin Invest* 1991 August;88(2):643-55.

32 van den Maagdenberg AM, Hofker MH, Krimpenfort PJ et al. Transgenic mice carrying the apolipoprotein E3-Leiden gene exhibit hyperlipoproteinemia. *J Biol Chem* 1993 May 15;268(14):10540-5.

33 Carlson LA, Oro L. Effect of treatment with nicotinic acid for one month on serum lipids in patients with different types of hyperlipidemia. *Atherosclerosis* 1973 July;18(1):1-9.

34 Hoogwerf BJ, Bantle JP, Kuba K, Frantz ID, Jr., Hunninghake DB. Treatment of type III hyperlipoproteinemia with four different treatment regimens. *Atherosclerosis* 1984 May;51(2-3):251-9.

35 Kamanna VS, Kashyap ML. Mechanism of action of niacin. *Am J Cardiol* 2008 April 17;101(8A):20B-6B.

36 Fabbrini E, Mohammed BS, Korenblat KM et al. Effect of fenofibrate and niacin on intrahepatic triglyceride content, very low-density lipoprotein kinetics, and insulin action in obese subjects with nonalcoholic fatty liver disease. *J Clin Endocrinol Metab* 2010 June;95(6):2727-35.

37 Grundy SM, Mok HY, Zech L, Berman M. Influence of nicotinic acid on metabolism of cholesterol and triglycerides in man. *J Lipid Res* 1981 January;22(1):24-36.

38 Wang W, Basinger A, Neese RA et al. Effect of nicotinic acid administration on hepatic very low density lipoprotein-triglyceride production. *Am J Physiol Endocrinol Metab* 2001 March;280(3):E540-E547.

39 Lamon-Fava S, Diffenderfer MR, Barrett PH et al. Extended-release niacin alters the metabolism of plasma apolipoprotein (Apo) A-I and ApoB-containing lipoproteins. *Arterioscler Thromb Vasc Biol* 2008 September;28(9):1672-8.

40 Kleemann R, Verschuren L, van Erk MJ et al. Atherosclerosis and liver inflammation induced by increased dietary cholesterol intake: a combined transcriptomics and metabolomics analysis. *Genome Biol* 2007;8(9):R200.

41 Wu BJ, Yan L, Charlton F, Witting P, Barter PJ, Rye KA. Evidence that niacin inhibits acute vascular inflammation and improves endothelial dysfunction independent of changes in plasma lipids. *Arterioscler Thromb Vasc Biol* 2010 May;30(5):968-75.

42 Foks AC, Frodermann V, ter Borg M et al. Differential effects of regulatory T cells on the initiation and regression of atherosclerosis. *Atherosclerosis* 2011 September;218(1):53-60.

43 Digby JE, McNeill E, Dyar OJ, Lam V, Greaves DR, Choudhury RP. Anti-inflammatory effects of nicotinic acid in adipocytes demonstrated by suppression of fractalkine, RANTES, and MCP-1 and upregulation of adiponectin. *Atherosclerosis* 2010 March;209(1):89-95.

44 Boden WE, Probstfield JL, Anderson T et al. Niacin in patients with low HDL cholesterol levels receiving intensive statin therapy. *N Engl J Med* 2011 December 15;365(24):2255-67.

45 Giugliano RP. Niacin at 56 years of age--time for an early retirement? *N Engl J Med* 2011 December 15;365(24):2318-20.

46 The AIM-HIGH Investigators. The role of niacin in raising high-density lipoprotein cholesterol to reduce cardiovascular events in patients with atherosclerotic cardiovascular disease and optimally treated low-density lipoprotein cholesterol: baseline characteristics of study participants. The Atherothrombosis Intervention in Metabolic syndrome with low HDL/high triglycerides: impact on Global Health outcomes (AIM-HIGH) trial. *Am Heart J* 2011 March;161(3):538-43.

Supplemental data

Supplemental table 1 **RT-PCR primer sequences.**

	Forward primer	Reverse primer
Gene		
HPRT	TTGCTCGAGATGTCATGAAGGA	AGCAGGTCAGCAAAGAACTTATAG
36B4	GGACCCGAGAAGACCTCCTT	GCACATCACTCAGAATTTCAATGG
CETP	CAGATCAGCCACTTGTCCAT	CAGCTGTGTGTTGATCTGGA

HPRT, hypoxanthine-guanine phosporibosyltransferase; 36B4, acidic ribosomal phosphoprotein PO; CETP, cholesteryl ester transfer protein.

CHAPTER 8

General discussion

General discussion

Despite advances in diagnosis and therapy, cardiovascular disease (CVD) remains a major cause of morbidity and mortality in Western society and is an increasing problem especially in low-to-middle income countries. The most prevalent cardiovascular disorders are myocardial infarction (MI) and stroke, both are predominantly caused by atherosclerosis. Atherosclerosis is a complex disease associated with a variety of genetic and environmental factors. Main pathogenic phenomena underlying atherosclerosis are disturbed lipid metabolism and inflammation. The studies described in this thesis have explored the effects of specific aspects of these two components on atherosclerosis and MI. In this chapter, the main conclusions and implications of these findings are discussed.

Gender, nutrition and cardiac function

In the first part of this thesis, the effect of high-fat diet feeding (HFD) on cardiac function with and without an MI was studied. We first set out to investigate if feeding a diet rich in saturated fatty acids (SFA) resulted in cardiac dysfunction. **Chapter 2** describes that long term HFD feeding led to alterations in cardiac function solely in male mice, although the observed increase in body weight and plasma lipids due to HFD feeding was independent of gender. We therefore concluded that male mice are the preferred model to investigate effects of ischemia and drug treatments on cardiac function in a setting of HFD-induced obesity.

The observation that female mice seem protected from HFD-induced cardiac dysfunction is probably related to beneficial effects of sex hormones and in particular estrogen. In animal studies beneficial effects of estrogen treatment are reported in models of cardiac hypertrophy[1, 2], ischemia/reperfusion[3, 4] and atherosclerosis[5]. These effects are likely mediated by effects of estrogen on cardiomyocytes and endothelial cells, but effects on other cell types including inflammatory cells and stem cells may be involved as well. In addition, estrogen exerts a part of its protective effect via beneficial effects on serum lipoproteins, e.g. an increased high-density lipoprotein (HDL)-cholesterol and a decreased low-density lipoprotiein (LDL)-cholesterol, accounting for approximately one third of the observed clinical benefits.[6] Thus, in animal studies, treatment with estrogen results in predominantly favorable effects.

In premenopausal women, the incidence of atherosclerotic diseases is relatively low and a sharp increase is observed with the occurrence of the menopause.[7] Results from these observations and established results of positive effects of estrogen on the cardiovascular system, including increased vasodilatation and an inhibited response of blood vessels to injury[8], suggested that hormone replacement therapy could have beneficial effects on CVD in postmenopausal women. However, two large prospective studies, the Women's

Health Initiative and the Heart and Estrogen/Progestin Replacement study, found that hormone replacement therapy did not lead to an improvement in cardiovascular outcomes, even though lipid profiles were improved and incidence of type 2 diabetes was reduced.[9-11] A possible explanation for these outcomes could be age-related metabolic changes, partly independent of estrogen or the estrogen receptor, thereby reducing the protective effect or even leading to detrimental rather than cardioprotective effects.[12] In addition, the Women's Health Initiative study was prematurely aborted since an increased risk for invasive breast cancer was observed.[10] Therefore, hormone replacement therapies for prevention of CVD, and possibly other chronic diseases, are currently not recommended.

The results in **Chapter 2** underscore the detrimental effects of a SFA rich HFD on cardiac health. From meta-analysis of randomized controlled trials[13] it is recommended to replace dietary SFA by polyunsaturated fatty acids (PUFA) to reduce coronary heart disease (CHD). Consumption of PUFAs lowers the total cholesterol to HDL-cholesterol ratio and may improve insulin resistance and reduce systemic inflammation. The two best known PUFAs are omega-3 and omega-6 PUFAs which are present in mainly fish, shellfish and seeds, respectively. Although the beneficial effects of omega-6 regarding CHD have been under debate, the American Heart Association recommended recently that a minimum daily consumption of 5-10% of energy from omega-6 PUFAs is sufficient to reduce CHD risk.[14]

Regarding omega-3 PUFAs; national and international guidelines have converged on consistent recommendations for adults to consume at least 2 servings of fish (particularly fatty species) per week. However, clinical trials have not indisputably proven that omega-3 PUFAs have beneficial effects on CVD.[15, 16] Possibly omega-3 does not solely contribute to the observed effects and the interplay between omega-3 and other nutrients in fish is also important.[17] For the vulnerable CVD patient population, especially those on suboptimal pharmaceutical treatment or those who have additional risk factors as a result of comorbidities, intake of omega-3 fatty acids in form of oily fish is advised as they may benefit the CVD patient.[17]

Chapter 3 continues with examining the effect of HFD feeding in presence of an MI. Unexpectedly, no aggravated cardiac dysfunction was observed upon HFD feeding and subsequent induction of MI. However, there was a tendency towards an increase in the amount of macrophages in the infarcted area compared to the low-fat diet (LFD) fed group. After an MI an extensive inflammatory response takes place which is a critical factor in the balance between cardiac repair and adverse ventricular remodeling. Since macrophages have an important contribution in this inflammatory process occurring post-MI, it is possible that in the longer term this secondary effect could aggravate cardiac dysfunction after MI. However, since the follow-up period after MI was only 2 weeks no long-term conclusion could be drawn from this study.

Although it seems relevant to adapt diet and nutrition style after an MI and other symptoms of heart failure, scarce information is provided in the major heart failure management guidelines.[18, 19] The most recent guidelines from the Heart Failure Society of America present a comprehensive recommendation on diet and nutrition.[19] They

report that, besides a sodium restriction for all heart failure patients, dietary instructions are mainly recommended in patients with heart failure in combination with diabetes, dyslipidemia, or severe obesity. Often patients need personalized dietary advice and it has been shown that supervision by dieticians benefits their wellbeing with a decreased sodium intake, fluid retention and increased quality of life score.[20, 21] Unfortunately, it is difficult to provide general recommendations since diet is generally disregarded as factor in observational studies and dietary intake is highly heterogeneous.

Inflammation and cardiac function

The metabolic system and the inflammatory system are evolutionary conserved, as survival of organisms depends on the ability to fight infections and to withstand starvation.[22] Coupling of metabolism and immunity is important since mounting an immune response requires much energy and thus regulation of energy homeostasis is essential. As a result, there is a delicate balance between the two systems and dysfunction of one leads to dysfunction of the other, with malnutrition and immune suppression on one side and obesity and immune activation on the other side.[23] The current chronic caloric overload in the Western world results in complications at the intersection of metabolism and immunity, including obesity-linked inflammatory diseases like diabetes, fatty liver disease and CVD.

The liver, adipose tissue, immune cells and blood cells, which perform key metabolic and inflammatory functions in humans, have evolved from one functional unit, the 'fat body', which is still present in the fruit fly *Drosophila melanogaster*.[22] The fat body coordinates a variety of actions including nutrient sensing, pathogen and survival responses. Although in humans, the different organs acquired specialized functions, they maintained their developmental heritage. Partly overlapping pathways regulate both metabolic and immune functions through shared signaling systems.[22] Consequently, nutrients and especially fatty acids (FAs) act through pathogen-sensing systems like Toll-like receptors (TLRs), giving rise to metabolically or nutritionally induced inflammatory responses.[22, 24] It was discovered that in particular TLR2 and TLR4 dependent pathways are activated by FAs and contribute via this pathway to the low-grade inflammation in several metabolic diseases. However, in **Chapter 6** we demonstrate that HFD-induced cardiac dysfunction, as observed in **Chapter 2**, is not likely to be mediated by TLR2 and/or TLR4. Very mild beneficial changes in cardiac function are observed in TLR-deficient mice, suggesting that TLR2 and TLR4, if anything, play a moderately protective role in HFD-induced cardiac dysfunction. A possible explanation for the absense of cardiac dysfunction might be that in absence of one TLR, another TLR is upregulated as a compensatory effect, resulting in a comparable inflammatory status that does not lead to cardiac dysfunction. Such a compensatory mechanism is not inconceivable in an evolutionary conserved process.

Although we did not observe HFD-induced TLR2 and TLR4-mediated dysfunction in the heart, others reported that TLR4 exerts an important role in myocardial infarction

healing and left ventricular (LV) remodeling.[25] This difference is probably caused by the strong inflammatory activation which is exerted post-MI and the subsequently released 'danger' signals activate the TLR pathway. The importance of the TLR signaling pathway is also emphasized in **Chapter 5** where we show that RP105, a negative regulator of TLR4, is involved in post-infarction cardiac remodeling. Deficiency of the accessory molecule RP105 aggravates systolic and diastolic cardiac function indices after MI, indicating that reduced inhibition (=activation) of TLR4 signaling aggravates cardiac dysfunction.

The influence of the TLR pathway on infections in general and cardiac function specifically opens opportunities as a therapeutic target. Targeting of TLRs is explored for the treatment of e.g. cancer, rheumatoid arthritis, sepsis and cardiac malfunctioning.[26] Different strategies are being considered to pharmaceutically modify TLR2 and TLR4 including receptor agonists and antagonists and inhibition of the signal transduction pathway.[27] Despite the evidence shown by animal studies that TLRs are involved in several pathological cardiovascular processes, this has so far not been translated into clinical applications. The only drugs thus far that have been evaluated for treatment of ischemia/reperfusion injury are the TLR4 antagonist Eritoran and the TLR2 antibody OPN-305. Preclinical results showed that inhibition of TLR2 by OPN-305 preserved cardiac function.[28] TLR4 inhibition by Eritoran, in a similar murine model, led to a reduced infarct size and decreased cytokine production.[29] Although Eritoran was studied in a Phase III clinical trial for sepsis, cardiovascular events were not part of the study end points.[30] However, the results in **Chapter 5** provide new opportunities for therapeutic approaches to reduce cardiac remodeling through RP105 and thereby improve cardiac function after a myocardial event.

High-density lipoprotein, atherosclerosis and cardiac function

An inverse correlation of plasma HDL-cholesterol with CVD risk is found in numerous epidemiological studies [31, 32], resulting in the concept that by increasing HDL-cholesterol levels, the risk for CHD could be reduced. This risk reduction can be achieved via therapeutic elevation of HDL-cholesterol levels, including treatments with niacin and cholesteryl ester transfer protein (CETP) inhibitors. Niacin is one of the most potent HDL-cholesterol-raising compounds clinically available. Relatively small secondary prevention studies have shown positive effects of niacin in combination with statin therapy leading to a reduced progression or even regression of atherosclerosis compared to statin treatment alone.[33-35] These results were supported by animal studies demonstrating anti-atherogenic properties of niacin.[36-38] Despite these initially promising data, two large clinical trials investigating the effects of niacin on top of LDL-lowering treatment revealed no beneficial effect of niacin treatment (HPS2-THRIVE[39] and AIM-HIGH[40]). In **Chapter 7** we aimed to investigate the reason for the failure of these trials and showed that niacin decreases atherosclerosis development mainly by reducing non-HDL-

cholesterol. In addition, the additive effect of niacin on top of simvastatin treatment is mostly dependent on the non-HDL-cholesterol-lowering capacities, thereby suggesting that beneficial effects of niacin for patient treatment may only be observed when niacin lowers LDL-cholesterol on top of related lipid-lowering therapy.

Niacin is not the only HDL-raising drug that did not meet the expectations. Trials with the CETP inhibitors torcetrapib and dalcetrapib were also prematurely terminated due to off-target toxic effects and the absence of effect, respectively.[41, 42] These results indicate that the relation between increased plasma HDL-cholesterol levels and reduction of CVD risk is rather complex. Although increasing plasma HDL-cholesterol levels as such could be relevant, HDL function might be more important in preventing CVD. An increase in plasma HDL-cholesterol levels *per se* does not necessarily translate into a decreased CVD risk when the HDL particle is 'dysfunctional'. However, assessment of HDL quality in clinical situations is rather difficult, whereas quantification of HDL quantity is easily achieved by measuring plasma HDL-cholesterol levels.

HDL exerts many functions such as mediating cholesterol efflux from macrophages as a first step of reverse cholesterol transport (RCT). Although in **Chapter 7** we concluded that RCT is not the driving force behind the anti-atherogenic effects of niacin, in general RCT is thought to be an important contributor to cardioprotection. Other properties of HDL, including the anti-inflammatory, anti-thrombotic and anti-apoptotic effects, may contribute to the anti-atherogenic effects of HDL. It remains difficult to discriminate between these different functions especially since the effects are achieved via a variety of mechanisms.

Recently, it was proposed that the cholesterol efflux capacity by macrophages may be an appropriate tool to measure HDL functionality.[43] Consistent with studies in animals, an inverse association was observed in patients between early steps in the RCT pathway and carotid intima-media thickness and the likelihood of coronary artery disease assessed by angiography. However, these effects were independently of HDL-cholesterol levels, indicating that increasing HDL levels *per se* does not necessarily lead to a reduction in the atherosclerotic burden. Importantly, issues related to the reported clinical results[44, 45], including the measurement of cholesterol efflux transport[46], remain the subject of on-going discussions, therefore requiring further investigations before measuring cholesterol efflux as a marker of HDL functionality can be of clinical value.

Alternative strategies are actively being explored to develop HDL-targeted therapeutics and specifically drugs that increase cholesterol efflux from the arterial wall. One of the mechanisms by which cholesterol content in the atherosclerotic lesion, and indirectly CVD risk, is reduced is via RCT by removal of cholesterol from the arterial macrophage foam cells to the liver for biliary excretion. Active cholesterol removal is mediated by the ATP-binding cassette transporters ABCA1 and ABCG1. Deletion of both transporters in macrophages results in an impaired cholesterol efflux and a rapid development of atherosclerosis.[47, 48] Furthermore, prevention of ABCA1 mRNA degradation by administration of antagomirs of miR-33, resulted in an enhanced expression of ABCA1 in the macrophages present in the lesion and a subsequent improved cholesterol removal.[49] These results support the anti-atherogenic properties of increasing RCT

and suggest a promising tool for the treatment of CVD. Although numerous studies have been conducted on the effects of ABCA1 on atherosclerosis, no studies have been published on the role of ABCA1 after an MI. In **Chapter 4** we found much to our surprise, that despite its protective effects regarding the development of atherosclerosis, ABCA1 exerts detrimental effects on cardiac function after MI. This is possibly caused by a reduced activation status of immune cells resulting in less efficient repair after MI. Although ABCA1 is considered as a potential therapeutic target for the treatment of atherosclerosis, our data clearly indicate that it is of great importance to carefully consider potential adverse effects of ABCA1 on cardiac remodeling post-MI.

Concluding remarks

The ever increasing prevalence of CVD in the Western world urges industry and society to develop novel solutions to decrease this burden. Since lifestyle interventions to reduce CVD risk prove difficult to realize, novel solutions and therapies are needed. However, for the development of new drugs and therapies it is essential to evaluate their effects on both lipid metabolism and inflammation in all aspects of the development of cardiac pathophysiology. In this thesis we show that HFD feeding has mild but significant detrimental effects on cardiac function. In contrast to our expectations, this effect is not likely to be mediated by TLR2 or TLR4. Also, we demonstrated in mice that HFD feeding does not significantly aggravate cardiac dysfunction post-MI. Despite these findings, it would be of great scientific and societal interest to conduct a more in depth investigation on these effects in a prospective obese patient population.

Deficiency of RP105, a modulator of inflammation, improved cardiac function after induction of MI. In addition, ABCA1 had adverse effects on cardiac function post-MI, possibly via a reduced activation of immune cells. This confirms the important role of inflammation in recovery after an MI. Furthermore, we elucidated a possible reason for the failure of niacin in recent clinical trials and found that niacin's anti-atherogenic properties are most potent by lowering LDL-cholesterol on top of statin treatment. Altogether, these results provide novel insights and targets for the prevention or treatment of CVD.

References

1 Donaldson C, Eder S, Baker C et al. Estrogen attenuates left ventricular and cardiomyocyte hypertrophy by an estrogen receptor-dependent pathway that increases calcineurin degradation. *Circ Res* 2009 January 30;104(2):265-75, 11p.

2 van Eickels M, Grohe C, Cleutjens JP, Janssen BJ, Wellens HJ, Doevendans PA. 17beta-estradiol attenuates the development of pressure-overload hypertrophy. *Circulation* 2001 September 18;104(12):1419-23.

3 Booth EA, Marchesi M, Kilbourne EJ, Lucchesi BR. 17Beta-estradiol as a receptor-mediated cardioprotective agent. *J Pharmacol Exp Ther* 2003 October;307(1):395-401.

4 Lagranha CJ, Deschamps A, Aponte A, Steenbergen C, Murphy E. Sex differences in the phosphorylation of mitochondrial proteins result in reduced production of reactive oxygen species and cardioprotection in females. *Circ Res* 2010 June 11;106(11):1681-91.

5 Bourassa PA, Milos PM, Gaynor BJ, Breslow JL, Aiello RJ. Estrogen reduces atherosclerotic lesion development in apolipoprotein E-deficient mice. *Proc Natl Acad Sci U S A* 1996 September 17;93(19):10022-7.

6 Effects of estrogen or estrogen/progestin regimens on heart disease risk factors in postmenopausal women. The Postmenopausal Estrogen/Progestin Interventions (PEPI) Trial. The Writing Group for the PEPI Trial. *JAMA* 1995 January 18;273(3):199-208.

7 Witteman JC, Grobbee DE, Kok FJ, Hofman A, Valkenburg HA. Increased risk of atherosclerosis in women after the menopause. *BMJ* 1989 March 11;298(6674):642-4.

8 Mendelsohn ME, Karas RH. The protective effects of estrogen on the cardiovascular system. *N Engl J Med* 1999 June 10;340(23):1801-11.

9 Margolis KL, Bonds DE, Rodabough RJ et al. Effect of oestrogen plus progestin on the incidence of diabetes in postmenopausal women: results from the Women's Health Initiative Hormone Trial. *Diabetologia* 2004 July;47(7):1175-87.

10 Rossouw JE, Anderson GL, Prentice RL et al. Risks and benefits of estrogen plus progestin in healthy postmenopausal women: principal results From the Women's Health Initiative randomized controlled trial. *JAMA* 2002 July 17;288(3):321-33.

11 Shlipak MG, Chaput LA, Vittinghoff E et al. Lipid changes on hormone therapy and coronary heart disease events in the Heart and Estrogen/progestin Replacement Study (HERS). *Am Heart J* 2003 November;146(5):870-5.

12 Murphy E. Estrogen signaling and cardiovascular disease. *Circ Res* 2011 September 2;109(6):687-96.

13 Mozaffarian D, Micha R, Wallace S. Effects on coronary heart disease of increasing polyunsaturated fat in place of saturated fat: a systematic review and meta-analysis of randomized controlled trials. *PLoS Med* 2010 March;7(3):e1000252.

14 Harris WS, Mozaffarian D, Rimm E et al. Omega-6 fatty acids and risk for cardiovascular disease: a science advisory from the American Heart Association Nutrition Subcommittee of the Council on Nutrition, Physical Activity, and Metabolism; Council on Cardiovascular Nursing; and Council on Epidemiology and Prevention. *Circulation* 2009 February 17;119(6):902-7.

15 Rizos EC, Ntzani EE, Bika E, Kostapanos MS, Elisaf MS. Association between omega-3 fatty acid supplementation and risk of major cardiovascular disease events: a systematic review and meta-analysis. *JAMA* 2012 September 12;308(10):1024-33.

16 Chowdhury R, Stevens S, Gorman D et al. Association between fish consumption, long chain omega 3 fatty acids, and risk of cerebrovascular disease: systematic review and meta-analysis. *BMJ* 2012;345:e6698.

17 de Goede J, Geleijnse JM. The role of fatty acids from fish in the prevention of stroke. *BMJ* 2012;345:e7219.

18 Jessup M, Abraham WT, Casey DE et al. 2009 focused update: ACCF/AHA Guidelines for the Diagnosis and Management of Heart Failure in Adults: a report of the American College of Cardiology Foundation/American Heart Association Task Force on Practice Guidelines: developed in collaboration with the International Society for Heart and Lung Transplantation. *Circulation* 2009 April 14;119(14):1977-2016.

19 Lindenfeld J, Albert NM, Boehmer JP et al. HFSA 2010 Comprehensive Heart Failure Practice Guideline. *J Card Fail* 2010 June;16(6):e1-194.

20 Kuehneman T, Saulsbury D, Splett P, Chapman DB. Demonstrating the impact of nutrition intervention in a heart failure program. *J Am Diet Assoc* 2002 December;102(12):1790-4.

21 Arcand JA, Brazel S, Joliffe C et al. Education by a dietitian in patients with heart failure results in improved adherence with a sodium-restricted diet: a randomized trial. *Am Heart J* 2005 October;150(4):716.

22 Hotamisligil GS. Inflammation and metabolic disorders. *Nature* 2006 December 14;444(7121):860-7.

23 Wellen KE, Hotamisligil GS. Inflammation, stress, and diabetes. *J Clin Invest* 2005 May;115(5):1111-9.

24 Shi H, Kokoeva MV, Inouye K, Tzameli I, Yin H, Flier JS. TLR4 links innate immunity and fatty acid-induced insulin resistance. *J Clin Invest* 2006 November;116(11):3015-25.

25 Timmers L, Sluijter JP, van Keulen JK et al. Toll-like receptor 4 mediates maladaptive left ventricular remodeling and impairs cardiac function after myocardial infarction. *Circ Res* 2008 February 1;102(2):257-64.

26 Dunne A, Marshall NA, Mills KH. TLR based therapeutics. *Curr Opin Pharmacol* 2011 August;11(4):404-11.

27 O'Neill LA, Bryant CE, Doyle SL. Therapeutic targeting of Toll-like receptors for infectious and inflammatory diseases and cancer. *Pharmacol Rev* 2009 June;61(2):177-97.

28 Arslan F, Smeets MB, O'Neill LA et al. Myocardial ischemia/reperfusion injury is mediated by leukocytic toll-like receptor-2 and reduced by systemic administration of a novel anti-toll-like receptor-2 antibody. *Circulation* 2010 January 5;121(1):80-90.

29 Shimamoto A, Chong AJ, Yada M et al. Inhibition of Toll-like receptor 4 with eritoran attenuates myocardial ischemia-reperfusion injury. *Circulation* 2006 July 4;114(1 Suppl):I270-I274.

30 Eisai Inc. A Controlled Comparison of Eritoran Tetrasodium and Placebo in Patients With Severe Sepsis, NCT00334828. *http://clinicaltrials gov* 2013. Accessed February 12, 2013.

31 Gordon T, Castelli WP, Hjortland MC, Kannel WB, Dawber TR. High density lipoprotein as a protective factor against coronary heart disease. The Framingham Study. *Am J Med* 1977 May;62(5):707-14.

32 Miller NE, Thelle DS, Forde OH, Mjos OD. The Tromso heart-study. High-density lipoprotein and coronary heart-disease: a prospective case-control study. *Lancet* 1977 May 7;1(8019):965-8.

33 Taylor AJ, Sullenberger LE, Lee HJ, Lee JK, Grace KA. Arterial Biology for the Investigation of the Treatment Effects of Reducing Cholesterol (ARBITER) 2: a double-blind, placebo-controlled study of extended-release niacin on atherosclerosis progression in secondary prevention patients treated with statins. *Circulation* 2004 December 7;110(23):3512-7.

34 Taylor AJ, Lee HJ, Sullenberger LE. The effect of 24 months of combination statin and extended-release niacin on carotid intima-media thickness: ARBITER 3. *Curr Med Res Opin* 2006 November;22(11):2243-50.

35 Taylor AJ, Villines TC, Stanek EJ et al. Extended-release niacin or ezetimibe and carotid intima-media thickness. *N Engl J Med* 2009 November 26;361(22):2113-22.

36 van der Hoorn JW, de Haan W, Berbee JF et al. Niacin increases HDL by reducing hepatic expression and plasma levels of cholesteryl ester transfer protein in APOE*3Leiden.CETP mice. *Arterioscler Thromb Vasc Biol* 2008 November;28(11):2016-22.

37 Parwaresch MR, Haacke H, Mader C. Efficacy of hypolipidemic treatment in inhibition of experimental atherosclerosis: the effect of nicotinic acid and related compounds. *Atherosclerosis* 1978 December;31(4):395-401.

38 Kamanna VS, Kashyap ML. Mechanism of action of niacin. *Am J Cardiol* 2008 April 17;101(8A):20B-6B.

39 Merck Announces HPS2-THRIVE Study of TREDAPTIVE™ (Extended-Release Niacin/Laropiprant) Did Not Achieve Primary Endpoint. *Merck Newsroom* 2012 December 20;Available at: URL: http://www.mercknewsroom.com/press-release/prescription-medicine-news/merck-announces-hps2-thrive-study-tredaptive-extended-relea. Accessed February 7, 2013.

40 Boden WE, Probstfield JL, Anderson T et al. Niacin in patients with low HDL cholesterol levels receiving intensive statin therapy. *N Engl J Med* 2011 December 15;365(24):2255-67.

41 Barter PJ, Caulfield M, Eriksson M et al. Effects of torcetrapib in patients at high risk for coronary events. *N Engl J Med* 2007 November 22;357(21):2109-22.

42 Schwartz GG, Olsson AG, Abt M et al. Effects of dalcetrapib in patients with a recent acute coronary syndrome. *N Engl J Med* 2012 November 29;367(22):2089-99.

43 Khera AV, Cuchel M, Llera-Moya M et al. Cholesterol efflux capacity, high-density lipoprotein function, and atherosclerosis. *N Engl J Med* 2011 January 13;364(2):127-35.

44 Gupta A. Cholesterol efflux capacity and atherosclerosis. *N Engl J Med* 2011 April 14;364(15):1472-5.

45 Frohlich J, Al-Sarraf A. Cholesterol efflux capacity and atherosclerosis. *N Engl J Med* 2011 April 14;364(15):1474-5.

46 de Vries R, Groen AK, Dullaart RP. Cholesterol efflux capacity and atherosclerosis. *N Engl J Med* 2011 April 14;364(15):1473-4.

47 Yvan-Charvet L, Ranalletta M, Wang N et al. Combined deficiency of ABCA1 and ABCG1 promotes foam cell accumulation and accelerates atherosclerosis in mice. *J Clin Invest* 2007 December;117(12):3900-8.

48 Out R, Jessup W, Le Goff W et al. Coexistence of foam cells and hypocholesterolemia in mice lacking the ABC transporters A1 and G1. *Circ Res* 2008 January 4;102(1):113-20.

49 Rayner KJ, Sheedy FJ, Esau CC et al. Antagonism of miR-33 in mice promotes reverse cholesterol transport and regression of atherosclerosis. *J Clin Invest* 2011 July;121(7):2921-31.

Summary

Summary

Cardiovascular diseases (CVD) are the leading cause of death in the Western world and despite greatly improved treatment options during the last decades, the number of patients suffering from CVD is still increasing. The risk for CVD is determined by a variety of factors, including genetic variation, gender, age, lifestyle, blood pressure and plasma lipid levels. Myocardial infarction (MI) and stroke caused by atherosclerosis are the most prevalent cardiovascular disorders. Atherosclerosis is a complex disease mainly caused by a disturbed lipid metabolism and inflammation. The studies in this thesis address specific aspects of inflammation and dietary lipids in the development of CVD. These two components are of particular interest as each, both individually and collectively, can lead to the onset or maintenance of pathological cardiac conditions.

An increased availability of high-fat diet (HFD) derived fatty acids (FA) may lead to excess FA uptake in non-adipose organs like the heart, as adipose tissue has a limited capacity to expand. The ectopic storage of FA in the form of TG is probably inert, but accumulation of toxic FA intermediates in the heart may affect cardiac function. In **Chapter 2** we investigated to what extent HFD feeding leads to alterations in left ventricular function and whether this depends on gender and (or) duration of HFD feeding. For this purpose we used wild-type (WT) male and female C57Bl/6J mice and subjected them to a low fat diet (LFD) or HFD for an intermediate (6 weeks) or long term (12 weeks) period. We demonstrated that HFD gradually increased body weight and plasma lipid levels in mice independent of gender. Furthermore, cardiac function assessed by combined echocardiography and invasive pressure-volume loop (PV-loop) measurements, was only affected in male mice, but not in female mice after long term HFD feeding. This was indicated by an increased end-systolic volume and end-systolic pressure and decreased ejection fraction, all symptoms of a reduced systolic function. We concluded from these data that male mice are the preferred model to investigate effects of ischemia and drug treatment on cardiac function in a setting of diet induced obesity.

Obesity is accompanied by low-grade systemic inflammation that is associated with increased risk of CVD including MI. Furthermore, inflammation in the heart, by for example local macrophage accumulation, might impair cardiac function. We therefore investigated in **Chapter 3** if HFD feeding results in aggravated cardiac dysfunction after an MI, due to an increased inflammatory response as compared to LFD feeding. We subjected WT male mice to a long term LFD and HFD and induced MI by permanent ligation of the left anterior descending coronary artery or performed sham surgery. Two weeks hereafter, cardiac function was determined by echocardiography and PV-loop measurements. Comparable with previous findings, HFD feeding increased body weight and induced dyslipidemia in mice. In addition, the sham surgery group showed that HFD feeding *per se* induced mild cardiac dysfunction. No differences in mortality rate nor in infarct sizes were observed between LFD and HFD mice with MI. Additionally, HFD did not further aggravate cardiac dysfunction after MI, despite a more prominent macrophage infiltration in the infarcted myocardial area in HFD MI mice compared to LFD MI mice. We concluded that long term HFD did not aggravate cardiac dysfunction two weeks after MI induction.

ATP-binding cassette transporter A1 (ABCA1), a transporter involved in cellular cholesterol transport, exerts anti-atherogenic functions in the pathogenesis of atherosclerosis. Since the actual role of ABCA1 during MI, is not established, we explored the role of ABCA1 after MI induction in **Chapter 4**. To this end, we induced an MI in ABCA1 knockout (KO) mice, WT controls and WT mice transplanted with ABCA1 KO or WT bone marrow. Surprisingly, compared to their respective WT controls, reduced infarct sizes were found in ABCA1 KO mice as well as WT mice transplanted with ABCA1 KO bone marrow. No effect of ABCA1 deficiency on infarct size was found in isolated hearts, as investigated in an *ex vivo* Langendorff perfusion system. The smaller infarct size *in vivo* in ABCA1 KO mice was thus likely due to a secondary effect of ABCA1 deficiency on myocyte function. Interestingly, after *in vivo* MI, ABCA1 KO mice compared to WT controls, showed higher levels of circulating leukocytes. After bone marrow transplantation no differences in leukocyte numbers were observed. However, white blood cell counts were increased compared to the first experiment. We concluded that despite the fact that ABCA1 has a protective role in atherosclerosis, it has adverse effects on cardiac function after MI. In addition, the observed detrimental effects are possibly caused by a reduced activation status of immune cells resulting in less efficient repair after MI. As a consequence, strategies aiming at up-regulation of ABCA1 function should be pursued with care in the light of potential adverse effects on cardiac remodeling post MI.

The innate immune system of the heart becomes activated after MI injury. Toll-like receptor 4 (TLR4), a receptor of the innate immune system, is suggested to negatively affect cardiac function after MI. RP105 is a TLR4 homolog which lacks the intracellular signalling domain that competitively inhibits TLR4-signalling. In **Chapter 5,** we hypothesized that deficiency of RP105, via an amplified signalling of TLR4, aggravates cardiac dysfunction after MI. First we proved that an increased inflammatory response was present in RP105 KO mice after TLR4 stimulation by LPS as compared to WT male C57Bl/6N mice. Subsequently, we found that baseline heart function, assessed by PV-loop measurements, revealed no differences between RP105 KO and WT mice. In addition, MI was induced and 15 days post MI, infarct size measurements revealed no differences between groups. However, PV-loop measurements showed that RP105 deficiency promoted cardiac dilatation after MI Furthermore, histological analysis of the myocardium and the infarcted area showed that in the area adjacent to the infarct zone, expression of RP105, TLR4 and the endogenous TLR4 ligand fibronectin-EDA and macrophage count were increased compared to healthy myocardium. However, no differences between RP105 and WT were found. Taken together, we showed that deficiency of the endogenous TLR4 inhibitor RP105 led to an enhanced inflammatory status and more pronounced cardiac dilatation after MI induction. Our findings underscored the role of the TLR4 pathway in post MI remodelling and modulating RP105 may be an interesting new therapeutic strategy.

TLR2 and TLR4 are hypothesized to be activated by ligands associated with HFD exposure such as (modified) FAs. Although TLR2 and TLR4 are involved in inflammation in cardiac disease, a direct relationship between HFD, TLR activation and cardiac dysfunction has not been reported. In **Chapter 6** we studied the role of TLR2 and 4 in the impairment of cardiac function after exposure to HFD. TLR2 KO, TLR4 KO mice and

their corresponding WT littermates received a long term HFD. No differences in body weight or plasma lipid levels were observed between the genotypes after HFD feeding. In TLR2 KO mice PV-loop measurements showed an increased end-diastolic volume, whereas other parameters of cardiac function were not different from WT littermates. In TLR4 KO mice trends were observed of a decreased pressure half time and an increased end-systolic elastance. These findings showed that deficiency for TLR2 or TLR4 only mildly impaired cardiac function in mice on HFD. This suggested that TLR2 and TLR4,

The primary goal of lipid-modifying therapy in patients with atherosclerotic disease is the lowering of LDL-cholesterol. Statins are currently the standard treatment for CVD, however a substantial residual risk for adverse cardiovascular outcomes remains. Treatment of low HDL-cholesterol is currently considered a secondary lipid target in the reduction of cardiovascular risk, since low HDL- cholesterol is an independent risk factor for CVD. Niacin is the most potent HDL-cholesterol raising drug clinically used and is considered as a novel therapy for reducing atherosclerosis. Despite evidence for an atheroprotective effect of niacin from previous small clinical studies, large outcome trials did not reveal additional beneficial effects of niacin on top of statin treatment. In **Chapter 7** we aimed to elucidate this apparent discrepancy by investigating the effects of niacin without and with simvastatin on atherosclerosis development and determine the underlying mechanisms in APOE*3Leiden.CETP mice. To this end, mice were fed a cholesterol-rich diet without or with niacin, simvastatin or their combination. Niacin treatment and the combination reduced total cholesterol and triglycerides, whereas simvastatin reduced total cholesterol. The combination treatment revealed a greater reduction of total cholesterol compared to simvastatin. Niacin decreased total cholesterol and triglycerides primarily by increasing VLDL clearance. Niacin increased HDL-cholesterol and mildly increased reverse cholesterol transport. All treatments reduced monocyte adhesion to the endothelium, atherosclerotic lesion area and severity. Compared to simvastatin, the combination increased the atherosclerotic plaque stability. Niacin and the combination reduced T-cells in the aortic root. Lesion area was strongly predicted by non-HDL-cholesterol and to a much lesser extent by HDL-cholesterol. In conclusion, niacin decreased atherosclerosis development mainly by reducing nonHDL-cholesterol with minor HDL-cholesterol-raising and additional anti-inflammatory effects. The additive effect of niacin on top of simvastatin was mostly dependent on its nonHDL-cholesterol-lowering capacities. These data suggest that clinical beneficial effects of niacin are largely dependent on its ability to lower LDL-cholesterol on top of concomitant lipid-lowering therapy.

Taken together, the studies in this thesis described the effects of both lipid metabolism and inflammation on several aspects of cardiac pathophysiology. We showed that HFD aggravated cardiac function, although this effect was likely not mediated by TLR2 or TLR4. Also, HFD has no detrimental effects on cardiac function post-MI. Deficiency of RP105 improved cardiac function after MI induction, whereas ABCA1 had adverse effects on cardiac function post MI. Last, we found that the anti-atherogenic properties of niacin were mostly dependent on its non-HDL-cholesterol-lowering capacities on top of statin treatment. Altogether, these studies offer novel strategies and insights for the prevention or treatment of CVD.

Nederlandse samenvatting voor niet-ingewijden

Nederlandse samenvatting

Introductie

Hart- en vaatziekten en de risicofactoren

Hart- en vaatziekten (HVZ) zijn de meest voorkomende doodsoorzaak in de westerse maatschappij. Ondanks nieuwe en succesvolle behandelmethodes, blijft het aantal patiënten met HVZ nog steeds stijgen. Er zijn verschillende factoren die het risico op het ontstaan van HVZ verhogen. Hierbij kan onderscheid gemaakt worden tussen factoren waar je zelf invloed op kunt uitoefenen (roken, overgewicht en vetrijke en eenzijdige voeding) en factoren die je zelf niet kunt beïnvloeden (genetische factoren, geslacht en leeftijd). Een gezonde levensstijl kan veel van de sterfgevallen als gevolg van HVZ voorkomen. Het blijkt echter dat het aanpassen van de levensstijl voor veel personen moeilijk haalbaar is. Ondanks de reeds bestaande therapieën voor de behandeling van HVZ is de verwachting dan ook dat HVZ de komende jaren wereldwijd doodsoorzaak nummer één zal blijven. Het is daarom noodzakelijk om inzicht te krijgen in de mechanismes die ten grondslag liggen aan het ontstaan van HVZ, waarmee nieuwe en effectievere behandelmethodes ontwikkeld kunnen worden.

Atherosclerose en hartinfarcten

De belangrijkste oorzaak van HVZ is atherosclerose (slagaderverkalking). Atherosclerose kenmerkt zich door vernauwingen in de bloedvaten als gevolg van de ophoping van vetten (waaronder cholesterol) en cellen van het immuunsysteem in de bloedvatwand. Dit kan uiteindelijk leiden tot een volledige afsluiting van het bloedvat. Als deze afsluiting in de kransslagaderen van het hart plaatsvindt, ontstaat een hartinfarct. Als gevolg hiervan worden delen van de hartspier niet langer van zuurstofrijk bloed voorzien. Aangezien het hart zuurstof nodig heeft om adequaat te kunnen functioneren, heeft een afsluiting als gevolg dat een deel van de hartspier afsterft en dat de kracht waarmee het hart het bloed door het lichaam pompt afneemt.

Vetstofwisseling

De belangrijkste vetten in ons dieet zijn cholesterol en triglyceriden (TG), die beiden essentieel voor het menselijk lichaam zijn. Cholesterol wordt onder andere gebruikt voor de aanmaak van sommige hormonen en TG zijn een belangrijke energiebron voor het lichaam. Omdat vetten slecht oplosbaar zijn in bloed worden ze voor transport door het lichaam opgenomen in zogeheten lipoproteïnen, die wel oplosbaar zijn in bloed. In het bloed circuleren vier klassen lipoproteïnen die variëren in samenstelling en dichtheid.

Tezamen zijn deze lipoproteïnen verantwoordelijk voor het transport van cholesterol en TG van en naar organen.

Vetten die na een maaltijd worden opgenomen in de darmen worden in chylomicronen verpakt en getransporteerd naar organen als vet, (hart)spier en de lever. Wanneer er enige tijd niet gegeten is worden TG in het vetweefsel afgebroken tot vetzuren (lipolyse), die via het bloed in de lever terecht komen. De lever is op dat moment de belangrijkste distributeur van lipoproteïnen. Om het lichaam van vetten te blijven voorzien, verhoogt de lever daarom de productie van lipoproteïnen met zeer lage dichtheid (Engels: VLDL). Chylomicronen en VLDL bevatten voornamelijk TG en daarom worden deze deeltjes ook wel TG-rijke lipoproteïnen genoemd. De vetzuren die onderdeel uitmaken van TG worden door de organen vervolgens uit het bloed opgenomen en verbrand waarbij energie vrijkomt. Daarnaast zijn er lipoproteïnen die relatief rijk zijn aan cholesterol: lipoproteïnen met lage dichtheid (LDL) en lipoproteïnen met hoge dichtheid (HDL). Cholesterol dat zich in de 'slechte' LDL-lipoproteïnen bevindt kan zich ophopen in de vaatwand, wat kan leiden tot de ontwikkeling van atherosclerose. Daarnaast zijn er de 'goede' HDL-lipoproteïnen, deze bevatten cholesterol dat vanuit de vaatwand naar de lever wordt getransporteerd. Daar wordt het hergebruikt of afgebroken om vervolgens via de darm het lichaam te verlaten. Waar hoge niveaus van het HDL-cholesterol het lichaam beschermen tegen HVZ, zijn hoge niveaus van het LDL-cholesterol juist een risicofactor voor HVZ.

Ontstekingen en het immuunsysteem

Een ontsteking is een proces dat het lichaam normaal gesproken beschermt tegen schadelijke stoffen, inclusief virussen en bacteriën. De ontsteking zorgt er op dat moment voor dat ziekteverwekkers netjes opgeruimd worden. Sinds een aantal jaar is bekend dat mensen met overgewicht een lichte mate van ontsteking hebben, onder andere in het vetweefsel. Dit wordt echter niet veroorzaakt door ziekteverwekkers, maar door de aanwezigheid van overtollig vet. Overgewicht ontstaat door een verstoorde balans, waarbij er in het lichaam meer energie binnenkomt dan verbruikt wordt. De overtollige energie kan in het vetweefsel worden opgeslagen, maar de opslagcapaciteit van het vetweefsel is beperkt. Bij te grote hoeveelheden wordt vet daarom ook opgeslagen in vitale organen zoals de lever en het hart, wat kan leiden tot een lokaal ontstekingsproces. Het gaat hier om een chronische ontsteking die de orgaanfunctie kan aantasten.

Er wordt gedacht dat de ontsteking in vetweefsel en vitale organen, als gevolg van overgewicht, ontstaat doordat vetzuren bepaalde receptoren van het aangeboren immuunsysteem activeren. Receptoren kunnen signalen van binnen of buiten de cel doorgeven nadat een signaalmolecuul zich aan de receptor gebonden heeft. Activatie van een receptor van het immuunsysteem, bijvoorbeeld door binding van een deel van een bacterie, leidt bijvoorbeeld tot een immuunreactie die de ziekteverwekker onschadelijk maakt. Recent is gebleken dat delen van vetzuren kunnen binden aan een aantal specifieke receptoren van het immuunsysteem, de zogeheten Toll-like receptoren (TLR), waardoor er een ontstekingsreactie op gang komt. Er zijn momenteel onderzoeken gaande naar de schadelijke gevolgen van het activeren van deze TLR door vetzuren voor het lichaam.

Wetenschappelijke studies

Doel van dit onderzoek en muismodellen

De studies die beschreven zijn in dit proefschrift hebben betrekking op twee specifieke processen, de vetstofwisseling en ontsteking, die zowel individueel als gezamenlijk invloed kunnen hebben op de ontwikkeling van atherosclerose en hartinfarcten. Om deze effecten te bestuderen werden onder andere gespecialiseerde hartfunctie-metingen uitgevoerd door middel van echocardiografie en druk-volume metingen (Engels: PV-loops). Dit is gedaan in de harten van gewone muizen en muizen waarbij belangrijke genen voor de vetstofwisseling of ontsteking waren uitgeschakeld. Door genen uit te schakelen kunnen de effecten van deze genen op het lichaam nauwkeurig bestudeerd worden. Het is zeer lastig om deze effecten met behulp van celkweken te onderzoeken, gezien de complexiteit en betrokkenheid van meerdere organen bij het ontstaan van HVZ. Ook de mogelijkheden rondom het gebruik van humaan weefselmateriaal zijn beperkt omdat de weefsels vaak alleen beschikbaar zijn na een chirurgische ingreep of als een patiënt overleden is, waarbij het ziekteproces zich vaak al in een eindstadium bevindt. Voor het ontwikkelen van nieuwe behandelmethodes is het juist noodzakelijk om meer te weten te komen over het ontstaan van HVZ. Diermodellen bieden hiervoor een belangrijke mogelijkheid.

Resultaten van de studies

In **Hoofdstuk 2** is onderzocht welke effecten vetrijke maaltijden hebben op de werking van het hart. Om te zien wat de bijdrage is van geslacht of de tijdsduur van het dieet, is dit onderzoek uitgevoerd bij zowel mannelijke als vrouwelijke muizen die een laag-vet dieet (LVD) of een hoog-vet dieet (HVD) kregen gedurende 6 of 12 weken. Het bleek dat door een HVD bij beide geslachten het lichaamsgewicht toenam en ook dat de cholesterol en TG niveaus in het bloed verhoogd waren. Een 12 weken HVD leidde echter alleen bij mannelijke muizen tot een slechtere hartfunctie. Een verklaring hiervoor zou kunnen zijn dat vrouwelijke hormonen een beschermende werking op het hart hebben. Uit deze studie is ook duidelijk gebleken dat mannelijke muizen het voorkeursmodel zijn om de effecten van dieet-geïnduceerde obesitas en de invloed van geneesmiddelen op de hartfunctie te onderzoeken.

In **Hoofdstuk 3** hebben we vervolgens onderzocht wat de effecten zijn van gezonde (LVD) of ongezonde voeding (HVD) op de hartfunctie na een hartinfarct in mannelijke muizen. Een HVD kan een chronische ontstekingsreactie tot gevolg hebben. Daarnaast treedt er na een hartinfarct een acute ontstekingsreactie op. Het is interessant om dit te bestuderen, omdat beide ontstekingsprocessen de hartfunctie kunnen beïnvloeden. De resultaten van deze studie laten zien dat het voor het herstel van het hart korte tijd na een hartinfarct niet veel uitmaakt of er gezonde (LVD) of ongezonde (HVD) voeding aan vooraf is gegaan. Het aantal ontstekingscellen in het geïnfarcteerde gebied van het hart was wel hoger in de HVD muizen, maar dit had vooralsnog geen invloed op de

hartfunctie. Deze resultaten, samen met die uit hoofdstuk 2, suggereren dat in muizen gezonde voeding een verslechterde werking van het hart kan voorkómen, maar dat een vetrijk dieet het herstel na een hartinfarct niet nadelig beïnvloedt.

Zoals al eerder genoemd kunnen HDL-deeltjes cholesterol vanuit de vaatwand naar de lever transporteren. Hierbij spelen ABC-transporters een belangrijke rol, omdat ze cholesterol vanuit de cellen in de vaatwand naar het HDL-deeltje kunnen transporteren. Eerdere studies hebben aangetoond dat de aanwezigheid van de ABC transporter A1 (ABCA1) beschermt tegen de ontwikkeling van atherosclerose. In **Hoofdstuk 4** hebben wij onderzocht of de aanwezigheid van ABCA1 ook beschermt tegen de schadelijke effecten van een hartinfarct. Echter, in tegenstelling tot de verwachting voortkomend uit de beschermende rol van ABCA1 tijdens de ontwikkeling van atherosclerose, bleek dat afwezigheid van ABCA1 in muizen juist zorgde voor minder schade aan de hartspier na een hartinfarct. Omdat activatie van het immuunsysteem invloed kan hebben op de infarctgrootte, hebben we de concentratie van immuuncellen in het bloed onderzocht. Hierbij zagen we een opmerkelijke verhoging van de concentratie immuuncellen bij ABCA1-deficiënte muizen. Om te bestuderen of het effect op infarctgrootte veroorzaakt werd door ABCA1 op immuuncellen zelf, hebben we vervolgens het beenmerg van normale muizen vervangen door dat van ABCA1 deficiënte muizen. Het bleek dat de afwezigheid van ABCA1 op de immuuncellen inderdaad resulteerde in kleinere infarcten. Hoe dit fenomeen tot stand komt moet nog verder uitgezocht worden. Deze resultaten laten zien dat therapeutische strategieën gericht op het activeren van ABCA1 ter preventie of behandeling van HVZ met zorg moeten worden overwogen, in verband met mogelijke schadelijke effecten op het hart.

Daarnaast hebben we onderzocht of Toll-like receptoren en RP105 een belangrijke rol spelen bij het herstel van het hart na een hartinfarct. TLR en RP105 zijn eiwitten die een belangrijke rol spelen in het immuunsysteem. Van TLR4 is al bekend dat deze receptor een negatieve invloed heeft op de hartfunctie na een hartinfarct. RP105 is een molecuul dat qua structuur veel op TLR4 lijkt, alleen kan dit molecuul, in tegenstelling tot de TLR4 receptor, geen signalen doorgeven. Wel kunnen signaalmoleculen die zich normaal gesproken aan TLR4 binden ook binden aan RP105. Dit zorgt uiteindelijk voor een verminderde ontstekingsreactie omdat TLR4 minder geactiveerd wordt. In **Hoofdstuk 5** testten wij de hypothese dat de afwezigheid van RP105, via een versterkte signalering van TLR4, leidt tot een verslechtering van de hartfunctie na een hartinfarct. De hartfunctie in muizen met normale en afwezige expressie van RP105 was niet verschillend voorafgaande aan het induceren van het infarct. Na een infarct zagen wij inderdaad dat, ondanks gelijke infarctgroottes tussen beide groepen, de RP105 deficiënte muizen een slechtere hartfunctie hadden ten opzichte van de normale muizen. Hoe dit effect precies tot stand komt is nu nog onbekend. Wel onderstrepen onze bevindingen de rol van TLR4 in het hart na een hartinfarct. Tevens kan het moduleren van RP105 een interessante nieuwe therapeutische strategie zijn om de schade na een hartinfarct te beperken.

In **Hoofdstuk 6** hebben we de effecten van TLR2 en TLR4 op de hartfunctie na blootstelling aan een HVD onderzocht. Hoewel bekend is dat TLR2 en TLR4 betrokken zijn bij ontsteking geassocieerd met HVZ, is er nog geen direct verband gevonden tussen

een HVD, de activering van TLR en een slechter werkend hart. In deze studie hebben we zowel normale muizen als muizen deficiënt voor TLR2 en TLR4 een HVD gegeven voor 12 weken. Na deze periode vonden we geen verschillen in lichaamsgewicht noch in cholesterol of TG niveaus in het bloed. Met behulp van de hartfunctiemetingen vonden we dat zowel TLR2- als TLR4-deficiënte muizen, zeer kleine verslechteringen in hartfunctie vertonen. Deze resultaten suggereren dat als TLR2 en/of TLR4 al een invloed heeft op de hartfunctie na HVD, dit een bescheiden rol zal zijn.

Als laatste hebben we in **Hoofdstuk 7** een medicijn bestudeerd waarvan bekend is dat het het goede HDL-cholesterol verhoogt, genaamd niacine. Recente experimentele patiënten-studies lieten zien dat niacine geen verlaging gaf van het risico op HVZ als het gegeven werd in combinatie met statines, ten opzichte van patiënten die alleen statines kregen. Statines zijn de huidige LDL-cholesterol verlagende middelen. Het ontbreken van de gunstige effecten van niacine is tegenstrijdig met eerder gevonden resultaten in kleinere groepen patiënten, waarbij de niacine leidde tot een stagnatie of zelfs een afname van de ontwikkeling van atherosclerose. Wij hebben in experimentele studies met muizen bestudeerd wat de effecten zijn van niacine in vergelijking met simvastatine alsook de combinatie behandeling van niacine met simvastatine. In deze studie hebben we ten eerste aangetoond dat de werking van niacine voornamelijk te verklaren is door verlaging van het nonHDL-cholesterol (dus voornamelijk het VLDL en LDL). Tevens zorgde niacine voor een milde verhoging van het HDL-cholesterol. Daarnaast zagen wij dat de behandeling met een combinatie van niacine en simvastatine ten opzichte van simvastatine alleen, een gunstig effect had op de ontwikkeling van atheroslcerose. Dit effect van niacine bovenop een statine bleek vooral te komen door een extra verlaging van het nonHDL-cholesterol. Deze resultaten wijzen er op dat de gunstige effecten van niacine in patiënten voor het grootste deel toe te schrijven zijn aan het verlagen van het LDL-cholesterol, in combinatie met reeds bestaande LDL verlagende medicijnen.

Conclusie

De in dit proefschrift gepresenteerde bevindingen beschrijven de gevolgen van zowel een verstoorde vetstofwisseling als ontsteking op verschillende aspecten van de hartfunctie. We hebben aangetoond dat een HVD de hartfunctie verslechtert, en dat dit effect vermoedelijk niet gemedieerd wordt door TLR2 en TLR4. Ook heeft een HVD geen extra schadelijke effecten op de hartfunctie na een infarct. Deficiëntie van RP105 verbetert de hartfunctie na een hartinfarct, terwijl de aanwezigheid van ABCA1 juist leidt tot een groter infarct. Als laatste hebben we gevonden dat de anti-atherosclerotische eigenschappen van niacine voornamelijk worden verklaard door het verlagen van LDL-cholesterol, en dat een combinatiebehandeling met statines tot betere effecten zou kunnen leiden. Tezamen bieden deze studies nieuwe strategieën en inzichten voor de preventie of behandeling van HVZ.

List of publications

List of publications (full papers)

Revsin Y, Rekers NV, Louwe MC, Saravia FE, De Nicola AF, de Kloet ER, Oitzl MS. Glucocorticoid receptor blockade normalizes hippocampal alterations and cognitive impairment in streptozotocin-induced type 1 diabetes mice. **Neuropsychopharmacology** (2009) 34, 747–758

Louwe MC, van der Hoorn JW, Jukema JJ, Romijn JA, Willems van Dijk K, Rensen PC, Smit JW, Steendijk P. Gender-dependent effects of high-fat lard diet on cardiac function in C57Bl/6J mice. **Applied Physiology, Nutrition, and Metabolism** (2012) 37 (2), 214-224

Louwe MC*, Kühnast S*, van Klinken JB, Smit JW, Havekes LM, Rensen PC, van der Hoorn JW, Princen HM†, Jukema JW†. Niacin reduces atherosclerosis progression and inflammation on top of simvastatin in APOE*3Leiden.CETP mice. *Both authors contributed equally, †These authors share equal responsibility for the manuscript. Accepted for publication in **PLOS ONE**

Louwe MC*, Karper JC*, de Vries MR, Bastiaansen AJ, van der Hoorn JW, Willems van Dijk K, Rensen PC, Steendijk P, Smit JW, Quax PH. RP105 deficiency aggravates cardiac dysfunction after myocardial infarction in mice *Both authors contributed equally. Submitted

Louwe MC, Maas S, van der Hoorn JW, Salvatori D, Rensen PC, Willems van Dijk K, Steendijk P, Smit JW. High-fat diet does not aggravate cardiac function after a myocardial infarction in C57Bl/6J mice. Submitted

Louwe MC*, Lammers B*, Frias MA, Foks AC, Hildebrand RB, Kuiper J, Smit JW, Van Berkel TJ, Rensen PC, Van Eck M. ABCA1 deficiency protects the heart against injury following myocardial infarction. *Both authors contributed equally. In preparation

Curriculum Vitae

Curriculum Vitae

Maria Cornelia Louwe (roepnaam Mieke) werd geboren op 31 mei 1984 te Egmond aan den Hoef. Na het behalen van haar VWO diploma in 2002 op het Petrus Canisius College te Alkmaar, startte zij datzelfde jaar met de studie Bio-Farmaceutische Wetenschappen aan de Universiteit Leiden. In 2006 behaalde zij haar Bachelor of Science.

Tijdens haar Master koos zij voor de specialisatie onderzoek en voerde zij twee stages uit. De eerste stage vond plaats bij de afdeling Medische Farmacologie van het Leiden/ Amsterdam Center for Drug Research aan de Universiteit Leiden, onder begeleiding van Prof. dr. M. Oitzl en Dr. Y. Revsin. Tijdens deze stage deed zij onderzoek naar de invloed van chronisch hoge corticosteron concentraties op het geheugen en het leergedrag in muizen met diabetes type 1. Haar tweede stage voerde zij uit aan de Uppsala Universitet in Uppsala, Zweden, onder begeleiding van Prof. dr. F. Nyberg en Dr. A-L. Svensson. Hier bestudeerde zij de effecten van opioïden- en neursteroïden-behandeling op de overleving van neuronale cellen.

Na haar afstuderen in mei 2008 startte ze in september datzelfde jaar met haar promotieonderzoek bij de afdeling Endocrinologie en Metabole Ziekten van het Leids Universitair Medisch Centrum onder supervisie van Prof. dr. J.W.A. Smit, Prof dr. K. Willems van Dijk en Dr. P. Steendijk. Als promovendus ontving zij voor de presentatie over haar onderzoek in 2010 de poster award op het 13^{e} symposium van de Dutch Atherosclerosis Society. Verder won zij tijdens de 2^{e} PREDICCt meeting in 2010 de schrijfwedstrijd 'scientific writing for the public'. Het promotieonderzoek, waarvan de resultaten zijn beschreven in dit proefschrift, werd afgerond in maart 2013.